Characterization of hMIA40 and hTOM40 as novel components of Fe/S cluster export machinery of mitochondria

Thesis submitted for the degree of

DOCTOR OF PHILOSOPHY

By

M. ANJANEYULU

Department of Biochemistry

School of Life Sciences

University of Hyderabad

Hyderabad-500046

INDIA

Enrollment No: 09LBPH13 June 2014

University of Hyderabad

School of Life Sciences

Department of Biochemistry

Hyderabad 500046 INDIA

CERTIFICATE

This is to certify that this thesis entitled **"Characterization of MIA40 and TOM40 as novel components of Fe/S cluster export machinery of mitochondria"** submitted to the University of Hyderabad by **Mr. M. Anjaneyulu**, for the degree of Doctor of Philosophy, is based on the studies carried out by him under my supervision. I declare to the best of my knowledge that this work has not been submitted earlier for the award of degree or diploma from any other University or Institution.

Dr. Naresh Babu V Sepuri

Supervisor

Head

Department of Biochemistry

Dean

School of Life Sciences

University of Hyderabad

School of Life Sciences

Department of Biochemistry

Hyderabad 500046 INDIA

DECLARATION

I hereby declare that the work presented in my thesis is entirely original, plagiarism free and was carried out by me in the Department of Biochemistry, University of Hyderabad, under the supervision of **Dr. Naresh Babu V Sepuri**. I further declare that this work has not been submitted earlier for the award of degree or diploma from any other University or Institution.

M. Anjaneyulu

Date

Dr. Naresh Babu V Sepuri

Supervisor

Acknowledgements

I thank **ALMIGHTY GOD** for giving me a nice, caring and kind supervisor, **Dr. Naresh Babu V Sepuri** who provided an opportunity to work in his lab. I am grateful to my supervisor, for his immeasurable patience, invaluable guidance, constant support, and timely help during entire course of my research work. My sincere appreciation goes to him for his continuous help in all stages of the thesis preparation despite of his busy schedule. No words can adequately express my deep gratitude to my supervisor for all his guidance and kindness.

I am thankful to former Deans Prof. A. S.Rahavendra, Prof. M. Ramanadham, Prof. R. P. Sharma, and Prof. Aparna Dutta Gupta, present Dean, School of Life Sciences, Prof. A. S. Raghavendra; former Heads of the department, Prof. M. Ramanadham, Prof. K. V. A, Ramaiah, Prof. O. H. Setty and present Head, department of Biochemistry, Prof. N. Siva Kumar, for allowing me to utilize facilities at the School and department level.

I thank my Doctoral committee members Dr. S. Rajagopal and Dr. K. Gopinath, for their valuable suggestions in carrying out my work.

I express my gratitude to Dr. S. Rajagopal, Dr. Y. Suresh and Prof. B. Senthilkumaran, for moral support, inspiration and encouragement.

I thank all faculty members of school of life sciences, I also thank all the non-teaching staff for their timely help.

I sincerely acknowledge Dr. Mohammed for his help in CD analysis, Dr. Krishanmoorthy for his help in AES studies.

I acknowledge Mrs. Monika for MS/MS analysis, Miss. Nalini for confocal microscopy studies and Mr. Durga Prasad for TEM analysis.

I am happy to mention my Lab members M. Aadinarayana, G. Madhavi, T. Prasad, A. Praveen, A. Chandra sekhar, V. Viswa Mitra, Dr. Pulla Reddy, T. Venkata Ramana, Fareed, B. Yerranna, K. Srenivasulu, Dr. Samule and lab attender G. Narasimha for providing

congenial atmosphere in the lab that led to smooth conduction of my research work. I feel very much happy to have such a nice lab mates.

I heartfully acknowledge the financial support of CSIR, ICMR, UGC, DBT, CREBB, DST-FIST, UPE-II and PURSE which helped me directly or indirectly in the school and university for carrying out my research work properly.

I cannot forget to mention fruitful discussions with G. Madhavi, A. Praveen and T. Prasad in personal, academic and research matters.

I will be failing my duty if I don,t mention my Friends Sujith, Rakesh, Abdul, B. Suresh, G. Madhu Babu, Rajesh, Kamusha vali, Raj kumar, M. Maruti, G. Mahesh, Shalu, Sweta, Harika and Ms. Jalaja, for cheerful environment and charging with happiness during my interactions with them. A simple word ‘thank you’ cannot suffice how much their friendship means to me.

I thank all my Friends for their love and affection which cannot be explained in words.

My greatest appreciation goes to my evergreen closest brother Dr. A. Venugopal, who was always in great support to me in all my struggles and frustrations. I would like to register my affection to my brother for his conversations and support.

I am kindful to my family members Mr M. Nasaraiah, Mrs M. Leelamma (Father and Mother), M. Jyothi, M. Ribka (sisters), M. Deena (Fiance) and M. Srenivasulu, M. Ravibabu and M. Krishna (Brothers), for unstinting love and affection during my research work.

M. Anjaneyulu

CONTENTS

CHAPTER-II

2. Characterization of human MIA40's function in iron homeostasis of the cell

Figures

ABBREVIATIONS

ABCB7	ATP binding cassette sub family member 7
APS	Ammonium persulphate
ATM1	ABC transporter of mitochondria
ATP	Adenosine triphosphate
Bp	Base pair
BSA	Bovine serum albumin
CD	Circular Dichroism
cDNA	Complementary DNA
CIA	Cytosolic Fe/S assembly
COX	Cytochrome oxidase
DMEM	Dulbecco's modified eagle medium
DMSO	Dimethylsulphoxide
DNA	Deoxyribonucleic acid
dNTP	Deoxyribonucleotide triphosphate
DPYD	Dihydropyrimidine dehydrogenase
DTT	Dithiothreitol
ECL	Enhanced chemiluminescence
EDTA	Ethylene diamine tetra acetic acid
EGTA	Ethylene glycol tetra acetic acid
ER	Endoplasmic reticulum
et al	et alii (Latin: and others)
FAD	Flavin adenine dinucleotide

FBS	Fetal bovine serum
FC	Ferrochelatase
Ft	Ferritin
FRDA	Friedreich's ataxia
g	Gram
GPAT	Glutamate Phosphoribosyl pyrophosphate Amidotransferase
GLRX	Glutaredoxin
HEK	Human embryonic kidney
HEPES	(N-(2-Hydroxyethyl)-piperizine-N'-(2-ethane sulfonic acid)
HRP	Horseradish peroxidase
IAA	Iodoacetamide
IgG	Immunoglobulin G
IMS	Inter membrane space
IN	Inner membrane
IPTG	Isopropyl β-D-thiogalactopyranoside
IRE	Iron responsive element
IRP	Iron regulatory proteins
ISC	Iron-sulfur cluster
Kb	Kilo base pair
kDa	Kilo Dalton
LB	Luria Bertani

M	Molar
MES	2-(*N*-morpholino) ethanesulfonic acid
MgCl2	Magnesium chloride
MIA	Mitochondrial inter membrane space assembly
Min	Minute
µM	Micro meter
mM	milli molar
mL	milli litre
MPP	Mitochondrial processing peptidase
mtDNA	Mitochondrial deoxyribonucleic acid
MW	Molecular weight
NaCl	Sodium chloride
NADH	Nicotinamide adenine dinucleotide
NADPH	Nicotinamide adenine dinucleotide phosphate
NC	Nitrocellulose
ND	NADH dehydrogenase
NIF	Nitrogen fixation
Ni-NTA	Nickel nitrilotriacetic acid
Nm	Nanometer
nM	Nano molar
OD	Optical density
OM	Outer membrane
PAGE	Polyacrylamide gel electrophoresis

PAM	Presequence translocase associated motor
PBS	Phosphate-buffered saline
PCR	Polymerase chain reaction
pH	-log (H^+) concentration
PPAT	Phosphoribosyl pyrophosphate amidotransferase
RNA	Ribonucleic acid
ROS	Reactive oxygen species
Rpm	Rotations per minute
RT	Reverse transcriptase
SAM	Sorting and assembly machinery
SDS	Sodium dodecyl sulphate
SUF	Sulphur-mobilization
Taq	*Thermophilus aquaticus*
TBS	Tris-buffered saline
TBST	Tris-buffered saline Tween20
TCA	Tricarboxylic acid
TEMED	N,N,N‘,N‘-tetramethylethylene diamine
Tf	Transferrin
TfR	Transferrin receptor
TIM	Translocase of inner mitochondrial membrane
TOM	Translocase of outer mitochondrial membrane
Tris	Tris-(Hydroxymethyl) aminoethane

tRNA	Transfer ribonucleic acid
U	Units
XDH	Xanthine dehydrogenase

CHAPTER I

INTRODUCTION

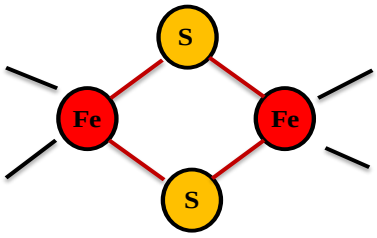

2Fe-2S

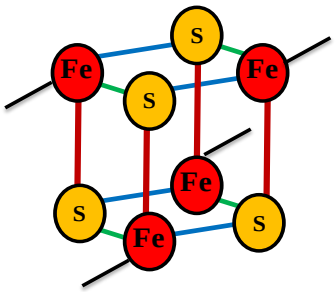

4Fe-4S

Introduction

1.1. Mitochondria

The mitochondrion is an unusual membrane bound organelle present in most eukaryotic cells (Henze and Martin 2003). Mitochondria can vary in size and number which depends on organism and tissue type. Mitochondria size is in range of 0.5-10 µm and the number varies from 1 to 1000. Mitochondria are the power house of the cell. Besides energy generation, mitochondria are necessary for number of essential functions of a cell. These include production of several metabolites, metal homeostasis, apoptosis, autophagy, lipid metabolism, generation of reactive oxygen species and metabolic signalling. To exhibit all these functions, mitochondria require approximately 10-15% of all gene products of eukaryotic cells.Mitochondria contain its own genome but it only codes for few proteins, 13 in humans and the remaining proteins required for mitochondrial function are encoded by nuclear DNA.

1.2. Structure of Mitochondria

Mitochondria contain two separate membranes, outer and inner membrane, dividing the organelle into four sub-compartments (Fig 1.1). The outer membrane constitutes a barrier between the organelle and the cytosol. The inner membrane separates innermost compartment, the matrix and the space between outer and inner membrane, intermembrane space. The inner membrane invaginates into the matrix to form cristae (Mannella, Pfeiffer *et al.,* 2001; Gilkerson, Selker *et al.,* 2003) that increases the surface area of inner mitochondrial membrane by several folds.

The outer mitochondrial membrane contains protein and phospholipids in the ratio similar to that of eukaryotic plasma membrane (1:1). Outer membrane is freely permeable to small

molecules due to presence of channel forming integral membrane proteins known as porins. These porins allow passive movement of molecules up to 5 kDa across the outer membrane. However, the high molecular weight proteins can only enter mitochondria through the multi-subunit protein complex known as Translocase of the Outer Membrane (TOM) (Herrmann and Neupert 2000).

The intermembrane space is a very tiny sub-compartment in between two membranes and occupies a space of few nano meters (Frey and Mannella 2000; Frey, Renken *et al.,* 2002). The concentration of small molecules in the intermembrane space is similar to cytosol as the outer membrane is freely permeable to small molecules (Bruce, Johnson*et al.,* 1994). Protein molecules that contain targeting information can only transfer across the outer membrane through a TOM complex and hence the protein composition in the IMS is different from the cytosolic protein composition.

Unlike outer membrane, inner membrane of mitochondria is enriched in protein and has a ratio of protein to phospholipids at around 3:1. The inner membrane is impermeable to most of the molecules due to presence of an unusual phospholipid known as cardiolipin (Bruce, Johnson*et al.,* 1994). Due to the impermeable nature of inner membrane, most of the ions and molecules require special transporters to enter or exit from the matrix. In addition, there is a membrane potential across the inner membrane formed by the action of enzymes of the electron transport chain. The inner mitochondrial membrane proteins are involved in oxidative phosphorylation, ATP synthesis, metabolite transport, protein import, mitochondrial fusion and fission (Bruce, Johnson*et al.,* 1994). The matrix is the space surrounded by the inner membrane and it contains about 2/3 of total proteins of a mitochondrion (Bruce, Johnson*et al.,* 1994). Mitochondrial matrix contains a highly concentrated mixture of enzymes, mitochondrial ribosomes, tRNA and multiple copies of

DNA. The major functions of mitochondrial matrix enzymes include oxidation of pyruvate and fatty acids, citric acid cycle, heme and Fe/S cluster biosynthesis, amino acid metabolism and Urea cycle (Bruce, Johnson*et al.*, 1994).

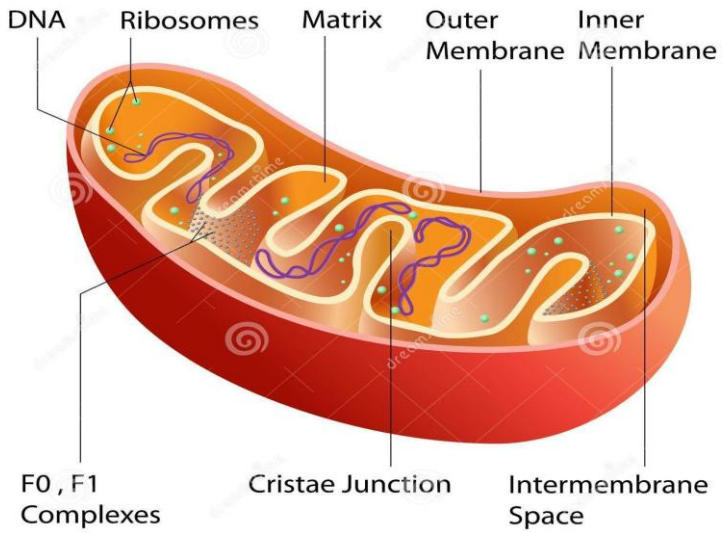

Figure 1.1. Structure of mitochondria. Mitochondria composed of two separate membranes, outer and inner membranes. The outer membrane constitutes a barrier between the organelle and the cytosol. The inner membrane separates innermost compartment, the matrix and the space between outer and inner membrane, intermembrane space. The inner membrane invaginates into the matrix to form cristae. The mitochondrial matrix contains ribosomes and DNA.

1.3. Mitochondrial Biogenesis

Mitochondria arises from growth and division of pre-existing mitochondria and do not arise *de novo*. The shape, size and number of mitochondria vary dramatically in different cell types depending on energy demands, physiological and environmental conditions. The number of mitochondria in a cell is directly connected to the biogenesis of the organelle (Attardi and Schatz 1988). The biogenesis of mitochondria per cell is tightly regulated by the activation of specific transcription factors and signalling pathways (Attardi and Schatz 1988; Moyes and Hood 2003).

Although mitochondria have their own genome, it encodes a small set of proteins and most of the proteins and enzymes that reside in the mitochondria are nuclear gene encoded products. The mitochondrial and nuclear encoded proteins together perform a role in synthesis of ATP through electron transport and oxidative phosphorylation. The other functions of nuclear encoded mitochondrial proteins include maintenance of organelle structure, pyrimidine and heme biosynthesis, transcription, translation machinery, components of mtDNA replication and other functions of mitochondria. The nuclear encoded mitochondrial proteins are imported into different sub-compartments of mitochondria by using complex protein import machineries present in the outer and inner membrane. On the other hand, 13 proteins that are encoded by mitochondrial DNA are mainly includes seven subunits of NADH dehydrogenase or Complex I (ND1, ND2, ND3, ND4, ND4L, ND5 and ND6), three subunits of cytochrome c oxidase or Complex IV (COI, COII and COIII), two subunits of F_0F1 ATPase or Complex V (ATPase6 and ATPase8) and one subunit of cytochrome c oxidoreductase or complex III (cytochrome B) (Attardi and Schatz 1988). Mammalian mtDNA also codes for two rRNAs and complete set of 22 tRNAs that are essential for protein synthesis in mitochondria. The assembly and functioning of the electron transport chain enzymes in mitochondria requires coordinated expression and interaction between mitochondrial and nuclear gene products (Poyton and McEwen 1996).

Mitochondria also import most of their phospholipids from the cytoplasm to maintain their membranes (Moyes and Hood 2003). Cardiolipin and hydrophobic phospholipid are required for the function of many mitochondrial proteins such as cytochrome c oxidase. The inner membrane is rich source of cardiolipin. Interestingly, the amount of cardiolipin present in the mitochondrial inner membrane changes in response to altered level of thyroid hormones,

chronic contractile activity of muscle and aging (Paradies and Ruggiero 1990; Takahashi and Hood 1993; Paradies, Petrosillo *et al.,* 1997).

1.3.1.mtDNA

Mammalian cell usually contain 2-10 copies of mtDNA and it is a circular double stranded DNA molecule (Robin and Wong 1988). Although the replication of mtDNA occurs throughout the cell cycle, it is predominant in late S phase and G2 phase of the cell cycle(Bogenhagen and Clayton 1977). In addition, the mtDNA replication, growth and division of the organelles do not take place at the same time (Shadel and Clayton 1997). Thus, mtDNA replication does not coupled with the mitochondrial proliferation. The copy number of mtDNA also varies with the cell type, physiological conditions and energy dependence of the cell (Moraes 2001). It has been shown that copy number of mtDNA in cells is modulated during cell growth and differentiation, treatment with hormones and exercise (Williams, Salmons *et al.,* 1986; Renis, Cantatore *et al.,* 1989; Shay, Pierce *et al.,* 1990; Wiesner, Kurowski *et al.,* 1992). However, under normal physiological conditions, mtDNA molecules are doubled in every cell cycle to maintain a constant amount of mtDNA molecules in each daughter cell mitochondrion.Protein components encoded by nuclear genes are involved in the mitochondrial biogenesis and maintenance of mtDNA copy number (Scarpulla 1997).

1.4. General Protein Import Machineries in Mitochondria

Mitochondria are considered to have originated through the process of endosymbiosis of alpha proteobacteria. However, during the course of evolution, most of the genes of primitive mitochondrial genome are transferred to nuclear DNA of the host cell and left with minimal amount of genome in mitochondria. In humans, the mitochondrial genome contains 16,580

bases. Further, acquired functions of mitochondria through evolution are attributed to the nuclear DNA. Thus, most of the proteins required for mitochondrial function and maintenance are dependent on nuclear encoded proteins. These proteins are synthesized on free ribosomes in the cytosol and imported into several sub-compartments of mitochondria (Neupert and Herrmann 2007; Bolender, Sickmann *et al.*, 2008).

Cells have evolved with a sophisticated import machineries at the outer, inner, and IMS of mitochondria to translocate nuclear encoded mitochondrial proteins into different sub-compartments of mitochondria. Proteins that are transported to the inner most compartments of mitochondria, the matrix, often bear import signals at N-terminus. The protein that is being translocated into mitochondria is also called as precursor protein or pre-protein. The N-terminal targeting sequences or pre-sequences usually consist of 10-80 amino acid residues and form an amphipathic α-helicesin the membrane environment. These helices contain hydrophobic amino acids on one side and positively charge amino acids on the other side (von Heijne 1986)). After the import of precursor protein into mitochondrial matrix, the N-terminal pre-sequence is cleaved by the mitochondrial processing peptidases in one or two steps to generate a mature protein. In contrast, most of the precursor proteins that are targeted to mitochondrial outer, inner and IMS do not contain any N-terminal pre-sequence and their targeting sequence is present within the mature protein (Gakh, Cavadini *et al.*, 2002).

Nearly all mitochondrial pre-proteins are imported through the generalentry gate known as the translocase of the outer membrane or TOM complex (Fig 1.2A). The TOM complex is a multi subunit protein complex that contains receptor proteins (Tom70, Tom20 and Tom22) for the recognition of the mitochondrial targeted precursor proteins and remaining other protein components constitute the translocation pore (Tom40, Tom5, Tom6 and Tom7) (Hachiya, Mihara *et al.*, 1995; Dekker, Ryan *et al.*, 1998; Kunkele, Heins *et al.*, 1998; Endo,

Yamamoto *et al.*, 2003; Pfanner, Wiedemann *et al.*, 2004; Neupert and Herrmann 2007). Cytosolic chaperones, Hsp70 and Hsp90, binds and prevents the aggregation of newly synthesized precursor proteins in the cytosol and delivers to the surface of mitochondria. Hsp70 preferentially binds and deliver the precursor proteins containing N-terminal pre-sequence and deliver to the TOM channel in an ATP dependent mechanism. Tom20 is the initial recognition sitefor pre-proteins containing pre-sequences at the N-terminus (Saitoh, Igura *et al.*, 2007). Tom20 binds andtransfers the pre-proteins to the central receptor, Tom22. In contrast, Hsp90 is involved in the binding of precursor proteins containing internal targeting sequences and delivering to the Tom70 receptor. Tom70forms the initial recognition site for inner membranemetabolite carrier proteins and transfers the precursor proteins to Tom22 (Kiebler, Keil *et al.*, 1993; van Wilpe, Ryan *et al.*, 1999). Precursor proteins are transferred from Tom22 and inserted into the Tom40 channel.After passing through the TOMcomplex channel, theprecursor proteins can follow one of four major import pathways (Koehler, Merchant *et al.*, 1999; Herrmann and Neupert 2000; Jensen and Johnson 2001; Pfanner and Geissler 2001; Endo, Yamamoto *et al.*, 2003); (i) Pre-proteins with a pre-sequence are transferred to thepre-sequence translocase of the inner membrane, also termed as TIM23 complex (Translocase of the Inner Membrane, TIM). Thepre-sequence translocase of Inner membrane forms a channel across the innermembrane and cooperates with the matrix heat shock protein70 (mtHsp70). The molecular chaperone mtHsp70 representsthe core of the pre-sequence translocase associated motor(PAM) which drives the completion of protein transport intothe matrix (Fig 1.2A). (ii) Many hydrophobic polytopic inner membrane proteins useschaperone like components in the intermembrane space and theprotein insertion machinery of the inner membrane carrier translocase known as TIM22 complex for targeting to the inner membrane (Fig 1.2A). (iii) The precursor of outer membraneproteins such as Porin and Tom40 are integrated into the outer membrane by the sorting and assembly

machinery(SAM complex) (Fig 1.2A). (iv) The number of precursorproteins that are targeted to the IMS utilizes the oxidative folding machinery of mitochondrial IMS machinery containing Erv1 and Mia40 or inner membrane TIM23 complex.

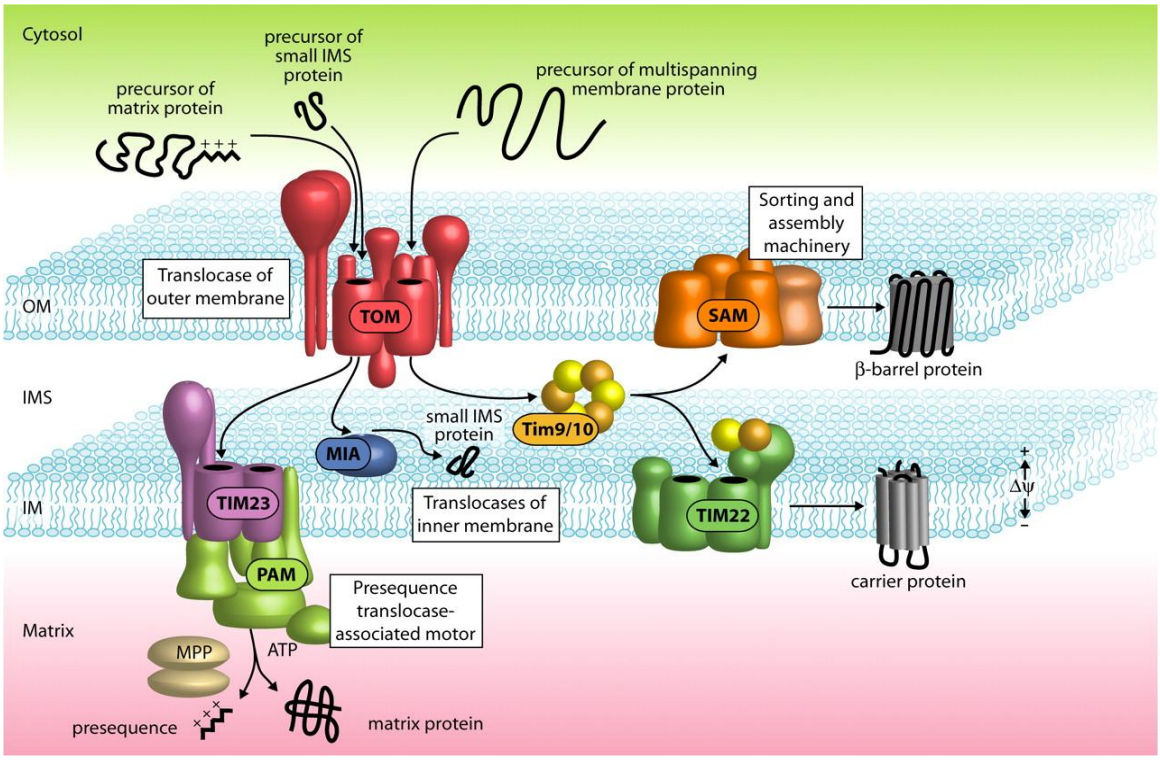

Figure 1.2.A. Mitochondrial protein import pathways. Nuclear encoded mitochondrial targeting proteins are imported by the TOM complex. Subsequently, they follow different sorting pathways. (i). Pre-sequence containing proteins are translocated through the TIM23 complex and motor PAM complex into the matrix, where mitochondrial processing peptidase (MPP) cleaves off the pre-sequences. (ii). Small proteins of the intermembrane space (IMS) are imported via the mitochondrial inter membrane space assembly machinery (MIA). (iii). β-barrel precursor proteins of the outer membrane (OM) are transferred from TOM to SAM complex. (iv). Precursor proteins of the inner membrane (IM) carriers use Tim9-Tim10 for transfer to the TIM22 complex that drives insertion into the inner membrane. Adapted from Stephan *et al.,* 2007.

1.4.1. Intermembrane Space (IMS)

Intermembrane space is an extremely small compartment of mitochondria, but, it contains various number of highly important proteins. These include the electron transporters, metal ions, enzymes required for metabolic reactions and group of pro-apoptotic proteins. Many

IMS targeted proteins do not contain any classical mitochondrial targeting signals. Intermembrane space targeted proteins can be divided into three classes based on their structural parameters, energy requirement and sorting routes (Fig 1.2B) (Herrmann and Hell 2005; Neupert and Herrmann 2007).

Class I proteins contain N-terminal mitochondrial targeting sequences followed by hydrophobic transmembrane domain. These proteins utilize the TOM and TIM23 complex for IMS targeting. Targeting of these proteins requires ATP and membrane potential. The targeting sequence at N-terminus translocates through the TIM23 complex, however, the hydrophobic domain present immediately after the pre-sequence arrests the precursor protein in the inner membrane and prevents further translocation into matrix. TIM23 complex inserts the hydrophobic domain into the inner membrane laterally. The mature proteins released into the IMS compartment by the action of inner membrane peptidase, which cleaves off the inserted hydrophobic domain from the exposed IMS domain (Glick, Brandt *et al.*, 1992). Class II proteins are typically low molecular weight (7-15 kDa) proteins and lack any detectable pre-sequences. These proteins contain conserved cysteine and histidine residues that are involved in the binding of metal ions or other cofactors. The cysteine residues present in these proteins enable them to form intra disulfide bonds to attain stable and mature protein confirmation. This disulfide mediated folding of proteins in IMS prevents them to diffuse back into the cytosol (Lutz, Neupert *et al.*, 2003; Mesecke, Bihlmaier *et al.*, 2008). Class III proteins of IMS contain neither pre-sequences nor any other import signal. The translocation of these proteins does not require ATP and the membrane potential. These proteins diffuse into the intermembrane space from cytosol and bind to high affinity sites present on IMS proteins. The energy that is being released during anchoring with intermembrane space

proteins is the driving force for the import of third category proteins into IMS (Steiner, Zollner *et al.*, 1995).

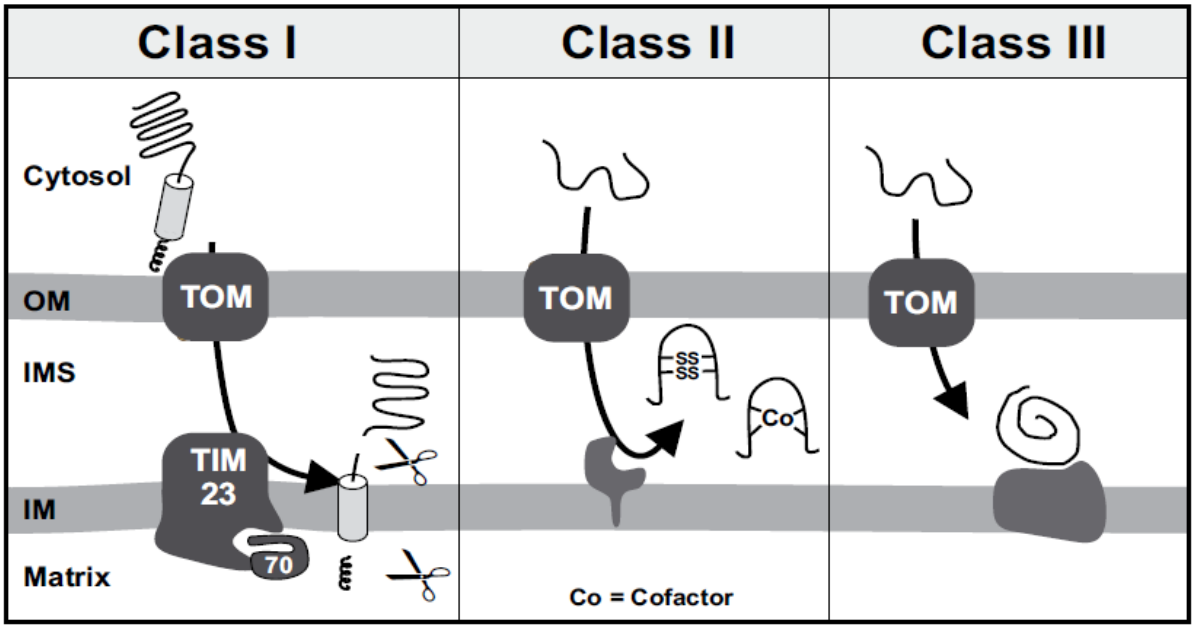

Figure 1.2.B. Categorization of intermembrane space proteins. Intermembrane space proteins are divided into three classes depending on their import signals. Class I proteins consist oftwotypes of import signal, such as a small helix and a hydrophobic anchoring domain. These proteins are processed after import. Class II proteins attain their native confirmation by formation of disulfide bonds or binding to cofactors. Class III proteins bind to high affinity site in the intermembrane space. OM - Outer Membrane, IMS - Intermembrane Space, IM - Inner Membrane, TOM - Translocase of the Outer Membrane, TIM - translocase of the Inner Membrane. Adapted from Bihlmaier*et al.,* 2007.

1.5. Iron trafficking in cells

Iron is essential molecule for all living organisms from single cell bacterium to humans. In living organisms, iron can exist in three different oxidation states and are ferrous (Fe^{2+}), ferric (Fe^{3+}) and ferryl (Fe^{4+}) form. Iron can participate in electron transfer and reversible binding to the ligands due to inter conversion of oxidative states. Further the electron spin state and redox potential of iron also plays a role in its chemical reactivity. Nitrogen, oxygen and sulfur are preferred biological ligands for iron. Thus iron is a suitable constituent for several

important biological molecules that are involved in oxygen transport (haemoglobin), oxidation-reduction (ferridoxin) and electron transfer (cytochromes).

Iron homeostasis is tightly regulated in a cell to avoid excess iron toxicity or iron deficiency. In humans, the systemic iron metabolism, uptake, trafficking, export and utilization of iron are highly regulated (Hentze, Muckenthaler *et al.,* 2004; De Domenico, McVey Ward *et al.,* 2008; Ganz 2008). In mammalian blood circulation, iron-laden transferrin (Tf) interacts with the transferrin receptor (TfR1) present on the plasma membrane,thereby leads to endocytosis of Tf-TfR1 complex (Fig 1.3). Upon acidification of the endosome the free iron is releases from the Tf complex. The released iron reduced to ferrous form and transported to the cytoplasm by the action of iron importer, DMT1. However, there are reports suggest that DMT1-independent iron transport from late endosomes and lysosomes to cytoplasm probably through a TRPML1 channel (Dong, Cheng *et al.,* 2008). The released iron can be assembled into Fe/S clusters for the maturation of cytosolic and nuclear proteins (Rouault 2006)) such as ribonucleotide reductase (Liu and Graslund 2000) or stored in the form of ferritin. The PCBP1 protein is involved in the storage of ferrous form of iron into ferritin (Shi, Bencze *et al.,* 2008). Free iron is also imported into mitochondria by mitochondrial importer, mitoferrin (Shaw, Cope *et al.,* 2006) and subsequently utilized in the formation of Fe/S clusters and heme.Mitochondria play a crucial role in iron metabolism as they are major iron consuming sub-cellular organelles in cells.

Further, surplus iron may also be exported from cytosol to plasma membrane by the action of ferroportin. Heme transporter, FLVCR, is involved in the transport of excess cytosolic heme to plasma membrane (Quigley, Yang *et al.,* 2004; Keel, Doty *et al.,* 2008). In cellular system, iron homeostasis is majorly regulated by two iron regulatory proteins known as IRP1 and IRP2 (Rouault 2006; Wallander, Leibold *et al.,* 2006).

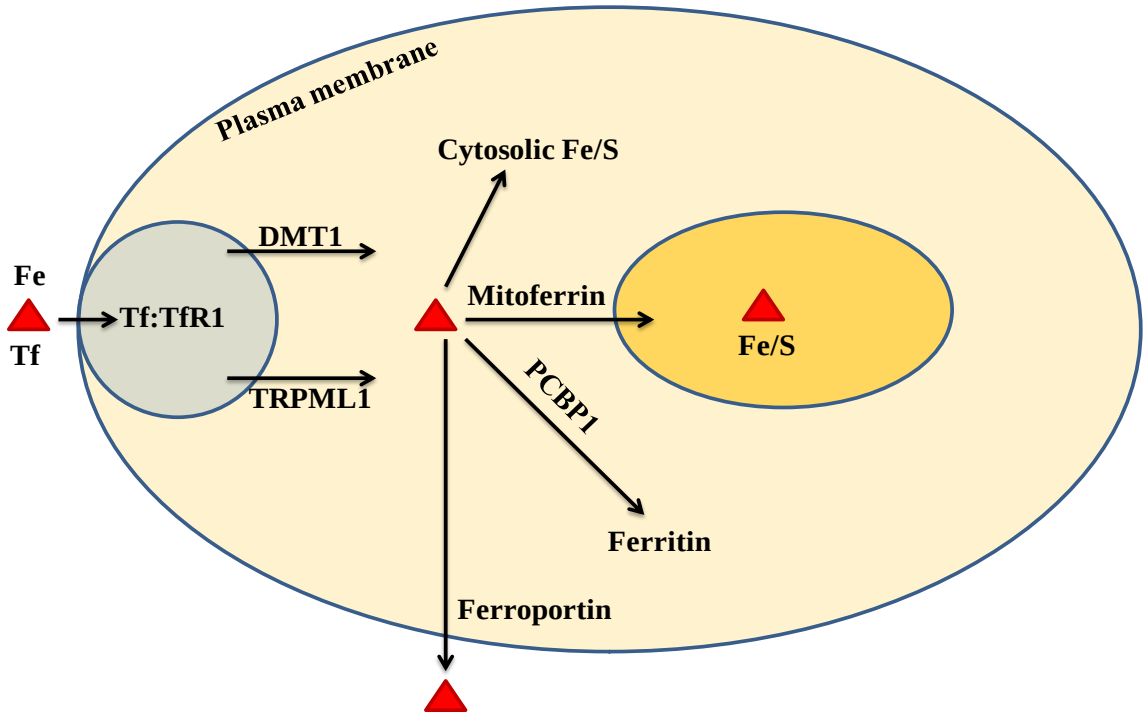

Figure 1.3. Mechanism of iron transport in human cells. Primarily, iron is bound to transferrin (Tf) in serum, which interacts with transferrin receptor 1 (TfR1) present on the cell membrane. This interaction leads to the formation of Tf-TfR1 complex and induces endocytosis. Iron releases from the Tf-TfR1 complex and exported to cytosol by DMT1 or TRPML1 upon endosome acidification. Cytosolic iron can be used by the cell in different ways such as it can be used to assemble Fe/S clusters in cytosol or it can transport into mitochondria throughthe mitoferrin (mitochondrial iron importer) or it can be stored in the form of ferritin with the help of PCBP1 chaperone or it can be exported by ferroportin. Imported iron is utilized in synthesis of Fe/S clusters and heme in the mitochondria.

1.6. Fe/S clusters

Iron is a component of Fe/S clusters, an ancient biological molecule that is essential for many fundamental processes including cellular respiration, electron transfer, redox catalysis, DNA replication, DNA repair and regulation of gene expression (Stephens, Jollie *et al.*, 1996; Beinert 2000; Ryter and Tyrrell 2000; Walden, Selezneva *et al.*, 2006; Boal, Yavin *et al.*, 2007; Netz, Stith *et al.*, 2012; Rouault 2012). They are evolutionarily ancient and are essentially present in all organisms including archea, bacteria, plants and animals. Initially, Fe/S clusterson proteins were discovered by Helmut Beinert and others in early 1960

(Beinert, Holm *et al.*, 1997; Rees and Howard 2003). The most common Fe/S clusters present in eukaryote proteins are 2Fe-2S and 4Fe-4S. These clusters are formed by tetrahydral coordination of iron atoms with sulphide and ligated to the protein through the cysteine residues (Fig 1.4).

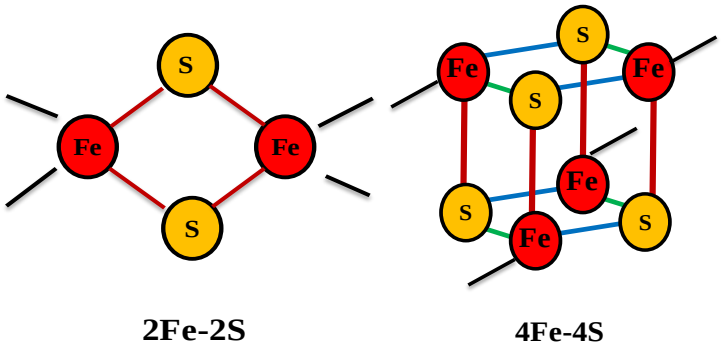

Figure 1.4. The structure of Fe/S clusters. The Fe/S clusters types that are most common are the 2Fe-2S and 4Fe-4S clusters. The clusters shown are colour coded by atom type: iron, red; sulfur, yellow; protein ligands are shown in black.

1.7. Fe/S cluster biogenesis

The pioneering research work on bacteria reveals that three different biosynthetic machineries are present to generate Fe/S proteins (Frazzon and Dean 2003). The first machinery, termed as nitrogen fixation (NIF) machinery, is dedicated to the assembly of the complex Fe/S protein nitrogenise. Nitrogenase is responsible for the conversion of N_2 to NH_3 in nitrogen fixing bacteria (Rees and Howard 2000; Frazzon and Dean 2002). The second machinery, iron sulfur cluster (ISC) assembly machinery which is majorly involved in the generation of cellular Fe/S proteins (Zheng, Cash *et al.*, 1998). The third machinery, SUF (sulphur-mobilization) machinery which is an independent system predominantly utilized under iron limiting or oxidative conditions (Fontecave, Choudens *et al.*, 2005; Johnson, Dean *et al.*, 2005). The mitochondria contain the components homologous to ISC machinery

whereas plastids contain the components homologous to SUF machinery of bacteria (Fig 1.5) (Lill and Kispal 2000; Balk and Lobreaux 2005).

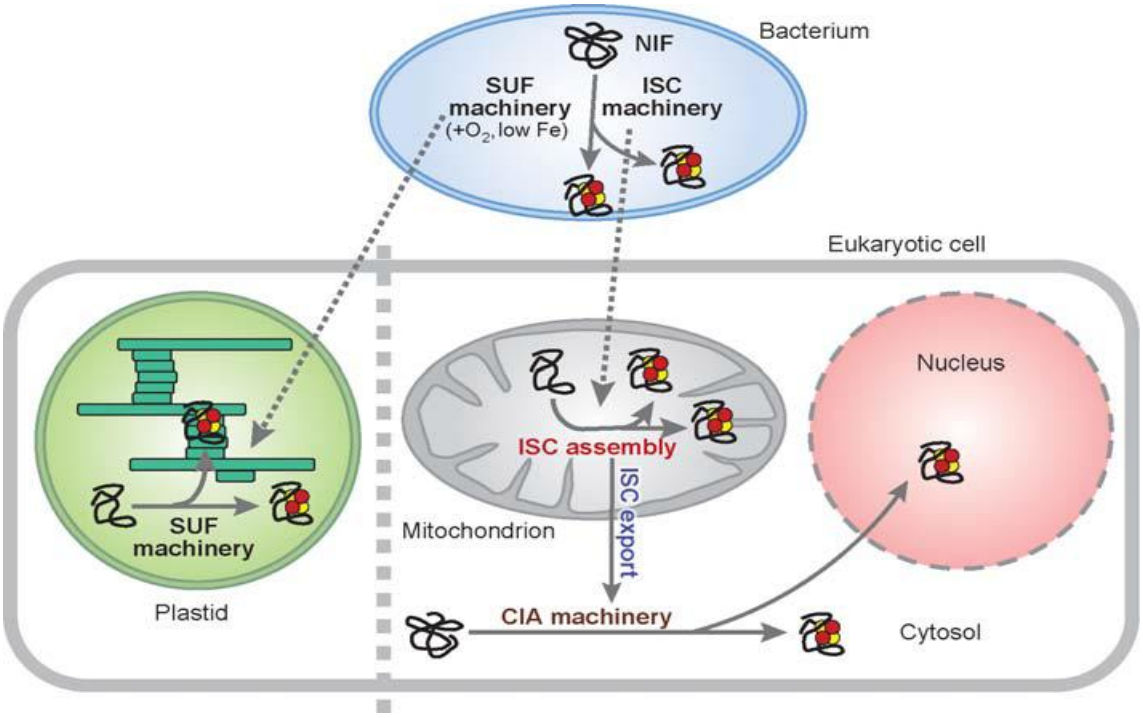

Figure1.5. Biogenesis& the evolutionary origin of Fe/S cluster proteins. In eukaryotes, Fe/S cluster proteins are present in mitochondria, cytosol and nucleus. The ISC assembly machinery of mitochondria was originated from the evolutionary ancestor,α-proteobacteria. The SUF machinery of plastids in plant cells may be transferred to the eukaryotic cell by endosymbiosis of a photosynthetic bacterium. The mitochondrial ISC assembly machinery,the ISC export system and the CIA machinery are required for the maturation of both cytosolic and nuclear Fe/S proteins. These three systems are highly conserved from lower to higher eukaryotes. The bacterial NIF machinery is principally required for the assembly of nitrogenase in bacteria. A small red and yellow circle denotes the Fe/S clusters. Adapted from Ronald Lill*et al.,,* 2006.

1.7.1. Role of Fe/S proteins in electron transfer

The Fe/S clusters possess redox properties and conducts electrons from one active site to the next. Several high molecular weight protein complexes and multi-protein electron transmit systemscontain Fe/S clusters to conduct electrons. Fe/S clusters present in respiratory chain complexes of mitochondria (ETC complex I, II and III)perform an electron transfer role. In humans, ETC complex I harbours eight iron sulfur clusters (Fe/S) with

diverse configurations. These Fe/S clusters together form a wire (Moser, Farid *et al.*, 2006) to transmitelectrons from NADH to ubiquinone through the complex I bound flavin group. Similar tocomplex I Fe/S clusters, the complex II clusters (Three) transmit electrons from the oxidation of succinate to ubiquinone. ETC complex II contains three different Fe/S clusters such as 2Fe-2S, 3Fe-4S and 4Fe-4S clusters. The third ETC complex, complex III, contains single Rieske type Fe/S cluster (2Fe-2S) and is coordinated by two cysteines and two histidine residues. The Rieske Fe/S protein is exposed towards the intermembrane space of mitochondria and accepts electrons from reduced ubiquinone through the cytochromes b and c1. Iron is also component of cytochrome c1 or b of respiratory chain complex III in the form of heme groups. Another Fe/S containing flavo-protein, a ubiquinone oxido-reductase conducts electrons to ubiquinone, and is required for the fatty acid oxidation (Ruzicka and Beinert 1975). A small mitochondrial matrix protein,adrenodoxin (Ferridoxin 1), that has a function in at least three biochemical pathways. One of the adrenodoxin roles is transferring electrons from NADPH to mitochondrial cytochrome P450 through its 2Fe-2S clusters for steroid biosynthesis. Other roles of adrenodoxin includes the conversion of heme b to heme a of cytochrome oxidase in concomitance with cox15 (Barros and Tzagoloff 2002) and the conversion of sulfide to reduced sulfur in the Fe/S protein biogenesis pathway (Muhlenhoff, Richhardt *et al.*, 2002).

1.7.2. Role of Fe/S proteins in metabolism

Aconitase is a Fe/S containing enzyme found in both the mitochondria and cytosol. The catalytically active form of mitochondrial aconitase, contains a 4Fe-4S cluster. In this cluster, three Fe atoms directly bind to the cysteines on the enzyme backbone and the fourth Fe is ligated to sulphur of the inactive 3Fe-4S cluster. This kind of Fe/S ligation provides a free coordination site and that is involved in the binding of substrates (Gardner and Fridovich

1992; Gardner 1997). In contrast, the cytosolic aconitase is a bifunctional enzyme with or without 4Fe-4S cluster. The holo form (4Fe-4S) has aconitase activity while the apo form (iron free) lacks enzymatic activity but involved in the regulation of intracellular iron levels. The apo form also known as iron regulatory protein (IRP1). A Lipoate synthase catalyses theproduction of lipoyl groups from octonoyl groups and it is belongs to the member of radical SAM (S-Adenosylmethionine) Fe/S cluster enzyme family. These enzymes bear two 4Fe-4S clusters and one of them involved in SAM dependent radical formation. The other Fe/S cluster present in Lipoate synthase acts as a source of sulfur in the formation of lipoic acid (Jarrett 2005).

In humans, there are three Fe/S cluster proteins that are involved in the nucleotide metabolism. Dihydropyrimidine dehydrogenase (DPYD) harbour four 4Fe-4S clusters that serves as a conduit for electron transport between the flavin adenine dinucleotide (FAD) and flavin mononucleotide (FMN) groups of the enzyme (Schnackerz, Dobritzsch *et al.,* 2004). This enzyme is involved in the catalyses of first and rate limiting step in pyrimidine degradation. The phosphoribosyl pyrophosphate amidotransferase (PPAT); also known as glutamate phosphoribosyl pyrophosphate amidotransferase, is involved in the catalysis of the committed and rate limiting step of purine biosynthesis and it contains a single 4Fe-4S cluster. Interestingly, Fe/S cluster associated with GPAT in *Bacillus subtilise*seems to be vital for both structural stability and amino terminal processing of the protein but does not appears to have a direct role in the enzymatic reaction (Makaroff, Paluh *et al.,* 1986; Grandoni, Switzer *et al.,* 1989). The prerequisite of Fe/S cluster incorporation into GPAT for protein stability has also been shown in human cell cultures.

1.7.3. Role of Fe/S proteins in iron metabolism

Iron sulfur clusters (Fe/S) and Heme represent the wide range of functional iron within the cell. However, the synthesis and abundance of these cofactors is tightly linked with the cellular uptake and distribution of iron. The enzyme ferrochelatase (FC) present in mitochondriathat catalysisthe insertion of ferrous iron into protoporphyrin IX in the final step of heme biosynthesis. Ferrochelatase contains a C-terminal 2Fe-2S cluster (Dailey 2002) cluster that is critical for ferrochelatase enzyme activity in humans. However, the precise role of Fe/S cluster in the enzymatic activity has not been elucidated (Shepherd, Dailey *et al.,* 2006). Further, the faithfulconnection between cellular iron metabolism and Fe/S cluster biogenesis is symbolized by the function of iron regulatory protein 1 (IRP1). It is a 4Fe-4S cluster containing protein and serves as a sensor for availability of cellular iron. In the absence of Fe/S cluster in IRP1, it becomes an active post-transcriptional regulator by binding to iron responsive elements (IREs) on several mRNAs that are involved in iron metabolism. For example, IRP1-IRE binding up regulates cellular iron uptake by stabilising transferrin receptor (TfR) mRNA and down regulates iron storage by occluding translation of ferritin (Ft) mRNA (Hentze, Muckenthaler *et al.,* 2004; Rouault 2006; Wallander, Leibold *et al.,* 2006). Thus the binding activity of IRP1 to IRE on mRNAs is inversely linked Fe/S cluster biogenesis activity. Indeed, several recent reports shows that perturbation of Fe/S cluster biogenesis pathway results in an enhanced IRE binding activity of IRP1 and consequently increased levels of transferrin receptor (Tf) (Stehling, Elsasser *et al.,* 2004; Biederbick, Stehling *et al.,* 2006; Song and Lee 2008; Stehling, Netz *et al.,* 2008).

1.7.4. Mechanism of Fe/S Cluster Assembly (ISC)

Under anaerobic conditions, iron sulfur clusters (Fe/S) can form extemporaneously from ferrous iron and sulfide. In a living cell, however, Fe/S cluster formation on proteins is catalysed by a variety of complex biosynthetic machineries thatpermit for the proper maturation of particularnascent target proteins. Iron sulfur cluster (ISC) assembly machinery is a fundamentalcomponent for the maturation of all Fe/S proteins present in non-green eukaryotic cells. In eukaryotes, the Fe/S cluster assembly (ISC) occurs in the mitochondria (Napier, Ponka *et al.,* 2005; Lill and Muhlenhoff 2008).This machinery not only required for the assembly of Fe/S clusters proteins present in the mitochondria but also involved in the maturation of non mitochondrial Fe/S proteins (Cytosolic and Nuclear Fe/S cluster proteins) by means of the ISC export machinery. Studies in yeast, zebra fish and plantshave shown that upto 20 different proteins are involved in Fe/S cluster biogenesis (Table1.1). The ISC system is required for maturation and functioning of mitochondrial Fe/S containing enzymes (Rouault 2012). The components required for the ISC system are present in the mitochondrial matrix. The iron sulfur cluster (ISC) assembly machinery can be subdivide into (i) the synthesis of a transient Fe/S cluster on a conserved dimeric scaffolding protein, ISCU and (ii) the transfer of Fe/S cluster from ISCU to the functional Fe/S cluster target proteins.

Table 1.1. Iron Sulfur Cluster (Fe/S) assembly components in eukaryotes

Protein	Full name	*Sc*homolog[a]	Localization	Function
Iron Sulfur Cluster Assebly Machinery				
NFS1	Cysteine desulfurase	Nfs1	Mitochondrial matrix, nucleus	Sulfur donor
ISD11	LYR motif containing 4	Isd11	Mitochondrial matrix, nucleus	In complex with Nfs1
FDXR*	Ferredoxinreductase	Arh1	Mitochondrial matrix, inner membrane	Ferredoxin-$NADP^+$reductase
FDX1*	Ferredoxin	Yah1	Mitochondrial matrix	Electron transport
FDX1L*	Ferredoxin-like	Yah1	Mitochondrial matrix	Electron transport
MFRN1	Mitoferrin 1	Mrs3, Mrs4	Mitochondrial inner membrane	Iron transport
MFRN2	Mitoferrin 2	Mrs3, Mrs4	Mitochondrial inner membrane	Iron transport
FXN	Frataxin	Yfh1	Mitochondrial matrix, cytosol (?)	Iron binding and delivery
ISCU	Fe/S cluster scaffold homolog	Isu1, Isu2	Mitochondrial matrix, cytosol	Scaffold
NFU*	Scaffold protein	Nfu1	Mitochondrial matrix, cytosol	Alternative scaffold protein (?)
GLRX5	Glutaredoxin 5	Grx5	Mitochondrial matrix	Cluster transfer
Grp75*	Heat shock 70 kDA protein 9	Ssq9	Mitochondrial matrix, cytosol (?)	Cluster transfer
HSCB*	HscB Fe/S cluster co-chaperon homolog	Jac1	Mitochondrial matrix	Cluster transfer
GrpE-L1/2*	GrpE like1/2	Mge1	Mitochondrial matrix	Cluster transfer
Ind1	Fe/S protein required NADH dehydrogenase	-	Mitochondrial matrix	Maturation of respiratory complex 1
ISCA1, ISCA2*	Fe/S cluster assembly 1/2 homolog	Isa1, Isa2	Mitochondrial matrix	Maturation of radical SAM dependent proteins and aconitase
IBA57	Fe/S cluster assembly factor for biotin synthase and aconitase like mitochondrial proteins with a mass of 57 kDa	Iba57	Mitochondrial matrix	Maturation of radical SSAM dependent proteins and aconitase
Iron Sulfur Export Machinery				

ABCB7	ABC-binding cassette transporter, subfamily B, member 7	Atm1	Mitochondrial inner membrane	Translocation of a sulphur compound to the cia machinery
ALR*	Augmenter of liver regeneration	Erv1	Mitochondrial inter membrane space	?
GSH*	Glutathione	GSH	Mitochondria, cytosol	?
Cytosolic Iron Sulfur Cluster Machinery				
NBP35	Nucleotide binding protein 1	Nbp35	Cytosol	Scaffold
CFD1	Nucleotide binding protein 2	Cfd1	Cytosol	Scaffold
IOP1	Nuclear prelamin A recognition factor like	Nar1	Cytosol, Nucleus	Cluster transfer
CIAO1	Cytosolic Fe/S protein assembl 1 homolog	Cia1	Cytosol, Nucleus	Docking platform, Cluster transfer
CIAPIN1*	Cytokine induced apoptosis inhibitor 1	Dre2	Cytosol, Mitochondrial intermembrane space (?)	(?)

[a]*Saccharomyces cerevisiae*, *Prediction, based on homology and/or functional studies. Adapted from Sheftel*et al.,,* 2010.

The initial step of Fe/S cluster biogenesis is accomplished by a multimeric protein complex which contains a core dimeric cysteine desulfurase (called IscS in *Escherichia coli*, Nfs1 in *S. cerevisiae* or NFS1 in mammals) and two monomers of a dedicated scaffold proteins (IscU in bacteria, Isu1 or Isu2 in yeast and ISCU in humans) (Fig 1.6.A). The two monomers of scaffold protein bind at either end of the complex (Shi, Proteau *et al.*, 2010). The NFS1 removes sulphur from cysteine amino acid and supplies to the ISCU. The ISCU provides a back bone structure of cysteine ligands on which a new cluster consisting of covalently bound iron and inorganic sulphur is synthesized (Bandyopadhyay, Chandramouli *et al.*, 2008; Raulfs, O'Carroll *et al.*, 2008; Lill 2009; Py and Barras 2010). Pyridoxal phosphate acts as cofactor for NFS1enzyme activity. In contrast to sulphur, the source of the iron for the nascent Fe/S cluster has not been clearly identified. Several reports suggest that the iron is

probably obtained from frataxin, (Stemmler, Lesuisse *et al.,* 2010) or from a complex containing glutathione and glutaredoxin that harbor's a Fe/S cluster (Qi and Cowan 2011). However, the structural modelling suggests that frataxin binds to a pocket like region in between NFS1 and ISCU. This model suggests that frataxin might be involved in either repression or stabilization or enhancing the activity of the core complex of Fe/S cluster biogenesis machinery (Prischi, Konarev *et al.,* 2010; Tsai and Barondeau 2010; Schmucker, Martelli *et al.,* 2011).

In eukaryotes the stability of cysteine desulfurase depends on its binding to a small partner protein called ISD11 (Adam, Bornhovd *et al.,* 2006; Wiedemann, Urzica *et al.,* 2006). ISD11 apparently became an indispensable binding partner for the eukaryotic cysteine desulfurase probably early in the evolution of eukaryotes (Richards and van der Giezen 2006). Isd11 is found in the mitochondrial matrix of *S. Cerevisiae*. However, ISD11 has been detected in mitochondrial matrix, cytosol and nuclear compartments in mammalian cells (Shi, Ghosh *et al.,* 2009). After the formation of a new Fe/S cluster on the core complex (composed of NFS1, ISD11, frataxin and ISCU in mammals) (Tsai and Barondeau 2010; Bridwell-Rabb, Winn *et al.,* 2011; Schmucker, Martelli *et al.,* 2011), the Fe/S cluster must be transferred to recipient proteins. Although many details of Fe/S cluster transfer process remains to be identified, several reports indicate that a highly conserved chaperone and co-chaperone system participates in the transfer of Fe/S cluster from core complex to target protein. A co-chaperone known as HSC20 in mammalian cells (Uhrigshardt, Singh *et al.,* 2010), HscB in bacteria (Vickery and Cupp-Vickery 2007) and Jac1 in *S. cerevisiae*(Craig and Marszalek 2002) binds to ISCU. In bacteria, co-chaperone HscB has been shown to form a complex with chaperone, HscA (in yeast Ssq1) a member of the HSP70 heat shock protein family and IscU. The homologue of Ssq1 has not been yet identified in mammalian cells. Recent studies

suggest that highly conserved residues in a hydrophobic region in the C-terminal portion of HscB are important to bind IscU (Fuzery, Oh *et al.*, 2011). Together, HscA (HSC70) and HscB (HSC20) might facilitate Fe/S cluster transfer from ISCU to target apo-proteins or to other secondary scaffolds protein complex (Vickery and Cupp-Vickery 2007; Bonomi, Iametti *et al.*, 2011). The question that remains to be answered is how the proteins are identified as apo-proteins for transfer of Fe/S as this process is highly selective and depends on specific interactions between apo-protein and binding sites on the chaperone-co-chaperone complex.

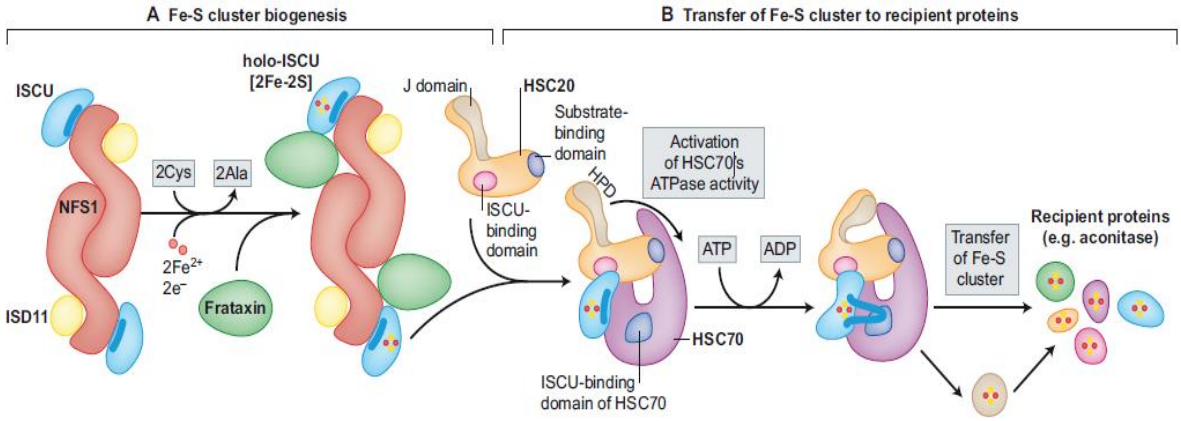

Figure 1.6.A. The mechanism of Fe/S clusters biogenesis in mammalian cells. (A). The dimeric cysteine desulfurase (NFS1) binds with the primary scaffold protein ISCU monomers of the complex. ISD11 is an obligate binding partner for NFS1 in eukaryotes. Frataxin donates Fe to the Fe/S scaffolding complex. NFS1 serves as inorganic sulfur donor to the nascent Fe/S cluster, and cysteines from ISCU contribute the sulfur that to the Fe/S cluster. (B). Following synthesis of the Fe/S cluster in mitochondrial matrix, it must be bringing to target proteins. A devoted chaperone-co-chaperone pair of proteins involved in theFe/S cluster transfer from ISCU, the primary scaffold protein, to the target Fe/S proteins. HSC20, a co-chaperone binds with primary scaffold protein ISCU and forms the HSC20-ISCU complex, and then probably it binds to its chaperone HSC70. This interaction leads to the activation of HSC70, and further conformational change is occurring in the substrate-binding domain of HSC70 that facilitates donation of its Fe/S cluster to target proteins. Adapted from Rouault *et al.*,, 2012.

Since Fe/S clusters are readily prone to oxidation, the biogenesis and transfer processes systems might have evolved to protect and hide newly synthesized Fe/S clusters. Studies on

the bacterial system suggest that it is likely that binding of human HSC20 protects the nascent iron sulfur cluster (Fe/S) on ISCU. Further, the energy released by ATPase activity of HSP70 induces a conformational change in the multi-subunit complex that might facilitate the protected transfer of Fe/S cluster from ISCU to recipient apo-proteins or to secondary scaffold proteins. From the secondary scaffold proteins, Fe/S may deliver to the defined group of recipient proteins. It is likely that apo-protein may be tethered to the chaperone-co-chaperone complex so that the release of Fe/S cluster from ISCU is coupled to acquisition of Fe/S cluster by apo-protein.

1.7.5. Iron sulfur cluster (Fe/S)assembly machinery in the cytosol and nucleus (CIA)

In mammalian system, the mechanism of Fe/S cluster protein assembly outside the mitochondria is beginning to be understood. In mammalian cells, a few of the ISC assembly machinery components such as NFS1 (Li, Tong *et al.*, 2006), ISD11 (Shi, Ghosh *et al.*, 2009) and frataxin (Acquaviva, De Biase *et al.*, 2005) are additionally localized in cytosol and nucleus besides in the mitochondrial matrix providing hints to the existence of a possible duplicate machinery of mitochondrial ISC in the cytosol/nucleus (Rouault and Tong 2005; Tong and Rouault 2006). However, there is no functional data available as yet to assist this hypothesis. In contrast, studies on both yeast and mammalian tissue culture models have identified a cytosolic Fe/S protein assembly (CIA) machinery that is dedicated to maturation of Fe/S proteins present in the cytosol and nucleus (Lill and Muhlenhoff 2008). The initial step in cytosolic-nuclear Fe/S protein assembly comprises the transient assembly of a Fe/S cluster on a scaffold complex formed by two soluble P-loop NTPases, CFD1 and NBP35. CFD1 and NBP35are themselves Fe/S proteins and related to the mitochondrial Ind1 (Netz, Pierik *et al.*, 2007; Stehling, Netz *et al.*, 2008) (Fig 1.6.B). The second step of non mitochondrial Fe/S protein biogenesis involves the cytosolic factors like IOP1 (Song and Lee

2008) and CIAO1 (Srinivasan, Netz *et al.*, 2007) which are homologous to the yeast proteins Nar1 (Balk, Pierik *et al.*, 2004) and Cia1 (Balk and Lobreaux 2005). Studies on yeast show that the assembly of endogenous Fe/S clusters on Nar1 requires both Cfd1 and Nbp35 function whereas Nar1 does not require for the assembly of Fe/S on Cfd1 and Nbp35. These evidences suggest that Nar1 and Cia1 are involved in later stages of Fe/S biogenesis (e.g. transfer Fe/S cluster to target proteins). Recently the role of yeast Dre2 as a CIA factor has been reported (Zhang, Lyver *et al.*, 2008). Nevertheless, the number of protein components required for CIA assembly machinery and its mechanistic details is not yet understood in detail.

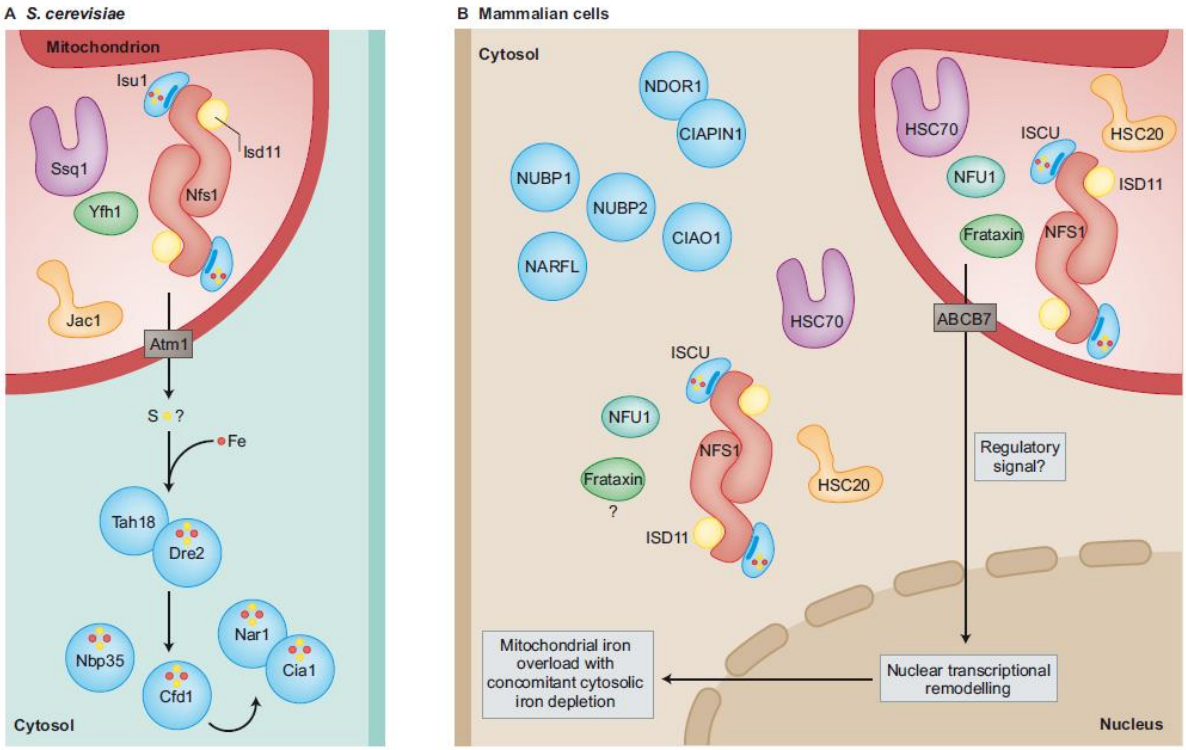

Figure 1.6.B. The differences in cytosolic Fe/S cluster proteins in *S. cerevisiae* versus mammalian cells.(A). In Yeast, mitochondria contain the basic Fe/S cluster biogenesis proteins, whereas cytosolic Fe/S cluster biogenesisdepends on the export of sulfur from mitochondria via the Atm1 transporter (ABCB7 in humans). Further biogenesis of cytosolic Fe/S cluster proteins depends on thedifferent set of proteins, including Tah18, Dre2, Nbp35, Cfd1, Nar1 and Cia1.These proteinscollectively called as cytosolic iron-sulfur assembly (CIA) proteins. (B). In contrast, most of the mammalian basic Fe/S cluster biogenesis proteins are expressed in mitochondria as well as in the

cytosolic and/or nuclear compartment. In addition, there are human counterparts to the proteins implicated in cytosolic Fe/S cluster biogenesis in yeast, including NDOR1 (homolog of Tah18), CIAPIN1, (homolog of Dre2), NUBP1 and NUBP2 (homologs of Nbp35 and Cfd1, respectively), and NARFL and CIAO1 (homologs of Nar1 and Cia1, respectively). Adapted from Rouault *et al.,,* 2012.

1.8. Medical Impact

The Fe/S cluster biogenesis pathway is fundamental for many cellular processes. Iron/Sulfur proteins are required for the function of citric acid cycle enzymes like succinate dehydrogenase and aconitase. All Fe/S proteins are also required for the function of respiratory chain complexes, I-III and number of protein functions in the mitochondria, cytosol and nucleus. Thus, it is not surprising that defects in Fe/S cluster biogenesis causes several human disorders. However, the disease phenotype with correlates with the protein factor that is defective in Fe/S biogenesis pathway (Table 1.2). For example, distinctly reduced expression of frataxin causes FRDA (Friedreich's ataxia) a neurodegenerative disease that is characterized by cardiac failure and death of specific neuronal cell types (Martelli, Napierala *et al.,* 2012). In contrast, ISCU myopathy, a disease resulting from a splicing mutation in ISCU gene affects skeletal muscles extensively and rarely has any cardiac effects (Kollberg, Tulinius *et al.,* 2009). Thus far, there has been no clear explanation as why these two diseases differ so dramatically in the choice of tissue while the main defect has been attributed to the derailment of the biogenesis of the iron sulfur cluster. The GLRX5 is required for efficient erythropoiesis in humans (Glutaredoxin5). Mutation in GLRX5 leads to a sideroblastic anaemia and the disease symptoms include microcytic anaemia, severe iron load and the presence of ring sideroblasts(Nordin, Larsson *et al.,* 2012).

Mutations in NUBPL, a chaperone required for the maturation of Complex I proteins, have been reported to cause mitochondrial encephalomyopathy, a severe multisystem infantile

disease. The diseases caused by defects in Fe/S cluster biogenesis has been mentioned in the Table 1.2.

Table 1.2. Diseases caused by defects in Fe/S cluster biogenesis

Disease	Cause	Clinical phenotype and incidence	Tissues affected
Friedreich's ataxia (FRDA)	Decreased expression of frataxin due to expansion of intronic GAA repeat	Ataxia, loss of sensation in extremities, heart failure; incidence: 1/50,000 births	Primerly affects dorsal root ganglia, cerebellum and heart
GLRX5 deficient sideroblasticanemea	Low expression of GLRX5 due to mis splicing	Sideroblasticanemia	Red blood cells
ISCU myopathy	Splicing defect in ISCU that diminishes expression	Exercise induced lactic acidosis and muscle weakness	Skeletal muscle and heart
Mitochondrial encephalomyopathy	Mutations in NUBPL impair the function of respiratory complex I	Developmental delay, myopathy ataxia	Neurons, skeletal muscle
Multiple mitochondrial dysfunctions syndrome (NFU type)	Mis-splicing of the NFU1, causes reduced expression	Weakness, lethargy progressing to death at 4 weeks of age, lactic acidosis, elevated blood levels of branched chain amino acids and glycine	No tissue specificity, possibly because of early onset severe systemic illness
Multiple mitochondrial dysfunctions syndrome (BOLA type)	Single exonic base pair duplication leads to frame shift and a premature stop codon in BOLA3	Hyper glycinemia, acidosis, dilated cardiomyopathy, epileptic encephalo myopathy, death at 11 months of age	Majorly affects central nervous system and heart

Adapted from Rouault *et al.*,, 2012.

1.9. Scope of the present study investigation

The ISC assembly machinery is required for the maturation and functioning of mitochondrial Fe/S cluster containing enzymes(Stehling, Elsasser *et al.*, 2004). In addition, the ISC machinery of mitochondria is also required for maturation of cytosolic or nuclear Fe/S cluster containing proteins (Kispal, Csere *et al.*, 1999; Muhlenhoff, Balk *et al.*, 2004). It has also been shown that mitochondria possess a Fe/S export system (Fig 1.7). However, the

precise component that is exported from the mitochondria for the maturation of non-mitochondrial Fe/S containing proteins is not known.

The central component of the Fe/S cluster export system in mammalian mitochondria is ABCB7 (Atm1 in yeast), a member of the ABC family (Kispal, Csere *et al.,* 1997; Kispal, Csere *et al.,* 1999). ABCB7 has been found to be present in the inner membrane of the mitochondria (Csere, Lill *et al.,* 1998). Systemic knock out of ABCB7 in mice has been found to be embryonically lethal. RNAi induced depletion of ABCB7 in human cell lines causes severe impairment in the maturation of cytosolic Fe/S cluster proteins while mitochondrial Fe/S proteins remain virtually unaffected (Pondarre, Antiochos *et al.,* 2006; Cavadini, Biasiotto *et al.,* 2007). A similar kind of phenotype has been observed in yeast when *ATM1* is depleted (Kispal, Csere *et al.,* 1999). This includes accumulation of iron in the mitochondria and defects in the maturation of cytosolic Fe/S cluster containing proteins. Reports suggest that Atm1 is required for the export of sulphur to cytosol. However, the exact component that is exported by Atm1 and the export mechanism are not known. Besides Atm1 additional components have also been implicated with potential roles in the export of mitochondrial Fe/S clusters. These include Erv1, a sulfahydral oxidase and glutathione as depletion of these components result in a phenotype similar to that of *ATM1* deficiency (Lange, Lisowsky *et al.,* 2001; Sipos, Lange *et al.,* 2002).

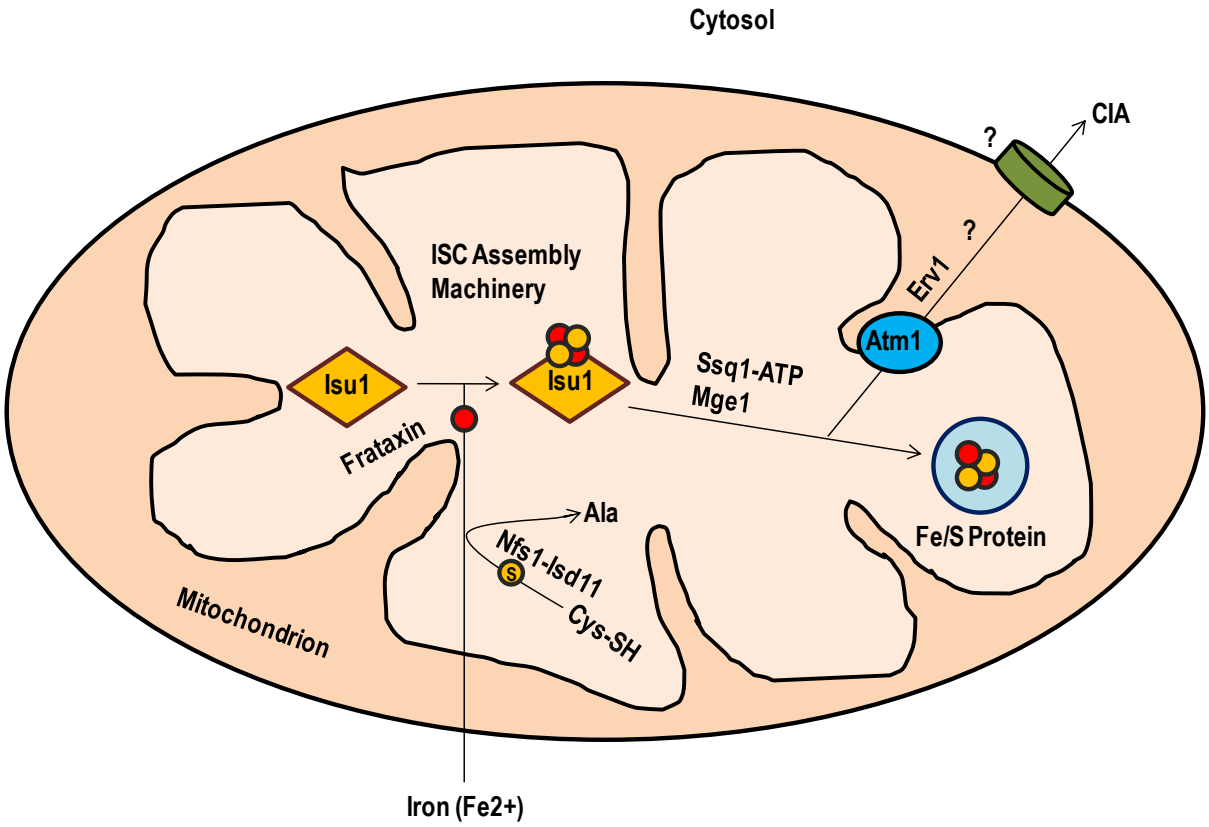

Figure 1.7. Current model for Fe/S cluster biogenesis in eukaryotes. The Fe/S clusters are synthesised in mitochondrial matrix by the ISC machinery. Extra-mitochondrial Fe/S cluster proteins depend on the mitochondrial ISC assembly and also on the ISC export machinery for their maturation and function. Previous studies suggested that the yeast Atm1 is involved in the export of Fe/S clusters across the inner membrane of mitochondria. However, it is not known that how these Fe/S clusters are exported to the cytosol across the IMS and outer membrane of mitochondria.

It has been shown by Daithankar, Farrell *et al.*, 2009that recombinant human MIA40 contains Fe/S cluster. A recent study by Spiller, Ang *et al.*, 2013, confirms that yeast Mia40 is indeed a 2Fe-2S containing protein. It was assumed that Fe/S cluster present in yeast or human MIA40 is probably required for its oxido-reductase activity (Spiller, Ang *et al.*, 2013). However, the precise functional and physiological significance of this Fe/S cluster in Mia40 is not known. Curiously, both Erv1 and Mia40 contain Fe/S clusters and both are present in the inter membrane space of mitochondria. Given that Erv1 has already been implicated in the export of Fe/S cluster, we hypothesized that human MIA40 may also be a component of

Fe/S export machinery of mitochondria. Testing this hypothesis, we find that human MIA40 is indeed involved in the cellular iron homeostasisand contains 4Fe-4S and 2Fe-2S clusters.

MIA40 being an inter membrane space protein, must act in concert with an outer membrane transporter to export Fe/S across outer membrane. To find out the downstream effectors of MIA40, we screened several mitochondrial outer membrane proteins for the presence of characteristic Fe/S binding cysteine motifs. Interestingly, we found characteristic cysteine motifs (CXC, CX_9C and CX_3C) in the outer mitochondrial protein import channel protein TOM40. **It is likely that mammalian TOM40 contains Fe/S cluster and probably is also involved in iron homeostasis of the cell.**

Tom40 is a channel forming central protein component of the TOM complex.Tom40 is an integral membrane protein with a β-barrel structure thatforms a channel for the translocation of pre-proteins across the outermembrane(Ahting, Thieffry *et al.*, 2001). Based on the above rationale, the objectives of the present study are as follows:

1. Characterization of human MIA40 function in iron homeostasis of the cell.
2. Characterization of human TOM40 as a Fe/S protein and its role in iron homeostasis of the cell.

CHAPTER II

Characterization of human MIA40 function in iron homeostasis of the cell

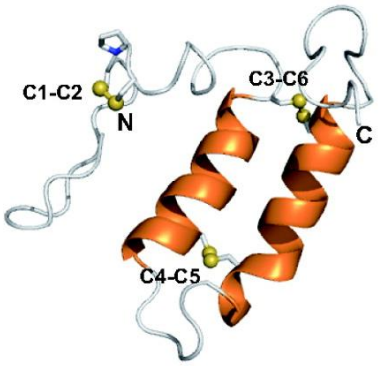

Kawano S et al. PNAS 2009

2.1. Introduction

Mia40 is a nuclear encoded 18 kDa mitochondrial intermembrane space protein. Mia40 harbours six conserved cysteine residues (C1-C6) that are clustered in the form of one CPC (C1 and C2) and two CX_9C motifs (C3-C6) (Fig 2.1). The CPC motif of Mia40 is redox sensitive. Initially, Mia40 is identified as a protein import component of IMS targeted proteins. Oxidized CPC motif in Mia40 is involved in the formation of transient disulfide mediated intermediates with free cysteine thiol motifs of intermembrane space targeted proteins. Subsequently, Mia40 draws the electrons from the precursor protein and becomes reduced. These events eventually promote the disulfide mediated oxidative folding and import of IMS targeted precursor proteins. Further, the reduced form of twin cysteine motif containing IMS precursor proteins can coordinate with metal ions like zinc (Lutz, Neupert *et al.,* 2003; Morgan, Ang *et al.,* 2009). During the oxidative folding process in the IMS these precursor proteins can pass their zinc ions to Mia40 and form complexes with Zn (Terziyska, Lutz *et al.,* 2005). The CX_9C motifs in Mia40 are involved in creating intra-molecular disulphide bonds for stabilizing the structure (Banci, Bertini *et al.,* 2009; Terziyska, Grumbt *et al.,* 2009).However, the reduced CPC motif in Mia40 must be re-oxidized to participate in another round of import cycle. The reduced form of Mia40 is re-oxidized by transferring electrons to Erv1, a FAD containing sulfahydral oxidase present in IMS (Fig 2.2) (Mesecke, Terziyska *et al.,* 2005). Erv1 is maintained in oxidative state by transferring electrons to molecular oxygen through cytochrome c coupled complex IV of electron transport chain.

The Erv1-Mia40 disulfide mediated oxidative folding of IMS proteins has been very well characterized from yeast to humans. Human MIA40 (CHCHD), a homologue of yeast Mia40 contain similar cysteine motifs and involved in the import of intermembrane space targeted proteins (Hofmann, Rothbauer *et al.,* 2005).However, yeast Mia40 is stably anchored

to the inner membrane of mitochondria through its N-terminal hydrophobic domain while the core domain is exposed to the intermembrane space, whereas human MIA40 lacks a trans-membrane domain and is present in the inter membrane space of mitochondria.

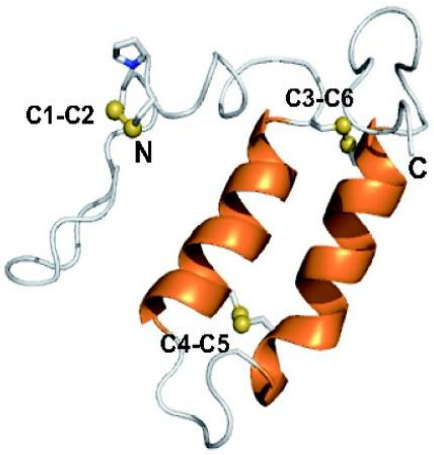

Figure 2.1. Structure of Mia40 (CHCHD4). The crystal structure of Mia40 has shown in ribbon form. The S atoms of cysteine in the three disulfide bonds showed as yellow colour spheres. Adapted from Kawano *et al.,,* 2009.

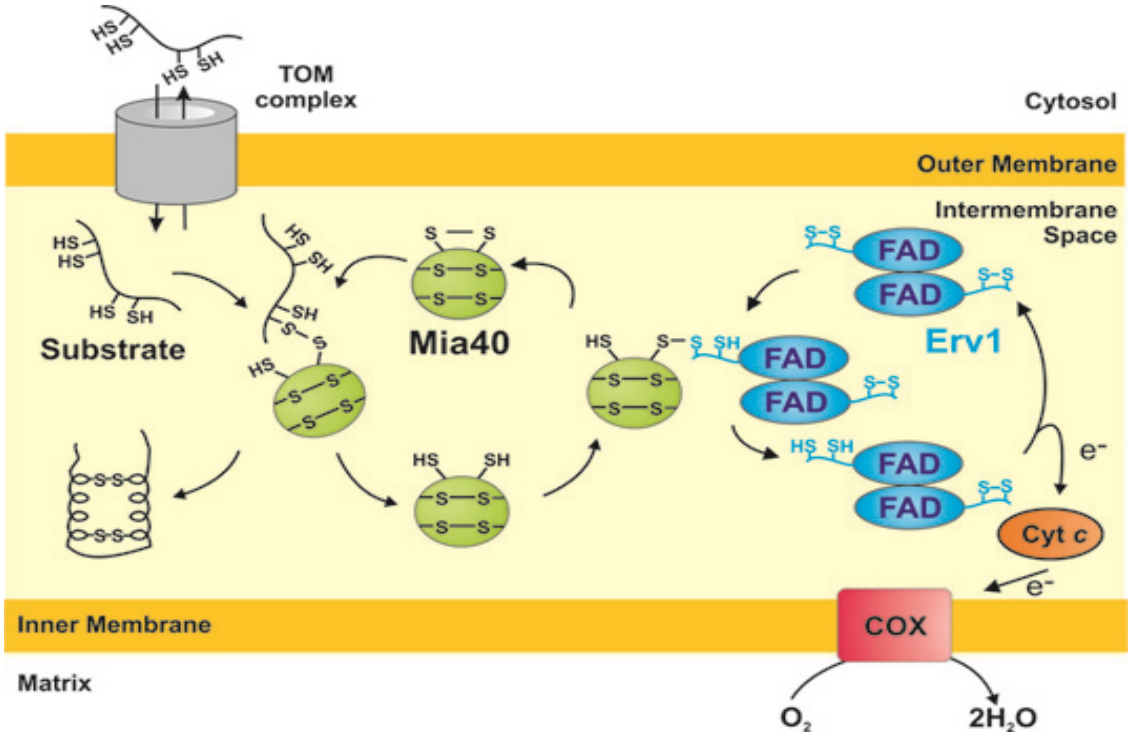

Figure 2.2. Model of the Mia40-Erv1 disulfide relay system. Schematic representation of the protein import into intermembrane space (IMS) of mitochondria. The oxidised active state of Mia40 interact with newly imported precursor proteins by inter molecular disulfide bonds and subsequently the substrate proteins getting into folded state. For the next cycle of protein import, Mia40 interacts directly with sulfhydryl oxidase Erv1 and converted into active oxidised Mia40. The sulfhydryl oxidase Erv1 is a dimeric FAD binding protein that maintains an oxidised state by the use of molecular oxygen as final electron acceptor. Adapted from Hell *et al.,,* 2008.

Mitochondria play an essential role for the maturation of cytosolic and nuclear proteins that contain Fe/S clusters (Kispal, Csere *et al.*, 1999; Muhlenhoff, Balk *et al.*, 2004). Atm1, an inner membrane protein of yeast mitochondria and its mammalian homolog ABCB7, has been identified as component of iron sulphur export machinery of mitochondria (Leighton and Schatz 1995; Kispal, Csere *et al.*, 1997; Kispal, Csere *et al.*, 1999). The phenotype that is associated with deficiency of Atm1 includes accumulation of iron in mitochondria and defects in maturation of cytosolic proteins that contain Fe/S clusters. Although there are reports suggesting that it may be exporting sulfur to cytosol, the exact component that is exported by Atm1 and the export mechanism are not known (Lill 2009; Netz, Stumpfig *et al.*, 2010). Besides Atm1, additional components have also been implicated in the Fe/S export machinery of mitochondria. These include Erv1, a sulfahydral oxidase and glutathione as depletion of these components result in a phenotype similar to that of Atm1 deletion (Lange, Lisowsky *et al.*, 2001; Sipos, Lange *et al.*, 2002). It has been assumed the Fe/S cluster is required for the oxido-reductase activity of both human and yeast Mia40. However, the precise physiological significance of Fe/S cluster in Mia40 and the role of this cluster in its function remain unknown.

Curiously, both Erv1 and MIA40 contain Fe/S clusters and both are present in the intermembrane space of mitochondria. Given that Erv1 has already been implicated in the export of Fe/S cluster, we hypothesized that MIA40 may also be a component of Fe/S export machinery of mitochondria. To understand the role of human MIA40, if any, in Fe/S cluster

export machinery of mitochondria and to determine the physiological role of Fe/S clusters present in hMIA40, the present study was, therefore, undertaken with the following objectives: (i) Cloning, expression and purification of recombinant hMIA40 (ii) Identification of hMIA40 as an Fe/S protein and (iii) Role of hMIA40 in cellular iron metabolism.

2.2. Materials and Methods

2.2.1. Materials

Bathophenonthroline was purchased from sigma Aldrich to measure the mitochondrial non-heme iron. Xanthine, isocitrate and decylubiquinone substrates were purchased from sigma Aldrich to measure the xanthine oxidase, cytosolic aconitase and mitochondrial complex I activity respectively. Radiolabel ^{55}Fe was purchased from American Radio Chemicals (USA) for measuring the iron uptake. Mouse polyclonal GPAT (Glutamate phosphoribosyl pyrophosphate amido transferse), aconitase, Hsp70, GAPDH (Glyceraldehyde-3-phosphate dehydrogenase) antibodies were purchased from abcam (USA). For the silencing of human MIA40, shRNA specific for Mia40 was purchased from ORIGENE. All reagents and chemicals used in the study were of high purity and purchased from either Hi-Media or Sigma.

2.2.2. Methods

2.2.2.A. Cloning of human MIA40

2.2.2.A.1. cDNA synthesis

HeLa cell total RNA (3 µg) (Bangalore GeNei) was used to clone the *MIA40* gene. In brief, the following components were added in the following order:

1.3 µg of total RNA

1 µl of random hexamer primer

8 µl of DEPC water

The contents were mixed and incubated at 65 ^{0}C for 10 min.

Then the reaction was chilled on ice and the following components were added: 4 µl of 5X Reaction buffer, 1 µl of RNase Inhibitor, 2 µl of 10 mM dNTP Mix and 2 µl of M-MuLV

Reverse Transcriptase. A total volume of 20 µl of reaction mixture was mixed and incubated at room temperature for 2 min followed by 60 min incubation at 37 ^{0}C. Finally, the reaction was terminated by heating at 95 ^{0}C for 2 min.

2.2.2.A.2. Polymerase Chain Reaction (PCR)

The*hMIA40* ORF was amplified by polymerase chain reaction using HeLa cells cDNA as a template. PCR was carried out in a final volume of 50 µl. The reaction mixture contains 10 pM of each forward primer NB73 Fwp: 5'CCCAG▾AATT▴CACC ATGTCCTATTGCCGGCAGGAA 3'- (*E.CoR1*) and reverse primer NB74 Revp: 5'CCAC▾ TCGA▴GTTAACTTGATCCCTCCTCTTCTTT 3'-(*Xho1*) primers specific for *hMIA40*, 2.5 mM each of four dNTPs, 0.5 U of DNA polymerase enzyme and 500 ng of cDNA. The amplification was performed with an initial denaturation step at 95 ^{0}C for 3 min, followed by 35 cycles of 94 ^{0}C: 30 sec, 58 ^{0}C: 30 sec and 72 ^{0}C: 2min; and a final extension at 72 ^{0}C for 10 min. The amplified product was visualised by 1.5% agarose gel electrophoresis and the amplified product was purified by gel extraction method (QUIAGEN). We also amplified *hMIA40* ORF without stop codon by using forward NB73 Fwp: 5'CCCAG▾AATT▴CACC ATGTCCTATTGCCGGCAGGAA 3'- (*E.CoR1*) andreverse primer NB165 Revp:5'CAAC▾ TCGA▴G ACTTGATCCCTCCTCTTCTTT3'-(*Xho1*) primers and processed as above.

2.2.2.A.3. Restriction Digestion

The amplified *hMIA40* and pET28 (a^+) / pcDNA3.1 Cmyc vectors were subjected to double digestion with *E.coR1* and *Xho1* restriction enzymes in a 50 µl reaction {(PCR product 30 µl; 10X Tango Buffer 10 µl (Fermentas); Milli Q water 9 µl; *E.coR1* 0.5 U; *Xho1* 0.5 U) and (pET 28 (a^+) / pcDNA3.1 Cmyc vector 30 µl; 10X Tango Buffer 10 µl; Milli Q water 9 µl; *E.coR1* 0.5 U; *Xho1* 0.5 U)} at 37 ^{0}C for overnight. The digested products were

visualised by 1.5 % Agarose gel electrophoresis and the products were excised and gel purified using QUIAGEN gel extraction method.

2.2.2.A.4. Cloning of *hMIA40* into pET28 (a^+)/pcDNA 3.1 Cmyc vector

The digested*hMIA40* fragment was ligated into a vector (pET 28 (a^+) / pcDNA 3.1 Cmyc) by using T4 DNA Ligase (Fermentas). The reactions were carried out in a final volume of 15 µl with 150 ng of vector, 3 fold excess of insert, 1 µl of T4 DNA Ligase and 1.5 µl of 10X T4 DNA Ligase Buffer. The reaction mixture was incubated at 18 ^{0}C for overnight and ligated product was transformed into DH5α cells.

2.2.2.A.5. Bacterial Transformation

E.coli DH5α / Rosetta gammie competent cells were used for transformation of ligated products and plasmids. About 10 µl of ligated product / 100 ng of pure plasmid was added to DH5α competent cells and incubated on ice for 30 min; heat shock was given at 42 ^{0}C for 1 min and chilled on ice for 2 min. To this reaction, 1 ml of LB medium was added and incubated at 37 ^{0}C shaker incubator for 60 min and the culture was plated on LB agar plate containing an antibiotic (Kanamycin / Ampicillin). The colonies were screened for the presence of cloned fragment with restriction digestion and sequence was confirmed by automated sequencer.

2.2.2.A.6. Site Directed Mutagenesis

For the creation of cysteine mutations (C-S) in *hMIA40*, we amplified the Pet28-*MIA40*/pcDNA-*MIA40* plasmid using Pfu DNA polymerase (Fermentas) and specific primers as described below. The amplified DNA was treated with Dpn1 enzyme at 37 ^{0}C for 2 hrs. The Dpn1 treated plasmid was transformed into DH5α Cells.The clones were confirmed

through the restriction digestion and sequencing. The primers used for the generation of cysteine mutant are listed below.

GB1 Fwp. 5'AAC TGG AAC TCC CCA TGC CTT3' (MIA40 C53S)
GB2 Revp. 5'AAG GCA TGG GGA GTT CCA GTT3' (MIA40 C53S)

GB3 Fwp. 5'AAC TGC CCA TCC CTT GGG GGA3' (MIA40 C55S)
GB4 Revp. 5'TCC CCC AAG GGA TGG GCA GTT3' (MIA40 C55S)

GB13 Fwp. 5'TGG AAC TCC CCA TCC CTT GGG3' (MIA40 C5355S)
GB14 Revp. 5'CCC AAG GGA TGG GGA GTT CCA3' (MIA40 C5355S)

GB5 Fwp. 5'AGC GGT CCC TCT GGA GAA CAG3' (MIA40 C64S)
GB6 Revp. 5'CTG TTC TCC AGA GGG ACC GCT3' (MIA40 C64S)

GB7 Fwp. 5'GCC TTT TCC TCC TTC CAC TAT3' (MIA40 C74S)
GB8 Revp. 5'ATA GTG GAA GGAGGA AAA GGC3' (MIA40 C74S)

GB9 Fwp. 5'GGG TCA GAC TCT GTA GAC CAG3' (MIA40 C87S)
GB10 Revp. 5'CTG GTC TAC AGA GTC TGA CCC3' (MIA40 C87S)

GB11 Fwp. 5'ATG CAG GAA TCC ATG CAG AAA3'(MIA40 C97S)
GB12 Revp. 5'TTT CTG CAT GGA TTC CTG CAT3' (MIA40 C97S)

2.2.2.B. Bacterial expression and protein purification

2.2.2.B.1. Expression of His tagged hMIA40

The plasmid pET28(a^+) harbouring *hMIA40* and *hMIA40*mutants (C-S) were transformed into *E.coli* Rosetta gammie strain. A colony carrying the pET28-*hMIA40* plasmid DNA was grown for overnight in LB medium containing kanamycin at 37 ^{0}C shaker incubator. The primary culture was diluted to 1:100 in 500 ml fresh LB medium, grown with vigorous agitation to mid logarithmic phase ($OD_{600\ nm}$: 0.6-0.8), and incubated at 37 ^{0}C by addition of 1 mM IPTG (Isopropyl-β-D-thiogalactopyranoside) for 3 hrs. Further the culture was centrifuged at 10,000 rpm for 10 min to pellet down the bacterial cells. The pellet was suspended in 50 mM Tris-HCl pH8.0 by 1/20th volume. The suspended bacterial cells were

ruptured by sonication. Then the soluble (Supernatant) and insoluble (inclusion bodies) fractions were separated by centrifugation at 10,000 rpm for 10 min. The expressed recombinant protein was present in soluble form. The soluble recombinant proteins were purified using Ni-NTA affinity column (Clontech).

2.2.2.B.2. Recombinant His-hMIA40 protein purification by Ni-NTA column

To the soluble protein fraction containing His-MIA40, an equal volume of buffer B (200 mM NaCl, 10 mM βME and 50 mM Tris-HCl pH 7.5) was added. The sample was then passed through the Ni-NTA column which was equilibrated with buffer A (100 mM NaCl, 5 mM βME and 25 mM Tris-HCl pH 7.5). The column was washed with Buffer A containing 10 mMimmidazole and the bound protein was eluted by using elution buffer (0.4 M Immidazole pH 7.0, 50 mM Tris-HCl pH 7.5, 100 mM NaCl and 5 mM βME).

2.2.2.B.3. Separation of affinity purified hMIA40 by Gel filtration chromatography

The affinity purified hMIA40 protein was subjected to gel purification on a sephadex-G100 column (1.5 X 86 cm, Sigma). About 100 ml of gel was packed into a glass column and equilibrated with buffer containing 50 mM Tris-HCl (pH 7.5) and 100 mM NaCl and followed by hMIA40 protein was loaded on to the column. Gel filtration was carried out at room temperature with buffer containing 50 mM Tris-HCl (pH 7.5) and 100 mM NaCl and eluted protein samples were collected as 2 ml fractions. The eluted sample absorbance was recorded at 280 nm by using UV-Vis spectrophotometer (HITACHIU-2910). The hMIA40 cysteine mutant proteins were also gel purified as described for the WT hMIA40. Initially the column was calibrated by using standard protein markers such as Alchohol dehydrogenase (150 kDa), Bovine serum albumin (66 kDa) and Carbonic anhydrase (29 kDa).

2.2.2.C. SDS-PAGE analysis

Purified recombinant proteins or HEK293T cell lysate were separated on 12% non-reducing and reducing SDS-PAGE (Laemmli 1970).To check the redox states of hMIA40, mitochondria were treated with or without DTT (Dithiothreitol) prior to resolving it on a 12% SDS-PAGE. For MALDI analysis purified hMIA40 protein was resolved on 12% SDS-PAGE followed by staining with coomassie blue R250 and the oligomeric form of hMIA40 band was excised for further analysis.

2.2.2.D. Western blot analysis

The proteins were resolved on 12% SDS-PAGE as described above and proteins were transferred to a Nitrocellulose membrane (NC membrane, Pall) overnight at 30 volts. The membrane was blocked with TBST (20 mM Tris-HCl pH 7.5, 150 mM NaCl and 0.05% Tween20) containing 5% milk powder for 1 hr at room temperature. The membrane was incubated with primary antibody in TBST solution at room temperature for 2 hrs. The membrane was washed with TBST solution for three times at each 15 min interval and incubated with HRP-conjugated secondary antibody for 2 hrs at room temperature. The membrane was washed three times with TBST solution for 15 min at room temperature and developed the blot using ECL reagents (GE Health care, USA) and Varsadoc (Bio-Rad).

2.2.2.E. Antibodies

Polyclonal antibodieswere raised againsthMIA40 recombinant protein in rabbit.The soluble recombinant hMIA40 was mixed either with Freund complete adjuvant or incomplete adjuvant (Bangalore GeNei) for initial and subsequent booster dose respectively (20 days interval for each booster) and injected into the rabbit. After subsequent booster doses, serum was collected from the rabbit blood. Human Mia40 mono specific antibodies were purified by

using antigen coupled sepharose beads (GE Health care).Pre-immune serum was collected from the rabbit prior to induce antibodies.

2.2.2.E.1. Purification of polyclonal Antibodies

The recombinant purified antigen (Rec.hMIA40 protein) was dialyzed against coupling buffer overnight (0.1 M $NaHCO_3$ pH 8.0 and 0.5 M NaCl) at 4 ^{0}C. The dialyzed antigen in coupling buffer was mixed with CNBr activated sepharose 4B beads and kept on rotisserie for 1 hr at room temperature or overnight at 4 ^{0}C. The beads were washed with coupling buffer and block the remaining active groups with the addition of 0.1 M Tris-HCl, pH 8.0 and incubated at room temperature for 2 hrs. Further, the column was washed 3 times with alternating pH cycle. Each cycle consist of a wash with 0.1 M Acetate buffer pH 4.0 containing 0.5 M NaCl followed by wash with 0.1 M Tris-HCl, pH 8.0 containing 0.5 M NaCl. Finally, the beads were kept in 1X PBS buffer pH 7.2 and stored at 4 ^{0}C. The dialyzed serum against 1X PBS pH 7.2 buffer was mixed with the ligand coupled CNBr activated sepharose beads and kept on a rotisserie for 2 hrs at 4 ^{0}C followed by centrifugation at 5000 rpm for 5 min to pellet down the sepharose beads. The beads were washed with 1X PBS pH 7.2 for 3 times. The bound Mono-specific antibodies were eluted by using 0.1 M Glycine pH 2.5. The eluted antibodies were neutralized with Tris buffer, concentrated and kept frozen at -20 ^{0}C for further use.

2.2.2.F. Spectroscopy analysis

2.2.2.F.1. UV Absorption Spectroscopy analysis

UV-Visible spectra were recorded in 10 mm path length quartz cuvettes using a HITACHI U-2910 spectrophotometer at room temperature in the range 200 nm-700 nm (Gorla and Sepuri 2014).

2.2.2.F.2. Atomic Emission Spectroscopy analysis

The hMIA40 recombinant protein was purified under reducing conditions by adding sodium dithionite (Sigma) followed by converted into protein ash. The protein ash was analysed by using Atomic Emission Spectroscopy (GSI, Hyderabad).

2.2.2.F.3. Circular Dichroism Spectroscopy analysis

Circular Dichroism spectroscopy (CD) measurements for hMIA40 and Fe bound form of hMIA40 were performed in a Jasco J-815 spectrophotometer using quartz cuvettes of 0.1 cm path length. Spectra wererecorded at 20^0C from 200 to 260 nm wavelength with a resolution of1.0 nm and an acquisition time of 50 nm/min. The final CD spectra were obtained by averaging three consecutive scans. CD scans were corrected for background noise bysubtracting spectra of protein-free samples recorded under identical conditions.

2.2.2.G. Cell culture and transfection

HEK293T cells were cultured in Dulbecco'smodified Eagle's medium (Invitrogen) containing 10% (v/v) fetal calf serum at 37 ^{0}C under an atmosphere of 5% CO_2. Cells growing on 175 mm flasks (60% confluence) were transfected with 20 µg of plasmid by using 20 µl of transfectant agent lipofectamine (Invitrogen) in serum free medium. After 6 hours of transfection, the serum free medium was changed with complete medium and cells were analyzed after 36 or 48 hrs of transfection.

2.2.2.H. Isolation of mitochondria from HEK293T cells

Mitochondria were isolated from HEK293T cell lines. Briefly, HEK293T cells were grown as monolayer's and suspended in mitochondria isolation buffer (20 mM HEPES pH 7.5, 1.5 mM MgCl2, 1mM EDTA pH 8.0, 1 mM EGTA, 210 mM Sucrose and 70 mM Mannitol).

The cell suspension was homogenized in a Dounce homogenizer. The homogenate was centrifuged at 1000 Xg for 10 min at 4 ^{0}C to separate nucleus and the supernatant was again centrifuged at 10,000 Xg for 15 min at 4 ^{0}C. The resultant mitochondrial pellet was suspended in a buffer containing 250mM Sucrose, 5 mM Magnesium Acetate, 80mM Potassium Acetate, 10 mM Sodium Succinate, 1 mM DTT and 20mM HEPES-KOH pH 7.4.

2.2.2.I. Measurement of Iron in mitochondria

The non-heme iron present in the mitochondria was measured by the bathophenonthroline method (Tangeras, Flatmark *et al.,* 1980). Briefly, mitochondria were suspended in medium containing 10 mM MES pH 4.5, 1 % sodium dodecyl sulphate and 0.5 mM dithionite. To this mixture, 50 µM bathophenonthroline was added, and the Fe (II)-chelate formation was measured in a dual-wavelength HITACHI spectrophotometer at 540 nm and 575 nm. For the measurement of mitochondrial ^{55}Fe content (specific Activity-10.18 mCi/mg), 80% confluent cells were incubated with 500 nM ^{55}Fe for 48 hrs. Mitochondria were washed with cold 500 µM bathophenonthroline to remove membrane bound ^{55}Fe. Radioactivity was quantified by using a Beckman scintillation counter.

2.2.2.J. Immunoprecipitation

HEK293T cells were transfected with mammalian expression vector harbouring the *hMIA40* gene by using lipofectamine transfection reagent (Invitrogen). After 36 hrs of transfection, cells were allowed to grow in serum free DMEM medium for 6 hrs and then incubated with radiolabel ^{55}Fe and 1 mM sodium ascorbate for 2 hrs. Cells were lysed with NP-40 buffer (20 mM Tris HCl pH 8.0, 137 mM NaCl, 10% Glycerol and 1% Nonidet P-40). Cell lysates were incubated with either polyclonal Mia40 antibody (1 µg) or pre immune serum for 90 min at room temperature followed by addition of protein A/G beads to the lysate

and kept on rotisserie for 90 min at room temperature. The supernatant was discarded after centrifugation and the beads were washed with IP buffer for 3 times. The labelled ^{55}Fe present in beads was measured using Beckman scintillation counter.

2.2.2.K. Enzyme assays

2.2.2.K.1. Xanthine oxidase activity

A spectrophotometric method was used to assay the cytosolic Xanthine oxidase enzyme activity (Viel, Benkirane *et al.*, 2008). Briefly, the cytosolic fraction was taken in a buffer containing 33 mM potassium phosphate (pH 7.5). The assay was initiated by the addition of xanthine substrate (0.05 mM) and the contents were mixed by inversion and equilibrated to 25 ^{0}C. The formation of uric acid was measured by monitoring the increase in absorbance at $A_{290\ nm}$ continuously for 5 minutes at 25 ^{0}C. One unit of enzyme activity was defined as the absorbance equivalent of 1 µmole of uric acid released per min per mL of the Xanthine oxidase enzyme solution (Sigma) under experimental conditions.

2.2.2.K.2. Aconitase activity

The cytosolic Aconitase activity was measured spectrophotometrically. The reaction mixture contains 50 mM Tris-HCl pH 7.5, 1 mM isocitrate as a substrate, 5 mM MgCl2 and cytosolic fraction. The conversion of isocitrate to cis-aconitate was measured as an increase in absorbance at $A_{240\ nm}$. One unit of enzyme activity was defined as the absorbance equivalent of 1 µmole of cis-aconitate released per min per mL of the enzyme solution under experimental conditions.

2.2.2.K.3. Mitochondrial complex I activity

The mitochondrial complex I activity (de Wit and Sluiter 2009) was determined by measuring the oxidation of NADH to NAD^+ at 340 nm with 380 nm used as a reference wavelength at 37 ^{0}C. The assay mixture contains 25 mM Potassium phosphate pH 7.4, 5 mM $MgCl_2$and 0.25% BSA. To this reaction, 5 mM NADH and 50 µg of mitochondria isolated from HEK293T cells were added. The contents were mixed and incubated for 1 min at 37 ^{0}C. The reaction was initiated by adding 3 mM decylubiquinone and monitored the decrease in absorbance at 340 nm for 5 min. The complex I activity was calculated by using the velocity of reaction (Δabsorbance/min) and the molar extinction coefficient of NADH (3.4 $mM^{-1}cm^{-1}$; at 340 nm).

2.3. Results

2.3.1. Cloning, Expression, Purification and Raising antibodies for hMIA40

To characterize the hMIA40 as a Fe/S containing protein, we have cloned *hMIA40* into pET28 (a+) vector. In brief, total cDNA was made from HeLa cells RNA (Bangalore GeNei) by using reverse transcriptase enzyme. From the total cDNA, the *hMIA40* was amplified by using *hMIA40* ORF specific primers (NB73 and NB74) and the amplified product was shown in Fig 2.3A. We cloned *hMIA40* gene into pET28 vector for bacterial expression as described in the methods (Fig 2.3B).

The expressed recombinant protein was present in soluble form. The soluble recombinant protein was purified on a Ni-NTA affinity column (Clontech) and separated on SDS-PAGE and coomassie stained (Fig 2.3C). Purified protein migrates as 18 kDa protein on SDS-PAGE as predicted from its sequence. However, we also find a small but significant amount of 70 kDa protein band in all our preparations of recombinant hMIA40 even under reducing conditions. We identified this 70 kDa band as MIA40 by MS-MS analysis (shown in Fig 2.4F).The polyclonal antibodies for hMIA40 protein were raised in rabbit. The mono-specific antibodies for Mia40 were purified as described in methods. To check the specificity of antibodies, the purified recombinant hMIA40 and mitochondrial fraction isolated from rat liver were separated on SDS-PAGE and western blotted (Fig 2.3D). The Mia40 antibody detects the 18 kDa and 70 kDa band in recombinant protein fraction lane (Fig2.3 D, lane 1) and 16, 30, and 70 kDa bands (lane 2) in mitochondrial extract lane. These high molecular weight cross reacting bands with hMia40 antibodies may represent the dimeric and tetrameric forms of MIA40 as described earlier by others (Hofmann, Rothbauer *et al.*, 2005).

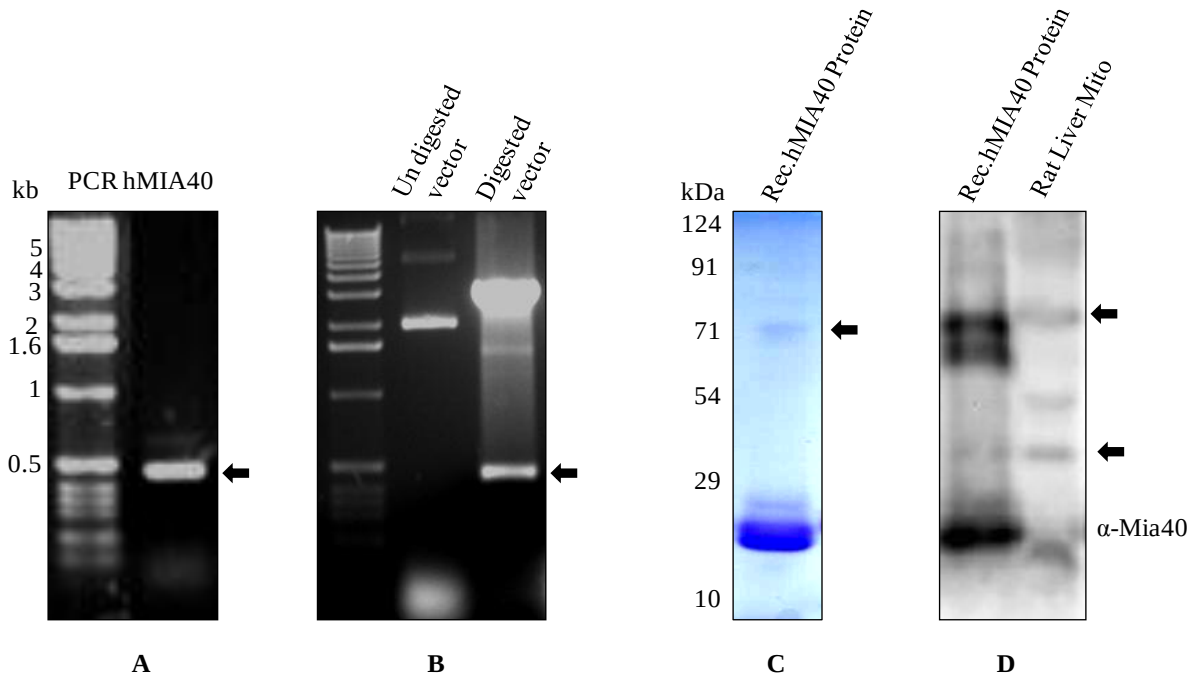

Figure 2.3. Cloning, Expression and Raising of antibodies against hMIA40. To characterize the hMIA40 *in vitro*, we cloned *hMIA40* into bacterial expression vector pET28 (a^+). **(A).** 1.5% Agarose gel electrophoresis analysis of PCR amplified *hMIA40* gene. Arrow indicates the *hMIA40* amplicon. **(B).** Restriction digestion of pET28-*hMIA40* with *EcoR1&Xho1* enzymes followed by 1.5% Agarose gel electrophoresis to confirm the presence of amplified insert. Arrow indicates the cloned fragment, *hMIA40*. **(C).** Recombinant hMIA40 protein was expressed and purified using Ni-NTA column and analysed by 12% SDS PAGE. Arrow indicates the oligomeric form of hMIA40. **(D).** Polyclonal antibodies were raised against hMIA40 in rabbit and purified. The cross reactivity was checked by western blot analysis both with recombinant hMIA40 and mitochondrial extract isolated from rat liver. Arrows indicates the oligomeric forms of hMIA40.

2.3.2. Human MIA40 is an Iron containing protein

Most of the purified Fe containing proteins are brownish in colour. The purified recombinant hMIA40 appears brownish in colour under reducing conditions indicating that it may contain Fe (Fig 2.4A). To determine whether hMIA40 contains Fe, the purified recombinant protein was further subjected to Atomic Emission Spectroscopy (AES) analysis (Spiller, Ang *et al.*, 2013). As shown in Fig 2.4B, recombinant hMIA40 indeed contains a significant amount of iron and a small amount of Mn. The molar ratio of protein to metal is

around 0.068 indicating that like its yeast homologue, a certain fraction of hMIA40 has the ability to bind to iron *in vitro*. It also confirms the study of Thorpe's group that human MIA40 is an iron binding protein *in vitro*.

We further investigated whether hMIA40 can bind to iron *in vivo*.To enrich endogenous hMIA40 *in vivo*, HEK293T cells were transiently transfected with plasmid containing pcDNA-*MIA40*and incubated with ^{55}Fe for 24 hrs. Thereafter, cells were harvested, lysed and the cell lysates were subjected to immunoprecipitation with Mia40 specific antibody or pre-immune serum. The amount of radioactivity present in the immunoprecipitate was determined in a scintillation counter (Fig 2.4C). Immunoprecipitate of cell lysate upon using Mia40 antibody was more enriched in ^{55}Fe compared to immunoprecipitate from pre-immune serum. We validated the immunoprecipitation of hMIA40 by probing the immunoprecipitated samples with the antibody specific for hMIA40 (Fig 2.4D). Taken together, our results indicate that hMIA40 binds to iron both *in vitro* and *in vivo.* Further, the ability of Mia40 to bind iron *in vivo* is found to be conserved from yeast to humans (Spiller, Ang *et al.*, 2013).

We have shown that recombinant or native hMIA40 can form higher order structures (Fig 2.3D). It is known that the metal containing higher order structures are resistant to reducing conditions (Spiller, Ang *et al.*, 2013). To further understand the nature of oligomeric structures and Fe content of hMIA40, the recombinant hMIA40 was separated on SDS-PAGE under reducing and non-reducing conditions and immunoblotted with Mia40 antibodies (Fig 2.4E.). In the absence of DTT, a fast migrating, monomeric and oxidized form of MIA40 and other higher order structures were detected. These higher order structures may be formed due to disulfide bridges or presence of metal ion. However, in the presence of DTT, a slow migrating monomeric reduced form and a small amount of 70 kDa protein was detected. This result indicates that most of the disulfide mediated higher order structures are reduced and

metal containing higher order structure are protected in the presence of DTT. We confirmed that 70 kDa higher order structure is indeed MIA40 by MS-MS analysis (Fig 2.4F).

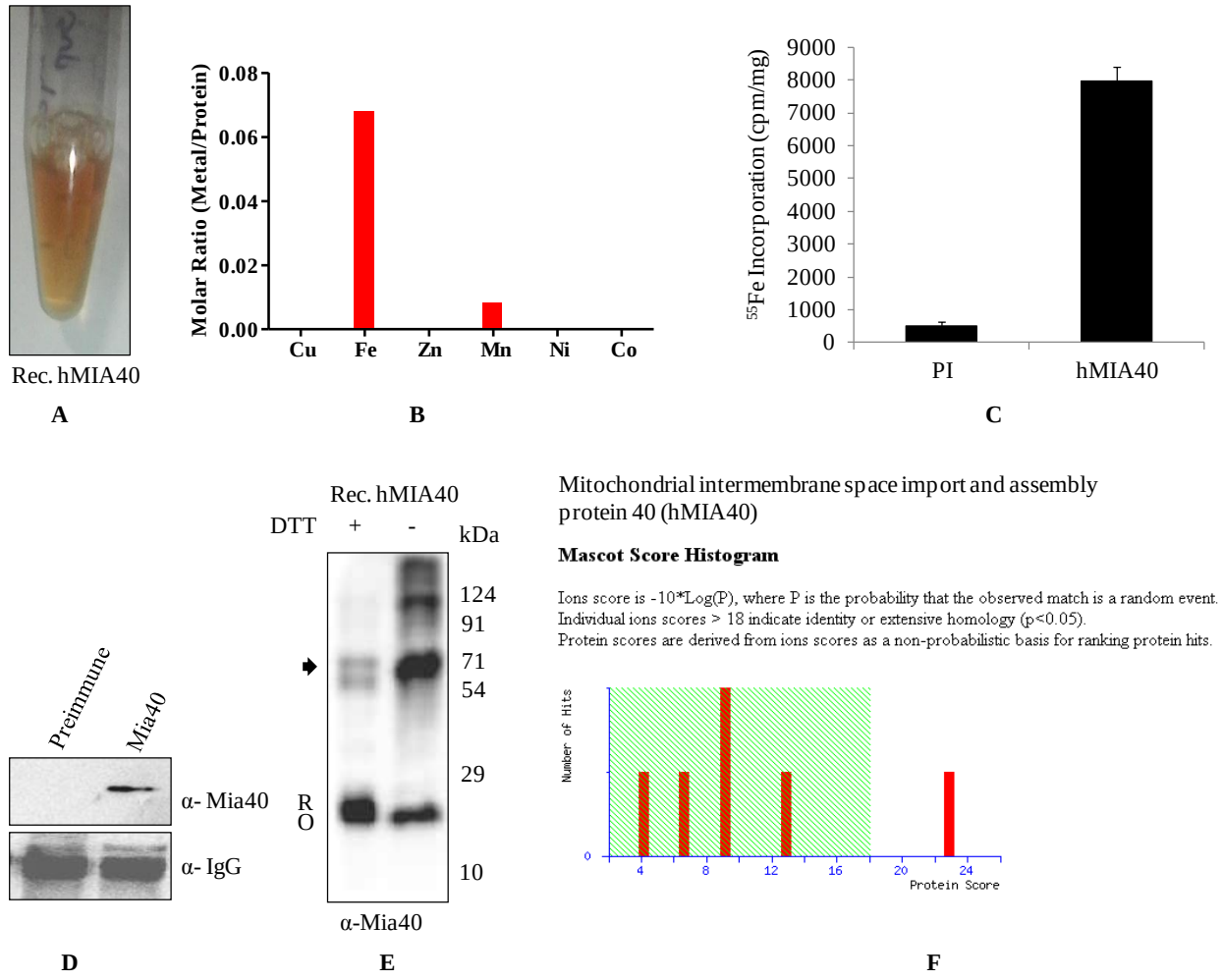

Figure 2.4. Human MIA40 is Iron binding protein. (A). *E.coli* lysate containing recombinant His-hMIA40 was purified by Ni-NTA column under reduced conditions and purified protein solution is brownish in colour. **(B).** AES analysis (GSI, Hyderabad) of purified recombinant His-hMIA40 was carried out as described under methods section and the metal content is shown here. **(C).** HEK293T cells were transiently transfected for over-expression of Myc-His-*hMIA40* followed by incubation with labelled ^{55}Fe. Cell lysate were prepared by using NP40 buffer as described in methods section. Immunoprecipitation was carried out with either pre-immune serum (PI) or Mia40 antibody. Labelled ^{55}Fe present in immunoprecipitate was measured in a scintillation counter and shown here as CPM/mg protein. **(D).** Immunoprecipitated samples were separated on SDS-PAGE and probed with antibodies specific for Mia40 and IgG. **(E).** Purified recombinant His-hMIA40 was separated on non reducing SDS-PAGE followed by western blot analysis. Recombinant His-hMIA40 migrated as both oxidised and reduced forms under reducing conditions. Arrow indicates the oligomeric form of

hMIA40. **(F).** Affinity purified His-hMIA40 protein was resolved on SDS-PAGE under reducing conditions. Human MIA40 migrates as a monomeric 18 kDa and as a tetrameric 70 kDa protein. The tetrameric form was excised and subjected to MS-MSanalysis to confirm the hMIA40.

2.3.3. Human MIA40 is a 4Fe-4S and 2Fe-2S cluster containing protein

In general Fe is associated with proteins as Fe/S cluster or heme group (Ruzicka and Beinert 1975; Rees 2002). To further characterize the nature of Fe present in hMIA40, we utilized the property of differential absorption maxima of different Fe/S in UV-Vis spectrum. Purified recombinant hMIA40 displayed absorption peaks at 410 nm and 460 nm in the visible spectrum which are characteristic spectral features of a protein harbouring 4Fe-4S (410 nm) and 2Fe-2S (460 nm) clusters (Fig 2.5A) (Cai, Frederick *et al.*, 2013). This result was surprising as yeast Mia40 is known to contain only 2Fe-2S clusters (Spiller, Ang *et al.*, 2013).

To further characterize the arrangement of iron sulfur clusters within hMIA40, we resolved recombinant hMIA40 on a sephadex G100 column as described under Methods section. Monomeric hMIA40 has a molecular weight of 18 kDa. However, upon gel filtration, purified hMIA40 was detected in three different fractions having molecular weight of approximately 70 kDa, 40 kDa and 20 kDa (Fig 2.5B) that corresponds to tetrameric (P1), dimeric (P2) and monomeric (P3) forms of hMIA40 respectively. Most interestingly, the tetrameric form of hMIA40 displays an absorption peak at 410 nm corresponding to 4Fe-4S cluster while dimeric form has absorption maxima at 460 nm that is characteristic of a 2Fe-2S cluster (Fig 2.5C). The monomeric form does not absorb in the visible spectrum (Fig 2.5C) despite comparable amount of protein being present. These studies indicate that recombinant hMIA40 can exist both as a tetramer and as a dimer *in vitro* that are capable of binding 4Fe-4S and 2Fe-2S clusters respectively while the monomeric form does not contain any Fe/S clusters. Further CD (Circular Dichroism) spectrum was used to analyze the secondary

structure of monomer and Fe/S bound oligomeric forms of hMIA40. There is no secondary structural change in the absence or presence of metal as monomer and Fe/S associated oligomers showed similar kind of CD spectrum (Figure 2.5D). These*in vitro* and *in vivo*studies suggest that hMIA40 is associated with Fe/S clusters as 4Fe-4S and 2Fe-2S confirmation.

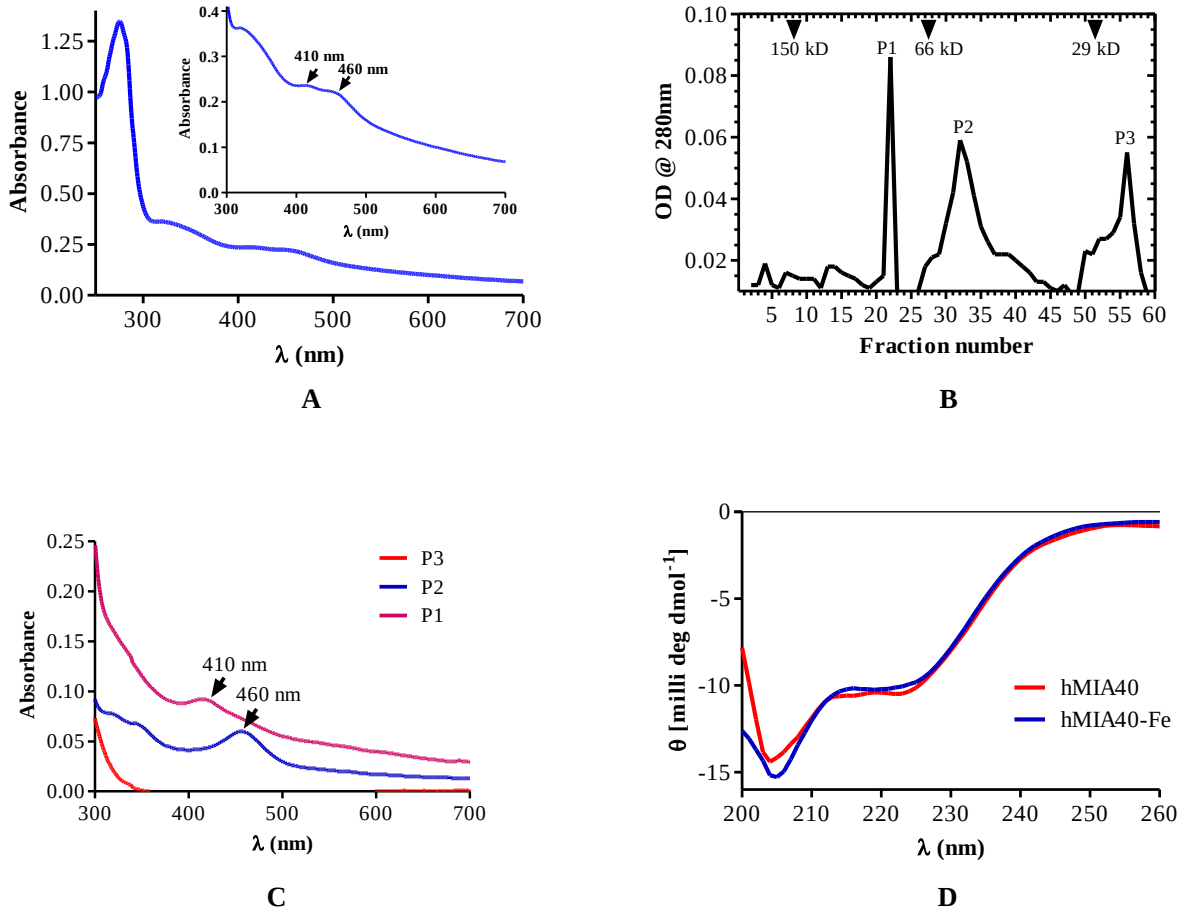

Figure 2.5. Human MIA40 is a Fe/S protein. (A). UV-Vis spectra (250 nm-700 nm) of purified recombinant His-hMIA40 were carried out as indicated in the Methods. Arrows indicate the characteristic 4Fe-4S and 2Fe-2S peaks at 410 and 460 nm. **(B).** Gel filtration profile (Sephadex G100) of purified recombinant His-hMIA40 that was monitored at 280 nm and plotted based on the standards markers profile. **(C).** UV-Vis spectra of P1 (Peak I), P2 (Peak II) and P3 (Peak III) samples obtained after gel filtration (B) of purified His-hMIA40. **(D).** CD spectrum (200 nm-260 nm) analysis of recombinant monomeric His-hMIA40 and Fe/S cluster bound oligomeric His-hMIA40 proteins.

2.3.4. Coordination of hMIA40 Fe/S clusters

Most of the Fe/S clusters associated with proteins are present either as 4Fe-4S or 2Fe-2S and arenormally coordinated by four cysteine amino acids resident in the protein. Human MIA40 contain six conserved cysteine residues that are ordered in the form of a CPC motif and two CX_9C motifs. The former serves as a redox active motif while the latter are involved in providing the structural framework in the form of disulphide bonds. Our aforementioned results clearly show that hMIA40 can exist as a tetramer with 4Fe-4S cluster or as a dimer with 2Fe-2S. We speculate that in a tetramer, the four CPC motifs from four protein molecules hold the 4Fe-4S cluster while in case of the dimer, the two CPC motifs from two molecules of hMIA40 coordinate the 2Fe-2S cluster.

To determine the importance of the CPC motifs, we carried out site directed mutagenesis of the cysteine residues within the CPC motif of recombinant hMIA40. We mutated either Cys 53 to Ser (C53S, M1) or Cys 55 to Ser (C55S, M2) or both (C5355S, M3) within the CPC motif. We also mutated the cysteines in CX_9C structural motifs to determine the role of these cysteines in the binding of hMIA40 to Fe/S cluster. We mutated either Cys 64 to Ser (C64S, M4) or Cys 87 to Ser (C87S, M5) within the CX_9C motifs (Fig 2.6A). These recombinant mutants were purified to homogeneity from bacterial cells (Fig 2.6B) and equimolar protein samples were analyzed forthe presence of Fe/S by UV absorption spectroscopy and gel filtration.Recombinant hMIA40 M1 and M2 displayed a significant reduction in absorption at 410 nm and 460 nm compared to recombinant hMIA40 wild type (Fig 2.6C) indicating low Fe/S content. Consistent with the low Fe/S content result, the metal to protein ratio of the hMIA40 M1 and M2 mutants were also significantly lowered compared to wild type hMIA40 (Fig 2.6D). Interestingly, the recombinant hMIA40 M1 and M2 mutants eluted as a tetrameric protein with low or negligible amount of dimeric or monomeric forms

(Fig 2.6E) in gel filtration indicating that the presence of either of the cysteine in CPC motif is sufficient to bind Fe/S albeit at lower efficiency. However, we cannot predict the exact coordination of Fe/S in tetrameric form of M1 and M2 mutant proteins as these structures show 4Fe-4S and 2Fe-2S characteristic absorption peaks (Fig 2.6C). In addition, we find that the recombinant hMIA40 M3 double mutant (C53S and C55S) did not show any absorption at 410 nm or 460 nm. These results directly implicate the CPC motif in hMIA40 as being critical for binding to Fe/S clusters. Most importantly, the double mutant did not exhibit any tetrameric form in the gel elution profile. It produced a large broad peak representing dimeric and monomeric forms (Fig 2.6F). The dimeric nature of CPC double mutant could be due to intra-disulfide mediated interaction of cysteines present in the structural motifs. In contrast, structural cysteine mutants M5 and M6 do not show any defect in Fe/S absorption at 410 or 460 nm (Fig 2.6G) and in the gel elution profile (not shown) when compared to wild type. These results suggest that the CPC motif and not the structural motifs are involved in coordinating Fe/S clusters in hMIA40 *in vitro*.

To further evaluate the role of CPC motif in hMIA40 to bind iron *in vivo*, HEK293T cells were transfected with plasmids harbouring*hMIA40* wild type or M3 respectively. HEK293T cells transfected with vector alone were used as internal control. The over expressed wild type and mutant *hMIA40* have both His and Myc epitopes. The transfected cells were incubated with ^{55}Fe for 24 hrs and the cell lysates were subjected Ni-NTA pull down. After incubation with the lysates, the Ni beads were washed and measured for ^{55}Fe content. Ni beads that were incubated with wild type hMIA40 lysates had relatively greater amount of radioactivity compared to Ni beads that were incubated with lysates from the hMIA40 double mutant (M3). Ni beads that were incubated with lysates from vector control were not enriched in ^{55}Fe indicating the specificity of the Ni-NTA pull down assay (Fig 2.6H). All the

transfected lysates were probed with Myc and Hsp70 antibodies to confirm the presence of equivalent amount of hMIA40 (in all samples except for vector control) and equal amount of lysate (Fig 2.6I). Taken together, our results irrefutably implicate the CPC motif in hMIA40 to be essential for efficient binding to iron both *in vitro* and *invivo*.

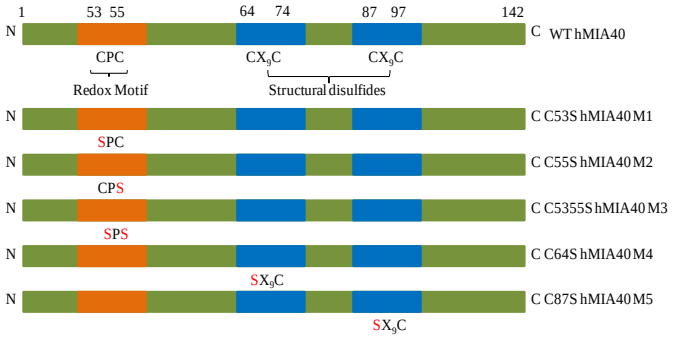

A

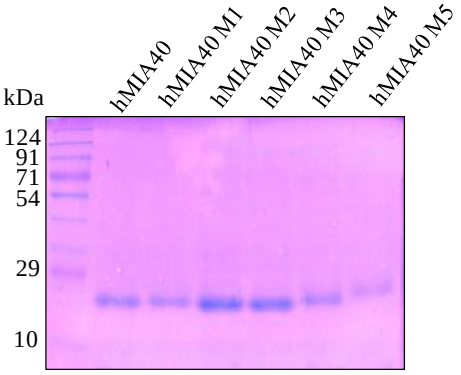

B

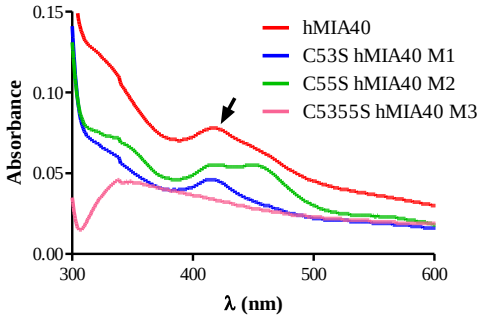

C

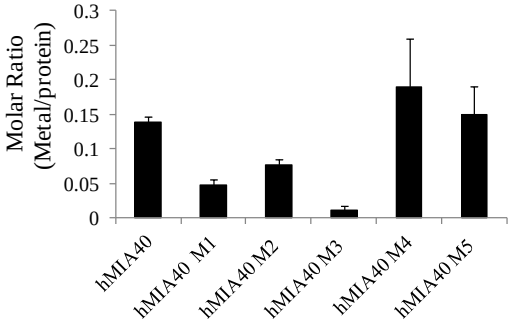

D

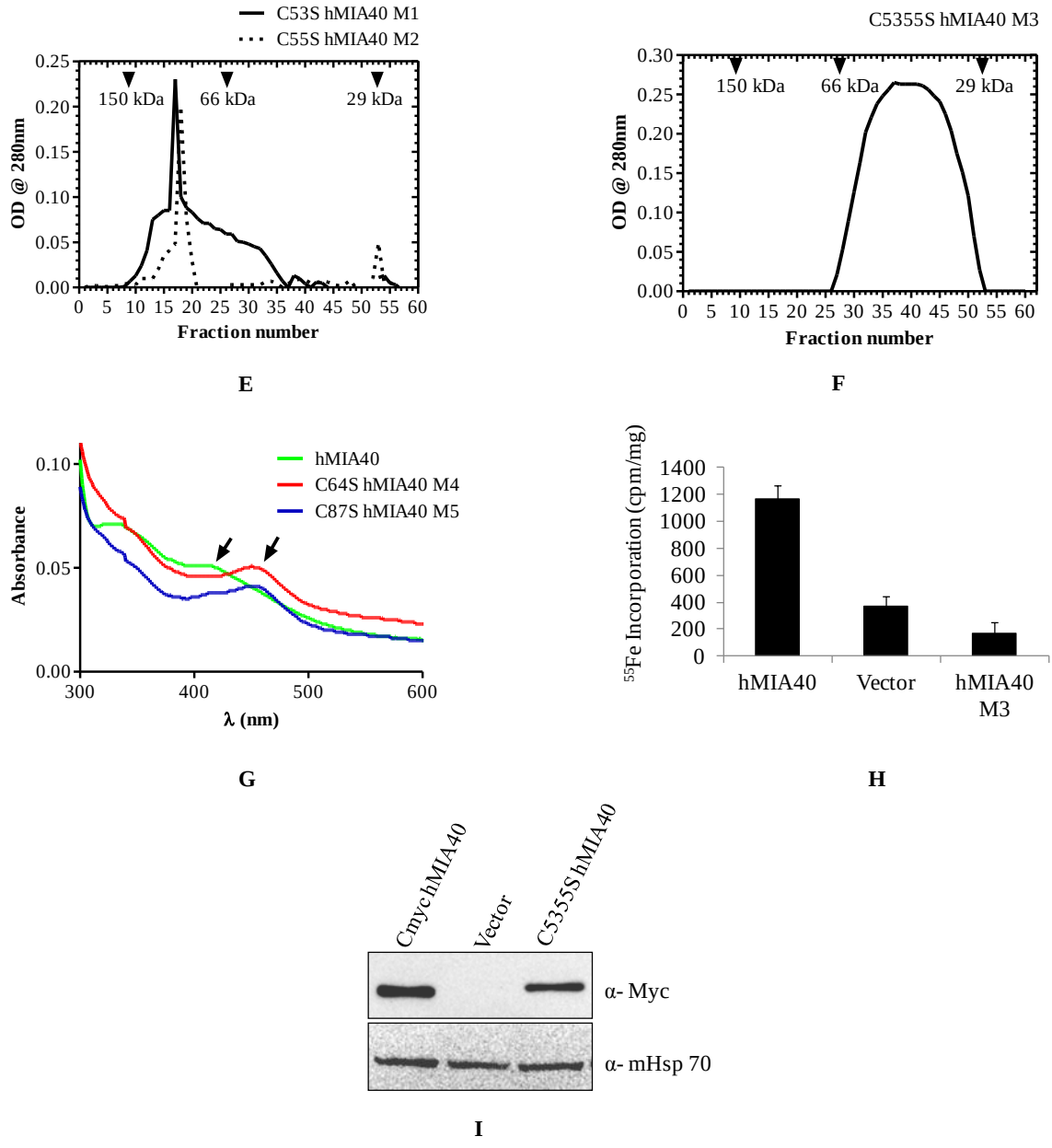

Figure 2.6 CPC motif in hMIA40 is required for binding to Fe/S cluster. (A). Schematic representation of hMIA40 (hMIA40 cysteine mutants) showing one CPC redox active motif and two CX_9C structural motifs. **(B).** Recombinant His-hMIA40 and cysteine mutants were purified by Ni-NTA column and separated on SDS-PAGE. The SDS-PAGE gel was stained with coomassie and is shown here. **(C).** UV-Vis spectra of purified recombinant His-hMIA40 WT, C53S hMIA40 (M1), C55S hMIA40 (M2) and C5355S hMIA40 (M3) mutant proteins. **(D).** Graphical representation of metal to protein ratio detected in recombinant His-hMIA40 and cysteine mutants (C & G)**. (E & F).** Gel filtration profile of purified recombinant C53S hMIA40, C55S hMIA40 and C5355S hMIA40 (F) mutant proteins. **(G).** UV-Vis spectra of affinity purified His-hMIA40, C64S hTOM40 (M4) and C87S hMIA40 (M5) mutant proteins. **(H & I).** HEK293T cells were transfected with either vector, WT Myc-His-*MIA40* or Myc-His tagged C5355S *hMIA40* plasmids.**(H)** The samples were processed through Ni-NTA beads as

indicated in the methods. The labelled ^{55}Fe present in beads was quantified by scintillation counter as CPM. **(I)** Western blot analysis of vector or Myc-*hMIA40* transfected HEK293T cell lysates probed with anti-Myc and anti- Hsp70.

2.3.5. Effect of redox reagents on hMIA40 Fe/S cluster stability

Fe/S clusters that are not an integral structural component of a protein are known to be sensitive to oxidative environment (Varghese, Tang *et al.*, 2003). To test the stability of the Fe/S clusters detected in hMIA40, absorption of purified recombinant hMIA40 at 410 nm and 460 nm wasmonitored after exposing it to oxidative and reducing conditions. A decrease or an increase in absorption at 410 or 460 nm can be directly correlated to a loss or an increase in stability of Fe/S clusters respectively. We observed a gradual decrease in absorption at 410 nm (Fig 2.7A) when hMIA40 was exposed to H_2O_2 at room temperature. These results suggest that the Fe/S clusters are sensitive to oxidation (Fig 2.7A). However, in the presence of reducing agent, there is a steady increase in the absorption at 410 nm for 10 minutes followed by a decline (Fig 2.7A & B). The initial increase in absorption at 410 nm could reflect the increased stabilization of 4Fe-4S clusters in presence of reducing conditions. However, this could paradoxically increase the exposure of the increased 4Fe-4S clusters to oxidation by air that is reflected in the drop in optical density at 410 nm after an initial increase. The spectrophotometric studies under oxidizing and reducing conditions suggest that the Fe/S clusters are not integral structural components of hMIA40 and are susceptible to oxidation and reduction. Based on these results, we hypothesize that the CPC motif may be coordinating the binding to Fe/S clusters.

We also analysed the effect of redox reagents on stability of Fe/S clusters associated with either recombinant or native hMIA40 by western blot. Purified recombinant hMIA40 or whole cell extract isolated from HEK293 cells was treated with or without H_2O_2 as indicated in the figure legend and separated either on non-reducing or reducing SDS-PAGE followed

by western blotting with antibodies specific for Mia40. In the absence of DTT, as expected, the recombinant and native protein displays a fast migrating oxidative form around 18 kDa (Fig 2.7C & D). In the presence of DTT, both native and recombinant protein displays only a reduced monomeric form (Fig 2.7C & D). Further, results show that the reducingenvironmentstabilized the dimeric and oligomeric forms of native hMIA40 when compared to the non-reducing environment. However, the oxidative conditions or treatment with H_2O_2 completely destabilizes tetrameric form and partially destabilizes the dimeric form of native hMIA40 indicating the sensitivity of Fe/S clusters towards oxidative environment. In contrast, reducing environment destabilizes the dimeric form of recombinant purified hMIA40 indicating the observed dimer is may be due to disulfide mediated or Fe/S cluster present in dimeric form is unstable (Fig 2.7C) *in vitro*. In addition, when HEK293T cells were treated with reducing agent followed by treatment with H_2O_2, a time dependent reduction in the reduced from of MIA40 was observed (Fig 2.7D). This indicates that the reduced form of hMIA40 is graduallygetting oxidized with disassembledIron sulfur cluster upon addition of H_2O_2 (Fig 2.7D). These results suggesting that for the stabilization of hMIA40 iron sulfur cluster requires reduced environment and these iron sulfur clusters are disassembled when the cells are exposed to oxidative stress. This result may also indicate that hMIA40 coordinated with iron sulfur clusters when CPC motif is in reduced form.Further, the oxidized form of CPC motif may have both intra and inter disulfides and cannot bind to the iron sulfur clusters. Further, the differences in recombinant and native protein in the formation and stability of Fe/S on SDS-PAGE may be due to native MIA40 redox status in the intermembrane space of mitochondria.

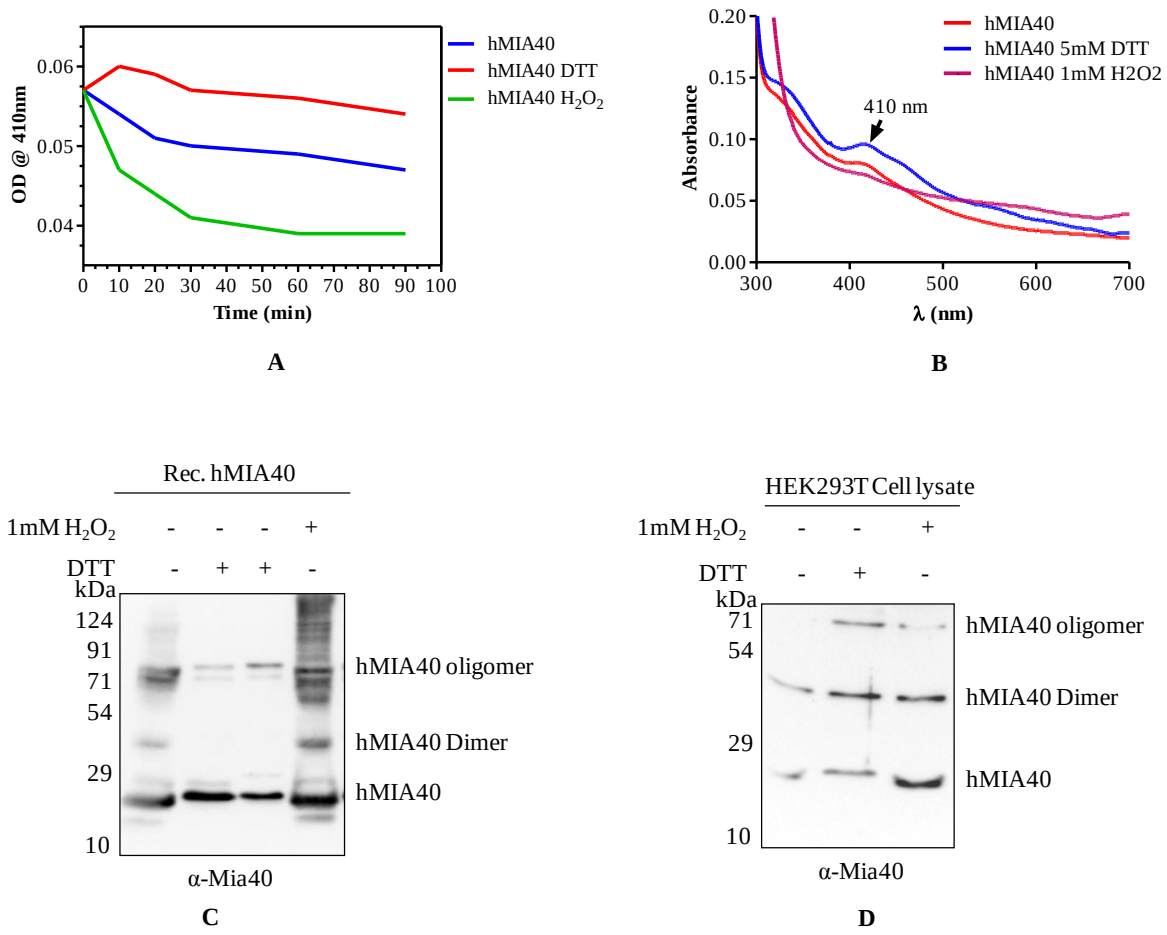

Figure 2.7. Effect of redox reagents on hMIA40 Fe/S cluster. (A). Time course of the absorption intensity changes of His-hMIA40 in the absence and presence of 5 mM DTT or 1 mM H_2O_2 at 410 nm is shown. **(B).** UV-Vis spectra of hMIA40 in the presence and absence of 5 mM DTT and 1 mM H_2O_2 is shown with wavelength on X- axis and absorbance on Y- axis. **(C).** Recombinant purified His-hMIA40 protein was analysed like as we did (C) for HEK293T cell lysate. **(D).** HEK293T cells were incubated with 5 mM DTT or 1 mM H_2O_2 followed by treated with 5 mM IAA. The cell lysates were resolved on SDS-PAGE and further analysed by western blot.

2.3.6. Role of hMIA40 in cellular iron homeostasis

Our *in vitro* and *in vivo* studies clearly demonstrate that hMIA40 binds to iron. Human MIA40 is known to interact with Erv1 (Bottinger, Gornicka *et al.*, 2012), a component of the ISC export machinery and protein import machinery of intermembrane space. Based on these findings, we further hypothesized that hMIA40 may be playing a role in cellular iron

homeostasis. To determine if hMIA40 has any effect on iron homeostasis, we initially depleted hMIA40 in HEK293T cells by transiently transfecting the cells with *MIA40* shRNA.

In parallel, we also transfected HEK293T cells with scrambled shRNA to serve as a control. To ascertain the level of hMIA40, SDS-PAGE followed by immunoblot analysis was carried out on mitochondria samples that were isolated from transfected cells (Fig 2.8A). Transfection with shRNA specifically reduced MIA40 levels by 70% compared to control cells while the level of mitochondrial Hsp70 was similar in both samples indicating equivalent loading (Fig 2.8A).

The amount of iron present in mitochondria that was isolated from the transfected cells was measured using bathophenonthroline. Depletion of hMIA40 is correlated to increased accumulation of non-heme iron in mitochondria (Fig 2.8B). We repeated this experiment by performing transfections in presence of radioactive iron. Consistent with the previous result, we observed accumulation of ^{55}Fe in mitochondria that was isolated from cells depleted in hMIA40 (Fig 2.8C). We rule out the possibility of cytosolic contamination as negligible amount of actin, a cytosolic marker protein was present in our mitochondrial preparations (Fig 2.8D). We conclude that hMIA40 may be required for export of Fe/S from mitochondria to cytosol.

Several cytosolic enzymes are dependent on Fe/S clusters that are exported from mitochondria for their activity (Kispal, Csere *et al.*, 1999). As depletion of hMIA40 affected the export of iron from mitochondria to cytosol, we additionally wished to probe if this affected the function of cytosolic enzymes that are associated with Fe/S clusters. We monitored the activity of cytosolic enzymes aconitase and xanthine oxidase in control cells and cells that were depleted for hMIA40 as described for the previous experiment. The

activities of aconitase and xanthine oxidase are significantly lowered in cytosolic fraction obtained from cells that were depleted for hMIA40 compared to control sample (Fig 2.8E & F). The stability of cytosolic Glutamate Phosphoribosyl Pyrophosphate Amidotransferase (GPAT) is dependent on the presence of 4Fe-4S cluster and hence its stability could serve as a hallmark for the presence of cytoplasmic 4Fe-4S assembly (Sheftel, Stehling *et al.,* 2010). The total cell extract of the hMIA40 depleted cells and control cells were resolved on SDS-PAGE and the level of GPAT enzyme was monitored by immunoblot analysis (Fig 2.8G). We find that depletion of hMIA40 reduces the stability of GPAT enzyme compared to control cells although comparable amount of GAPDH is present in both fractions. Further, we measured the mitochondrial aconitase protein levels by western blot in hMIA40 depleted cell lines. Aconitase is a 4Fe-4S protein and its stability is dependent on mitochondrial ISC machinery. We could not find any decrease in steady state levels of aconitase nor mitochondrial Hsp70 in hMIA40 depleted cells compared to control cells (Fig 2.8H). We also assayed for the Fe/S containing mitochondrial complex I enzyme activity and found no significant difference in the activity in the mitochondrial fractions of hMIA40 depleted cells and of scrambled shRNA treated cells (Fig 2.8I). These studies indicate that although hMIA40 does not affect mitochondrial Fe/S cluster assembly or Fe/S containing mitochondrial enzyme activities, it has a pronounced effect on the cytosolic Fe/S cluster assembly and on the activity and stability of cytosolic enzymes present in the cytosol. Taken together, our results suggest that hMIA40 has an important function in the mitochondrial Fe/S export machinery and thereby affects cellular iron homeostasis.

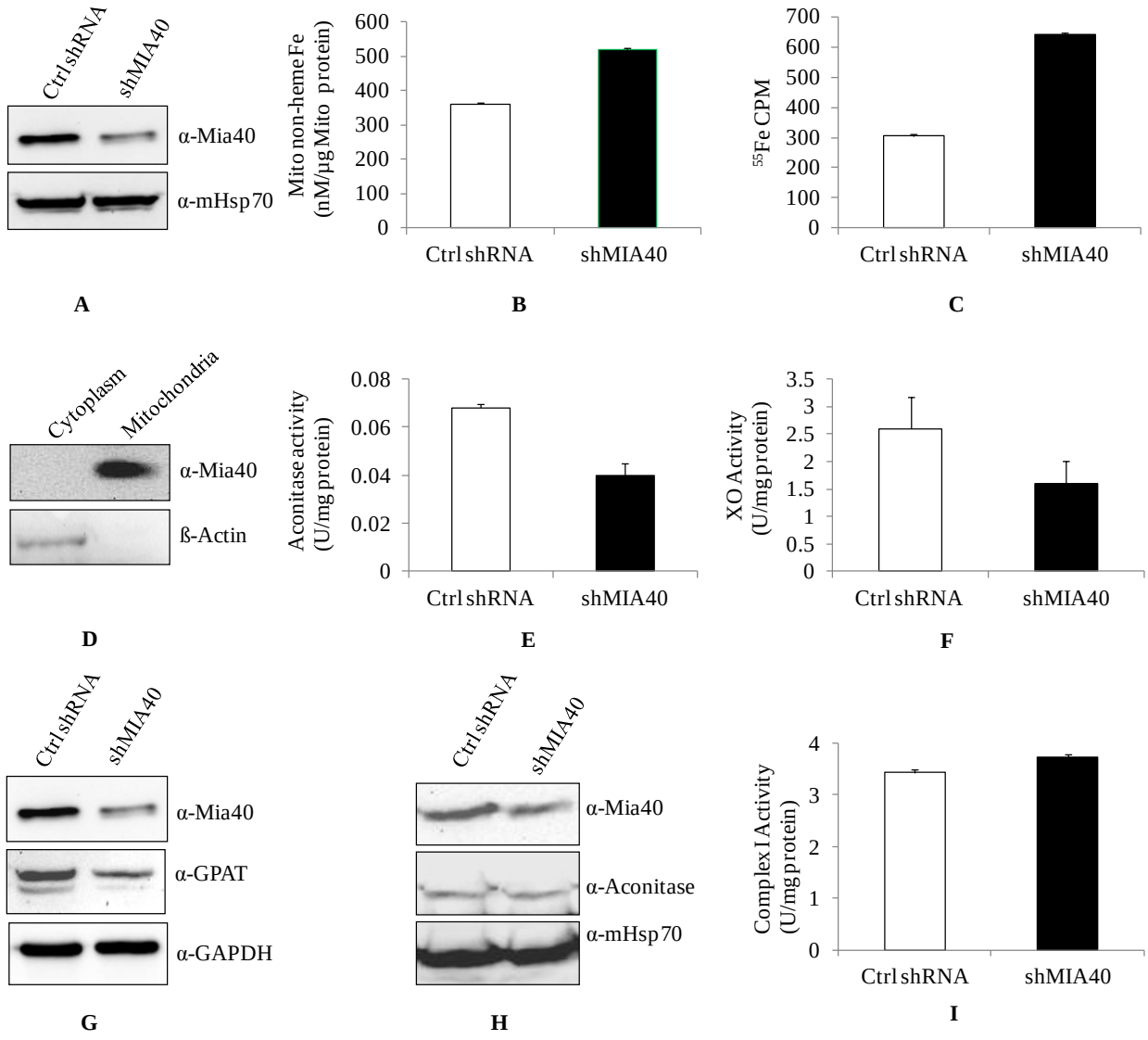

Figure 2.8. Knock down of hMIA40 result in increased levels of mitochondrial iron and decreased activity of cytosolic Fe/S proteins. (A). HEK293T cells were transfected with *MIA40* shRNA or scrambled shRNA vector. Western blot analysis of whole cell extracts of HEK293T cells. The blot was probed with Mia40 and HSP70 antibodies. HSP70 was used as an internal loading control. **(B).** Mitochondrial non-heme iron was measured by bathophenonthroline method as described in the methods section and shown here as nM/□ Mitochondrial non-heme iron **(C).** Radiolabelled ^{55}Fe present in mitochondria was measured in a Beckman scintillation counter and shown as CPM/mg. **(D).** Cytosolic and mitochondrial fractions from HEK293T cells were separated on SDS-PAGE and probed with antibodies specific for actin (cytosolic) and Mia40 (mitochondria). **(E).** Cytosolic aconitase activity was measured at 240 nm and shown here as units/mg protein. **(F).** XO (Xanthine Oxidase) activity was measured spectrophotometrically at 290 nm and the activity is shown here as units/mg protein. **(G).** Western blot analysis of the total cell extract of HEK293T cells treated with *hMIA40* shRNA and vector control. The blot was probed with antibodies against Mia40, GPAT

and GAPDH. GAPDH was used as an internal loading control. **(H).** Western blot analysis of mitochondrial fraction from HEK293T cells treated with *hMIA40* shRNA or vector control for the presence of aconitase, HSP70 and MIA40. **(F).** Reduction of hMIA40 protein levels not alter the mitochondrial biogenesis of Fe/S clusters. Complex I activity was measured in *hMIA40* shRNA cells and control cells spectrophotometrically at 340 nm and presented as units/mg protein.

2.4. Discussion

Mitochondrion is an essential organelle of the cell and has multifarious roles. One of the important functions of mitochondria is the regulation of cellular iron homeostasis. It forms the main hub for synthesis and export of Fe/S clusters. The enzyme components of the ISC synthesis pathway of the mitochondria have been well characterized genetically and biochemically in yeast and bacteria (Frazzon and Dean 2003; Lill and Muhlenhoff 2006). The cytoplasm and the nucleus in higher eukaryotes have their own Fe/S assembly machinery (CIA), nevertheless, perturbations in the mitochondrial ISC pathway causes maturation defects of nuclear and cytoplasmic enzymes that are dependent on Fe/S clusters. This underscores the importance of mitochondrial ISC system in the cellular iron homeostasis. Yet, the molecular mechanism by which the mitochondrial ISC system exports iron to the cytoplasm is to be fully elucidated.

Although, cytosol and nucleus in higher eukaryotes contain its own iron sulfur machinery (CIA), the defect in Fe/S cluster synthesis and exports lead to accumulation of iron in mitochondria and defect in maturation of Fe/S proteins in cytosol and nucleus. Atm1, an inner membrane protein has been identified as an iron sulfur exporter from mitochondria (Kispal, Csere *et al.,* 1997). Although the precise component that is exported by Atm1 from mitochondria is debatable, deficiency of Atm1 lead to iron overload in mitochondria, defect in cytosol and nuclear Fe/S cluster biogenesis and no effect on mitochondrial ISC machinery or stability of Fe/S clusters containing proteins (Kispal, Csere *et al.,* 1999; Lill 2009). The additional components of Fe/S export machinery that are probably working along with Atm1 includes Erv1, a sulfahydral oxidase and glutathione (Lange, Lisowsky *et al.*, 2001; Sipos, Lange *et al.,* 2002) as depletion of these proteins reflects the similar phenotype like Atm1 deficiency. Erv1 has been shown to play a role in combination with Mia40, an intermembrane

space protein, in the import of numerous cysteine rich inter membrane space proteins by an oxidative folding mechanism.

Our *AES* studies using recombinant hMIA40 shows that hMIA40 binds to iron (Fig 2.4B). Visible spectrum of recombinant hMIA40 showed an absorption peak at 410 and 460 nm (Fig 2.5A) which are characteristic peaks for 4Fe-4S and 2Fe-2S clusters respectively. We hypothesize that 4Fe-4S and 2Fe-2S forms are probably coordinated by four or two molecules of hMIA40 respectively through its CPC motif. Further, gel filtration and spectral analysis of recombinant hMIA40 suggest that majority of hMIA40 in a tetrameric state (Fig 2.5B) and probably has a cubane 4Fe-4S clusteras it shows a characteristic 4Fe-4S absorption peak at 410 nmwhereas dimeric form of hMIA40 showed a 460 nm absorption peak which is typical for 2Fe-2S cluster (Cai, Frederick *et al.,* 2013) (Fig 2.5C). Further, SDS-PAGE analysis of recombinant hMIA40 (Fig 2.7C) exhibits the partially stable form of tetramer and unstable dimeric state under reducing conditions. In addition, we observed that redox stability of 4Fe-4S form in the presence of DTT. Further these clusters are very sensitive to oxidative conditions as the addition of H_2O_2 to recombinant hMIA40 completely destabilizes the Fe/S clusters and formation of oligomers are observed which are probably through inter molecular disulfide bonds (Fig 2.7C). In contrast to recombinant protein, western blot analysis of hMIA40 from cell lines showed that majority of dimeric form is stable in the presence of DTT (Fig 2.7D). We cannot explain this ambiguity, but, it may be that 2Fe-2S cluster of hMIA40 is involved in oxidoreductase activity whereas 4Fe-4S cluster is involved in the export of clusters.

Mutation of either of cysteine in CPC motif in hMIA40 causes the decrease in iron binding (Fig 2.6C & D). However, gel filtration analysis shows that majority of single cysteine mutant protein is eluted as tetrameric protein and negligible dimeric and monomeric forms

(Fig 2.6E). The tetrameric form of cysteine mutant shows low level of Fe/S cluster formation. Further,Fe/S cluster in the single cysteine mutants are unstable as we observed mostly a monomeric form in SDS-PAGE. However, substitution of both cysteines with serine completely abolishes the formation Fe/S clusters (Fig 2.6C & D). These studies indicate the CPC motif in hMIA40 is involved in the formation Fe/S clusters.Thus we conclude that certain levels of reducing conditions were required for binding of Fe/S clusters with hMIA40.

The sulfhydryl oxidase activity of Mia40 requires oxidative conditions. Whenever Mia40 is in oxidised state, it is probably involved in the oxidative folding of IMS proteins (Hofmann, Rothbauer *et al.,* 2005; Banci, Bertini *et al.,* 2009; Terziyska, Grumbt *et al.,* 2009). We show that hMIA40 present in both oxidised and reduced state *in vitro* and *in vivo* (Fig 2.7C & D). Further, hMIA40 also exists in metal bound state and metal free state. Our findings suggest that the metal bound hMIA40 converted into oxidised hMIA40 upon exposure to hydrogen peroxide (H_2O_2). The presence of metal bound state and oxidised hMIA40 is probably depends on cellular environment.

The biological significance of Fe/S clusters on MIA40 is not known. Here we show that the role of hMIA40 in cellular iron homeostasis.We used ShRNA to deplete the levels of MIA40 in human cell lines (Fig 2.8A). To assess the mitochondrial iron, we have used two different methods i.e. bathophenonthroline and ^{55}Fe method. These results show a significant accumulation of mitochondrial iron and when we deplete the hMIA40 (Fig 2.8B & C). Further, we have analysed the activity and maturation of cytosolic Fe/S cluster containing enzymes in MIA40 depleted cell lines. The knock down of hMIA40 significantly reduced the activity of cytosolic Fe/S cluster containing enzymes (Aconitaseand Xanthine Oxidase) (Fig 2.8E & F). Further, the stability of GPAT (Glutamate Phosphoribosyl pyrophosphate

Amidotransferase) is altered in the hMIA40 knock down cells (Fig 2.8G). These results suggest that hMIA40 is involved in the export of mitochondrial Fe/S cluster.

Similar observations have also been reported when the dosage of Atm1 in yeast or ABCB7 in mammals, an inner mitochondrial membrane protein was reduced and thereby Atm1 was suggested to be a component of iron sulfur export machinery of mitochondria (Kispal, Csere *et al.,* 1999). Although the precise component that is exported by Atm1 from mitochondria is debatable, deficiency of Atm1 leads to an iron overload in mitochondria accompanied by defects in Fe/S cluster biogenesis that occurs in cytosol and nucleus. However, no apparent effect was observed on mitochondrial ISC pathway or stability of mitochondrial enzymes associated with Fe/S clusters (Kispal, Csere *et al.,* 1999).Besides Atm1, the Fe/S export machinery most likely includes Erv1 in yeast or ALR in mammalian cells, a sulfahydral oxidase and glutathione as depletion of these proteins results in a phenotype similar to that of Atm1 deficiency. We speculate that MIA40 works in conjunction with ALR to export Fe/S cluster from mitochondria as it has already been shown that ALR and MIA40 collaborate in the import of numerous cysteine rich mitochondrial space proteins by an oxidative folding mechanism (Allen, Balabanidou *et al.,* 2005). The genetic mutations in proteins that are involved Fe/S biogenesis may lead to several human disorders. These diseases are ranging from ataxia such as Friedreich's ataxia (FRDA), myopathies and anaemia (Mochel, Knight *et al.,* 2008; Ye, Jeong *et al.,* 2010; Koeppen 2011). Studying the Fe/S synthesis and export from mitochondria would eventually help in development of better therapeutics to various disorders due to genetic mutations in Fe/S cluster biogenesis.

CHAPTER III

Characterization of human TOM40 as a Fe/S protein and its role in iron homeostasis of the cell

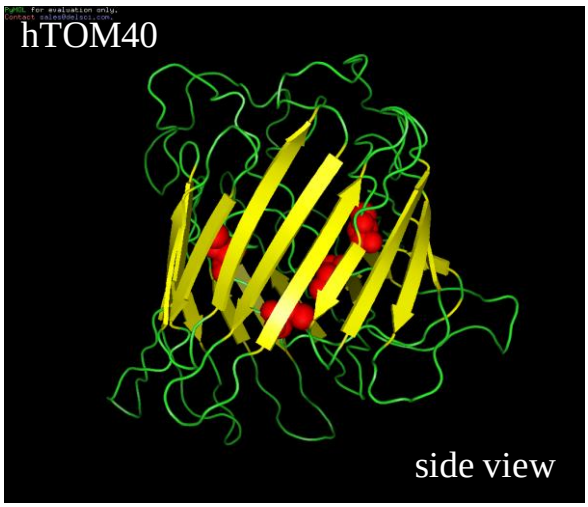

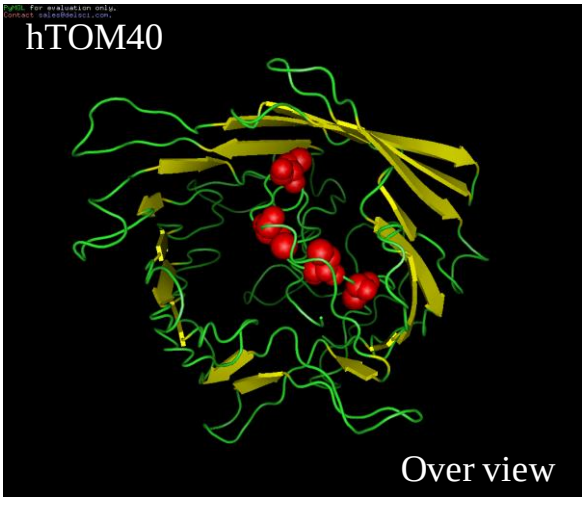

3.1. Introduction

Most of the cytosolic Fe/S clusters containing proteins depend on mitochondrial biogenesis of Fe/S clusters for their activity and stability. Besides the assembly and insertion of Fe/S clusters, the ISC system of mitochondria is also essential for the maturation of cytosolic and nuclear proteins that contain Fe/S clusters (Kispal, Csere *et al.,* 1999; Muhlenhoff, Balk *et al.,* 2004). This process probably uses the Fe/S clusters that are exported through the ISC export machinery that is present in the mitochondria. Atm1, an inner membrane protein of yeast mitochondria and its mammalian homolog ABCB7, Erv1, a sulfahydral oxidase and glutathione have been so far identified as components of iron sulphur export machinery of mitochondria (Leighton and Schatz 1995; Kispal, Csere *et al.,* 1997; Kispal, Csere *et al.,* 1999; Lange, Lisowsky *et al.,* 2001; Sipos, Lange *et al.,* 2002).

In this study, we have identified hMIA40 is involved in the export Fe/S clusters across the intermembrane space of mitochondria. MIA40 being an inter membrane space protein, must act in concert with an outer membrane transporter to export iron across outer membrane. To find out the downstream effectors of MIA40 in iron export, we have looked for the characteristic cysteine motifs in several outer mitochondrial membrane proteins. Interestingly, we found characteristic cysteine motifs (CXC, CX_9C and CX_3C) in outer mitochondrial channel protein TOM40. We hypothesize that these typical cysteine motifs that are present in TOM40 probably important for the binding of Fe/S clusters.

Tom40 is a central pore forming component of TOM complex. All mitochondrial targeted nuclear encoded pre-proteins are imported through the general entry gate, the translocase of the outer membrane or TOM complex (Fig 3.1), Tom40 is an integral membrane protein with a β-barrel structure thatforms the channel for pre-protein translocation across the outermembrane of mitochondria. Further, Tom40 is organized as an oligomer that constitutes

twoto three channels per each TOM complex (Ahting, Thieffry *et al.,* 2001; Model, Meisinger *et al.,* 2008). Tom40 is a component of a multi subunit complex comprising of the receptor proteins Tom20, Tom70 (Lithgow, Glick *et al.,* 1995), a central organizing subunit Tom22 which is involved in the TOM complex stability (van Wilpe, Ryan *et al.,* 1999) and three small proteins Tom5, Tom6 and Tom7 (Alconada, Kubrich *et al.,* 1995; Honlinger, Bomer *et al.,* 1996; Dietmeier, Honlinger *et al.,* 1997).Tom40 is synthesized in the cytosol and contains information in its mature protein for its mitochondrial targeting and assembly.*In vitro* studies with isolated mitochondria and labelled Tom40 reveal thathuman TOM40 assembled into three resolvable complexes in a timedependent manner. Initially human TOM40 precursors are found in a 500kDa complex (Intermediate 1) followed by a smaller 100 kDa complex (Intermediate II) andeventually forming a mature 380 kDa complex (TOM Complex) in a time dependent manner. The process of protein import into mitochondria through the Tom40 channel has been well characterized in lower eukaryotes. It is assumed that similar kind of role for mammalian TOM40 in transporting precursor proteins across outer membrane.

The present study was undertaken with the following objectives;(i) Cloning, expression and purification of hTOM40 (ii) Identification of hTOM40 as a Fe/S protein and (iii) Characterization of hTOM40 in cellular iron metabolism.

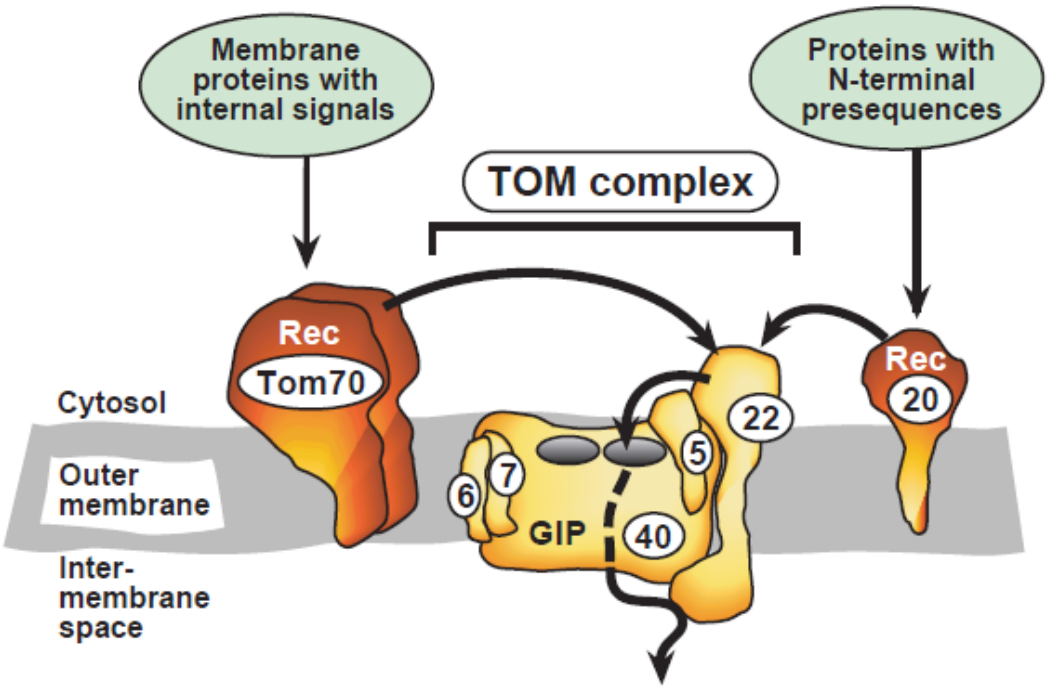

Figure 3.1. Schematic representation of mitochondrial TOM machinery. Mitochondrial precursor proteins synthesized in the cytosol are recognized by two types of receptor proteins integrated in the outer membrane (Tom70 and Tom20). The precursor proteins then transferred to the TOM complex via Tom22 and Tom5 and inserted into the Tom40 channel (General import pore). The small subunits Tom6 and Tom7 mediate the dynamic behaviour of the TOM complex. The precursor proteins reach the intermembrane space via additional interaction sites on the trans side of the membrane, provided by Tom40 and Tom20. Further translocation process then performed by coordination with specific translocation complexes in the inner membrane. Adapted from Wolfgang *et al.,,* 2003.

3.2. Materials and Methods

3.2.1. Materials

LDAO (Lauryl Dimethyl Amine Oxide) and Azolectin was purchased from Sigma Aldrich (USA). Uranyl acetate was purchased from Sigma for electron microscopy. Radiolabel ^{35}S-Methionine was obtained from BARC (Mumbai, India). Alexa conjugated secondary antibodies were purchased from Invitrogen for confocal microscopy. For the silencing of human *TOM40*, shRNA was purchased from ORIGENE. All reagents and chemicals used in the study were of high purity, and purchased either from Sigma or Hi-Media.

3.2.2. Methods

3.2.2.A. Cloning of human TOM40

3.2.2.A.1. cDNA synthesis

HeLa cell total RNA (3 µg) (Bangalore GeNei) was used to clone the *hTOM40* gene. In brief, the following components were added in the following order:

1.3 µg of total RNA,

1 µl of random hexamer primer

8 µl of DEPC water

The contents were mixed and incubated at 65 ^{0}C for 10 min.

Then the reaction was chilled on ice and the following components were added: 4 µl of 5X Reaction buffer, 1 µl of RNase Inhibitor, 2 µl of 10 mM dNTP Mix and 2 µl of M-MuLV Reverse Transcriptase. A total volume of 20 µl of reaction mixture was mixed and incubated at room temperature for 2 min followed by 60 min incubation at 37 ^{0}C. Finally, the reaction was terminated by heating at 95 ^{0}C for 2 min.

3.2.2.A.2. Polymerase Chain Reaction (PCR)

The *hTOM40* ORF was amplified by polymerase chain reaction using HeLa cells cDNA as a template. PCR was carried out in a final volume of 50 µl. The reaction mixture contains 10 pM of each forward primer NB57 Fwp: 5'CTTT GAATTC ACC ATG GGG AAC GTG TTG GCT GCC 3'- (*E.CoR1*) and reverse primer NB60 Revp: 5'CTTT CTCGAG TCA GCC GAT GGT GAG GCC AAA GCC 3'- (*Xho1*) primers specific for *hTOM40*, 2.5 mM each of four dNTPs, 0.5 U of DNA polymerase enzyme and 500 ng of cDNA. The amplification was performed with an initial denaturation step at 95 ^{0}C for 3 min, followed by 35 cycles of 94 ^{0}C: 30 sec, 58 ^{0}C: 30 sec and 72 ^{0}C: 3 min; and a final extension at 72 ^{0}C for 10 min. The amplified product was visualised by 1.5% agarose gel electrophoresis and the amplified product was purified by gel extraction method (QUIAGEN). We also amplified *hTOM40* ORF without stop codon by using forward NB57 Fwp: 5'CTTT GAATTC ACC ATG GGG AAC GTG TTG GCT GCC 3'- (*E.CoR1*) and NB164 Revp: 5'CTTT CTCGAG GCC GAT GGT GAG GCC AAA GCC 3'- (*Xho1*) primers and processed as above.

3.2.2.A.3. Restriction Digestion

The amplified *hTOM40* and pET28 (a^+) / pcDNA3.1 Cmyc vectors were subjected to double digestion with *E.coR1* and *Xho1* restriction enzymes in a 50 µl reaction {(Insert 30 µl; 10X Tango Buffer 10 µl; Milli Q water 9 µl; *E.coR1* 0.5 U; *Xho1* 0.5 U) and (pET 28 (a^+) / pcDNA3.1 Cmyc vector 30 µl; 10X Tango Buffer 10 µl; Millie Q water 9 µl *E.coR1* 0.5 U; *Xho1* 0.5 U)} at 37 ^{0}C for overnight. The digested products were visualised by 1% Agarose gel electrophoresis and the products were excised and gel purified by QUIAGEN gel extraction method.

3.2.2.A.4. Cloning of *hTOM40* with pET28 (a^+)/pcDNA 3.1 Cmyc vector

The digested*hTOM40* fragment was ligated into vector (pET 28 (a^+) / pcDNA 3.1 Cmyc) by using T4 DNA Ligase (Fermentas). The reactions were carried out in a final volume of 15 µl with 150 ng of vector, 3 fold excess of insert, 1 µl of T4 DNA Ligase and 1.5 µl of 10X T4 DNA Ligase Buffer. The reaction mixture was incubated at 18 ^{0}C for overnight and ligated product was transformed into DH5α cells.

3.2.2.A.5. Site Directed Mutagenesis

For the creation of cysteine mutations (C-A) in the *hTOM40*, we employed site directed mutagenesis by using Pfu DNA polymerase. The amplified DNA was treated with Dpn1 enzyme at 37 ^{0}C for 2hrs to digest the methylated DNA. The Dpn1 treated plasmid was transformed into DH5α Cells.The clones were confirmed through the restriction digestion and sequencing. The primers used in the study were listed below.

NB167 Fwp: 5'GAT GGG GCC GCA GGC TGC CTG3' (hTOM40 C74A)
NB168 Revp: 5'CAG GCA GCC TGC GGC CCC ATC3' (hTOM40 C74A

NB169 Fwp: 5'GCC TGC GGC GCA CTG CCC AAC3' (hTOM40 C76A)
NB170 Revp: 5'GTT GGG CAG TGC GCC GCA GGC3' (hTOM40 C76A)

NB171 Fwp: 5'TTC GAG GAGGCA CAC CGG AAG3' (hTOM40 C86A)
NB172 Revp: 5'CTT CCG GTG TGC CTC CTC GAA3' (hTOM40 C86A)

NB173 Fwp: 5'CAC CGG AAG GCA AAG GAG CTG3' (hTOM40 C90A)
NB174 Revp: 5'CAG CTC CTT TGC CTT CCG GTG3' (hTOM40 C90A)

NB175 Fwp: 5'GAG GAG GCA CAC CGG AAG GCA AAG GAG3' (hTOM40 C8690A)
NB176 Revp: 5'CTC CTT TGC CTT CCG GTG TGC CTC CTC3' (hTOM40 C8690A)

3.2.2.A.6. Bacterial Transformation

E.coli DH5α / Rosetta gammie competent cells were used for transformation of ligated products and plasmids. About 10 µl of ligated product / 100 ng of pure plasmid was added to DH5α competent cells and incubated on ice for 30 min; heat shock was given at 42 ^{0}C for 1 min and chilled on ice for 2 min. To this reaction, 1 ml of LB medium was added and incubated at 37 ^{0}C shaker incubator for 60 min and the culture was plated on LB agar plate containing an antibiotic (Kanamycin / Ampicillin). The colonies were screened for the presence of cloned fragment with restriction digestion and sequence was confirmed by automated sequencer.

3.2.2.B. Bacterial expression and protein Purification

3.2.2.B.1. Expression of His tagged hTOM40

The plasmid pET28 (a^{+}) harbouring *hTOM40* and *hTOM40* mutants (C-A) were transformed into *E.coli* Rosetta gammie strain. A colony carrying the pET28-*hTOM40* plasmid DNA was grown for overnight in LB medium containing kanamycin at 37 ^{0}C shaker incubator. The primary culture was diluted to 1:100 in 500 ml fresh LB medium, grown with vigorous agitation to mid logarithmic phase ($OD_{600\ nm}$: 1.0), and incubated at 37 ^{0}C by addition of 1 mM IPTG (Isopropyl-β-D-thiogalactopyranoside) for 3 hrs. Further the culture was centrifuged at 10,000 rpm for 10 min to pellet down the bacterial cells. The pellet was suspended in 50 mM Tris-HCl pH 8.0 by 1/20th volume. The suspended bacterial cells were ruptured by sonication. Then soluble (Supernatant) and insoluble (inclusion bodies) fractions were separated by centrifugation at 10,000 rpm for 10 min. The expressed recombinant proteins were present in inclusion bodies and the inclusion bodies were solubilised in 8 M

Urea buffer (50 mM Tris-HCl pH 8.0). The insoluble recombinant proteins (hTOM40 and hTOM40 cysteine mutants) were purified on a Ni-NTA affinity column (Clontech).

3.2.2.B.2. Recombinant His-hTOM40 Protein purification by Ni-NTA column

The inclusion bodies containing hTOM40 or mutants were solubilised in 50 mM Tris-HCl pH 8.0 and 8M urea. The solubilised inclusion bodies were spun at 10,000 rpm for 10 min and the supernatant was mixed with buffer A (8 M Urea and 50 mM Tris-HCl pH 8.0) equilibrated Ni-NTA beads and kept on rotisserie at room temperature for 2 hrs. Ni-NTA beads were washed with buffer containing 8 M Urea, 50 mM Tris-HCl pH 8.0 and 10 mM Immidazole. The bound protein was eluted by using elution buffer (0.4 M Immidazole pH 7.0, 8 M Urea and 50 mM Tris-HCl pH 8.0).

3.2.2.C. SDS-PAGE analysis

Purified recombinant proteins and HeLa cell lysate were separated on 10% non-reducing and reducing SDS-PAGE (Laemmli 1970).To check the redox states of hTOM40, Mitochondria and hTOM40 protein was treated with or without DTT (Dithiothreitol) prior to resolving it on a 10% SDS-PAGE.

3.2.2.D. Antibodies

The polyclonal antibodies for hTOM40 recombinant protein were raised in rabbit.Recombinant hTOM40 was separated on SDS-PAGE and the band corresponding to hTOM40 was excised, frozen with liquid N_2 and grinded with mortar and pestle. The powdered antigen was mixed either with Freund complete adjuvant or incomplete adjuvant (Bangalore GeNei) for initial and subsequent booster dose (20 days interval for each booster) and injected into the rabbit. After subsequent booster doses, serum was collected from the

rabbit blood. Human Tom40 mono specific antibodies were purified by using antigen coupled sepharose beads (GE Health care). Pre-immune serum was collected from the rabbit prior to raising the antibodies.

3.2.2.D.1. Purification of mono specific antibodies for hTom40

The recombinant purified antigen (Rec.hTOM40 protein) was dialyzed against coupling buffer overnight (0.1 M $NaHCO_3$ pH 8.0 and 0.5 M NaCl) at 4 ^{0}C. The dialyzed antigen in coupling buffer was mixed with CNBr activated sepharose 4B beads and kept on rotisserie for 1 hr at room temperature or overnight at 4 ^{0}C. The beads were washed with coupling buffer and block the remaining active groups with the addition of 0.1 M Tris-HCl, pH 8.0 and incubated at room temperature for 2 hrs. Further, the column was washed 3 times with alternating pH cycle. Each cycle consist of a wash with 0.1 M Acetate buffer pH 4.0 containing 0.5 M NaCl followed by wash with 0.1 M Tris-HCl, pH 8.0 containing 0.5 M NaCl. Finally, the beads were kept in 1X PBS buffer pH 7.2 and stored at 4 ^{0}C. The dialyzed serum against 1X PBS pH 7.2 buffer was mixed with the ligand coupled CNBr activated sepharose beads and kept on a rotisserie for 2 hrs at 4 ^{0}C followed by centrifugation at 5000 rpm for 5 min to pellet down the sepharose beads. The beads were washed with 1X PBS pH 7.2 for 3 times. The bound Mono-specific antibodies were eluted by using 0.1 M Glycine pH 2.5. The eluted antibodies were neutralized with Tris buffer, concentrated and kept frozen at -20 ^{0}C for further use.

3.2.2.E. *In silico* analysis

BLAST-P bioinformatics tool was used for TOM40 sequence alignment. The secondary structure of hTOM40 was predicted by using EASY Pred analysis. And the pore structure of hTOM40 was analyzed by using ITASSAR bioinformatics tool.

3.2.2.F. Spectroscopy analysis

3.2.2.F.1. UV Absorption Spectroscopy analysis

UV-Visible spectra were recorded in 10 mm path length quartz cuvettes using a HITACHI U-2910 spectrophotometer at room temperature in the range 200 nm-700 nm (Gorla and Sepuri 2014).

3.2.2.F.2. Atomic Emission Spectroscopy analysis

The hTOM40 recombinant protein was purified under reducing conditions by adding sodium dithionite (Sigma) followed by converted into protein ash. The protein ash was analysed by using Atomic Emission Spectroscopy (GSI, Hyderabad).

3.2.2.F.3. Circular Dichroism Spectroscopy analysis

Circular Dichroism spectroscopy (CD) measurements for 0.5% LDAO reconstituted (0.5% LDAO, 25 mM Tris HCl pH 8.0 and 1 mM EDTA pH 8.0) hTOM40 and hTOM40 cysteine mutants were performed in quartz cuvettes of 0.1 Cm path length using a Jasco J-815 spectrophotometer. Spectra wererecorded at 20^0C from 200 to 260 nm with a resolution of1.0 nm and an acquisition time of 50 nm/min. Final CD spectra were obtained by averaging three consecutive scans. Further, CD scans were corrected for background bysubtraction of spectra of protein-free samples recorded under the identical conditions.

Mean residue ellipticity (Q) was calculated based on the molar protein concentrationand the number of amino residues of the hTOM40 cysteine mutants. The protein concentrationused for CD spectroscopy was adjusted to 0.1 mg/ml. Sample buffer (0.5% LDAO) was usedfor baseline determination.

3.2.2.G. Reconstitution of TOM40 in liposomes

To prepare TOM40 proteo-liposomes, 1 gm of Azolectin (Sigma) was suspended in 20 ml of 10 mM MOPS pH 7.0 and sonicated the suspension for 7 x 10 Sec with 2 min interval to clear the vesicles (70% duty cycle and output control at 4). The vesicles were kept frozen at -80^{0}C for 30 min. The frozen vesicles were thawed at room temperature and mixed with MEGA-9 (Nonanoyl-N-Methylglucamide-9) detergent to 160 mM. 10 mg (220 µl) of the detergent solubilised vesicles were taken and incubated with 0.1 mg of recombinant urea denatured, purified hTOM40 protein at room temperature for 10 min followed by dialysis against 10 mM MOPS pH 7.0 buffer in the presence or absence of 1 mM DTT for 24 hrs. The dialyzed reconstituted TOM40 vesicles were stored at 4 ^{0}C for further analysis.

3.2.2.H. TEM (Transmission Electron Microscope) analysis of hTOM40 liposomes

TOM40 liposomes (0.1 mg protein/ml) were adsorbed to carbon-coated grids for 30 sec. The grids were washed twice with deionisedwater, blotted with filter paper and stained with 2% (wt/vol) aqueous Uranylacetate (Sigma) for 1 min. TOM40 liposome images were taken by transmission electron microscope operating at 120 kV.

3.2.2.I. Cell Culture and Transfection

HEK293T cells were cultured in Dulbecco'smodified Eagle's medium (Invitrogen) containing 10% (v/v) fetal calf serum at 37 ^{0}C under an atmosphere of 5% CO_2. Cells growing on 175 mm flasks (60% confluence) were transfected with 20 µg of plasmid by using 20 µl of transfectant agent lipofectamine (Invitrogen) in serum free medium. After 6 hours of transfection, the serum free medium was changed with complete medium and cells were analyzed after 36 or 48 hrs of transfection.

3.2.2.I.1. Confocal Microscopy

After 48 hrs of transfection of cells with desired plasmids as described above, the cells on cover slip were washed with 1X PBS buffer andfixed with ice cold (4%) Para-formaldehyde for 20min at room temperature. Cells were permiabilized withice cold acetone and methanol (1:3%) for 20 min followed by washing with TBS (20 mM Tris HCl pH 7.5 and 150 mM NaCl) for 3 times, with 5 min interval. The cells were blocked with 3% BSA in TBS buffer for 1 hr at room temperature. The permiabilized cells were incubated with primary antibody (Mouse C-Myc, 1:200 dilution) in 3% BSA solution at room temperature for 2 hrs followed by washing with TBS, TBST (20 mM Tris HCl pH 7.5, 150 mM NaCl and 0.05% Tween 20) and TBS buffers for 15 min each with shaking. Cells were incubated with secondary antibody (Mouse Alexa conjugated, Invitrogen, 1:200 dilution) at room temperature for 1 hr and washed with TBS, TBST and TBS buffers for 15 min each with shaking. Allowed the cover slip is to dry at room temperature and Anti fade reagent was added to prevent the bleaching of fluorescence.

3.2.2.I.2. Isolation of mitochondria from HEK293T cells

Mitochondria were isolated from HEK293T cell line. Briefly, HEK293T cells were grown as monolayer's and suspended in mitochondria isolation buffer (20 mM HEPES pH 7.5, 1.5 mM MgCl2, 1mM EDTA pH 8.0, 1 mM EGTA, 210 mM Sucrose and 70 mM Mannitol). The cell suspension was homogenized in a Dounce homogenizer. The homogenate was centrifuged at 1000 Xg for 10 min at 4 ^{0}C to separate nucleus and the supernatant was again centrifuged at 10,000 Xg for 15 min at 4 ^{0}C. The resultant mitochondrial pellet was suspended in a buffer containing 250mM Sucrose, 5 mM Magnesium acetate, 80mM Potassium Acetate, 10 mM Sodium Succinate, 1 mM DTT and 20mM HEPES-KOH pH 7.4.

3.2.2.I.3. Isolation of mitochondria from Rat heart

About 0.8-1 gm of rat heart (0.8-1.1 g) was taken into 10 ml of ice-cold medium A (10mM HEPES pH7.5, 220mM Mannitol, 70mM Sucrose, 1 mM EGTA and 2mg/ml BSA) and homogenized for 3 secwith a Polytron homogenizer.The heart tissue homogenate was diluted to 40 ml with medium B (medium A without BSA) and centrifuged at 1800 rpm for 10 min at 4 ^{0}C. The pellet fraction (Nucleus) was discarded and the supernatant was further centrifuged at 7000 rpm for 10 min.The resulting pellet fraction contains mitochondria and it was washed in 10 ml of medium B and centrifuged at 1800 rpm for 10 min.The supernatant was again centrifuged at 7000 rpm to collect the purified mitochondria.The mitochondrial pellet was resuspended in import buffer (250mM Sucrose, 5mM $MgCl_2$,80 mM KCl, 10mM Na-Succinate pH 7.2, 1mMDTT, 0.1mM ADP and 20 mM HEPES-KOH pH 7.4) and used for an *in vitro* import studies.

3.2.2.J. Measurement of Iron in mitochondria

The non-heme iron present in the mitochondria was measured by the bathophenonthroline method (Tangeras, Flatmark *et al.*, 1980). Briefly, mitochondria were suspended in medium containing 10 mM MES pH 4.5, 1 % sodium dodecyl sulphate and 0.5 mM dithionite. To this mixture, 50 µM bathophenonthroline was added, and the Fe (II)-chelate formation was measured in a dual-wavelength HITACHI spectrophotometer at 540 nm and 575 nm. For the measurement of mitochondrial ^{55}Fe content (specific Activity-10.18 mCi/mg), 80% confluent cells were incubated with 500 nM ^{55}Fe for 48 hrs. Mitochondria were washed with cold 500 µM bathophenonthroline to remove membrane bound ^{55}Fe. Radioactivity was quantified by using a Beckman scintillation counter.

3.2.2.K. Immunoprecipitation

HEK293T cells were transfected with mammalian expression vector harbouring the *hTOM40* gene by using lipofectamine transfection reagent (Invitrogen). After 36 hrs of transfection, cells were allowed to grow in serum free DMEM medium for 6 hrs and then incubated with radiolabel ^{55}Fe and 1 mM sodium ascorbate for 2 hrs. Cells were lysed with NP-40 buffer (20 mM Tris HCl pH 8.0, 137 mM NaCl, 10% Glycerol and 1% Nonidet P-40). Cell lysates were incubated with either polyclonal Myc antibody (1 µg) or pre immune serum for 90 min at room temperature followed by addition of protein A/G beads to the lysate and kept on rotisserie for 90 min at room temperature. The supernatant was discarded after centrifugation and the beads were washed with IP buffer for 3 times. The labelled ^{55}Fe present in beads was measured using Beckman scintillation counter.

3.2.2.L. Aconitase activity

The cytosolic Aconitase activity was measured spectrophotometrically. The reaction mixture contains 50 mM Tris-HCl pH 7.5, 1 mM isocitrate as a substrate, 5 mM MgCl2 and cytosolic fraction. The conversion of isocitrate to cis-aconitate was measured as an increase in absorbance at $A_{240\ nm}$. One unit of enzyme activity was defined as the absorbance equivalent of 1 µmole of cis-aconitate released per min per mL of the enzyme solution under experimental conditions.

3.2.2.M. *In vitro* Transcription and Translation

About 500 ng of pcDNA3.1 plasmid harbouring *hTOM40* and its cysteine mutants were incubated with 20 µl of TNT T7 master mix (Promega, USA) and 1 µl ^{35}S-Methionine (specific activity-1000 TBq/mmole) at 30 ^{0}C for 90 min. The translated proteins were

resolved on 10% SDS-PAGE and the proteins were transferred to the nitrocellulose membrane followed by autoradiography.

3.2.2.N. *In vitro* protein Import

Mitochondria were isolated from rat heart as described above. For *in vitro* protein import studies, ^{35}S-labeled hTOM40 and hTOM40 cysteine mutant proteins were incubated with isolated mitochondria at 37 ^{0}C for 60 min.The samples were subjected to 100 mg/ml Trypsin treatment in order to remove non-imported protein and pellet out the mitochondria by passing through sucrose cushion (0.8 M Sucrose and 10 mM HEPES pH 7.5).All mitochondrial pellets were washed with import buffer by centrifugation at 12000 rpm for 5 min and finally re-suspended in SDS sample buffer. The mitochondrial lysates were resolved on10% SDS-PAGE and analyzed by autoradiography.

3.3. Results

3.3.1. *In silico* analysis of hTOM40

We have shown that hMIA40 function as Fe/S cluster exporter in the intermembrane space of mitochondria. Being an inter membrane space protein hMIA40 must act in concert with an outer membrane transporter to export Fe/S across outer membrane. To find out the downstream effectors of hMIA40 in iron export, we have looked for the characteristic cysteine motifs in outer mitochondrial membrane proteins (Fig 3.2A). Interestingly, we found conserved characteristic cysteine motifs ($CXCX_9CX_3C$) in outer mitochondrial channel protein hTOM40. These typical cysteine residues are only present in higher eukaryotes and probably important for the binding of Fe/S clusters. Based on the EASY PRED and ITASSAR bioinformatics tools, the secondary structure of hTOM40 was predicted and it shows that majorly of TOM40 contains β-barrel structure like yeast counterpart and cysteine rich domain exposed towards the intermembrane space side (Fig 3.2B & C). These results suggest that hTOM40 contains typical cysteine motifs like other Fe/S cluster containing proteins.

CXC X9 C X3 C

```
H.sapiens          ATASASGAAEDGACGCLPNPGTFEECHRKCK---ELFPIQMEGVKLTVNKGLSN--HFQV
B.taurus           AAGSAAGTADDGACGCLPNPGTFEECHRKCK---ELFPIQMEGVKLTVNKGLSN--HFQV
M.musculus         AASGAAAASEDGSCGCLPNPGTFEECHRKCK---ELFPVQMEGVKLTVNKGLSN--RFQV
R.ratus            AASGAAASSNDGNCGCLPNPGTFEECHRKCK---ELFPVQMEGVKLTVNKGLSN--RFQV
D.melanogaster     EGLDSLAAAKD---AALENPGTVEELHKKCK---DIQAITFEGAKIMLNKGLSN--HFQV
S.cerevisiae       VVDTYKQLHSHRQSLELVNPGTVENLNKEVSRDVFLSQYFFTGLRADLNKAFSMNPAFQT
```

A

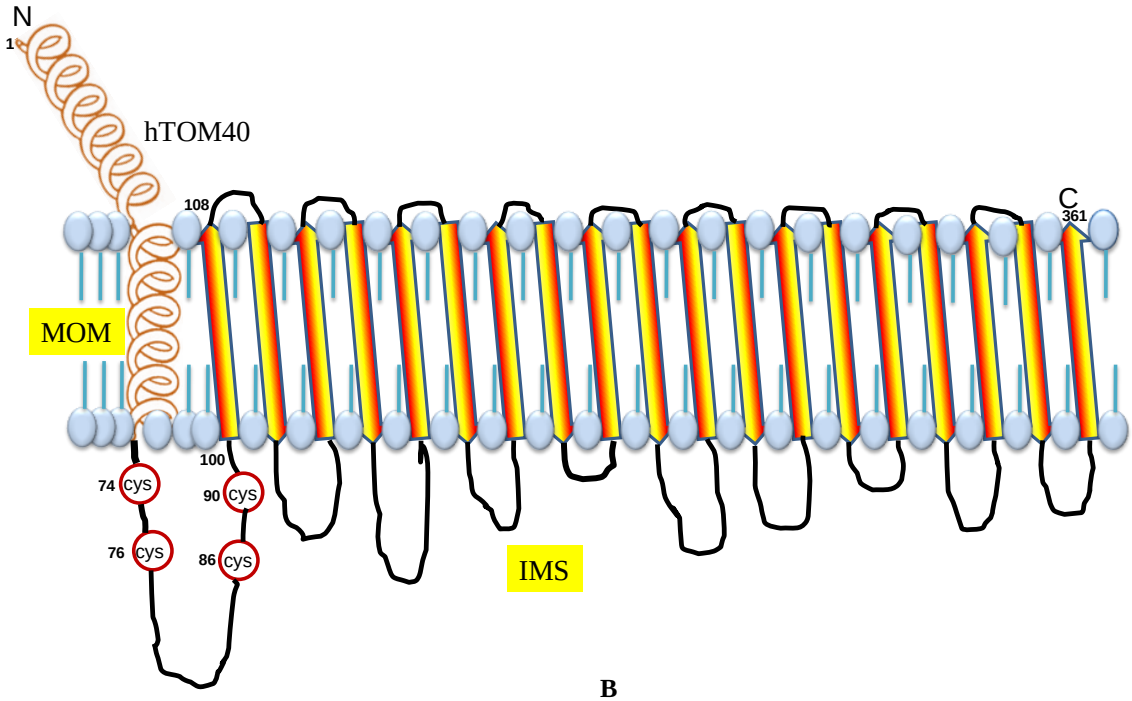

B

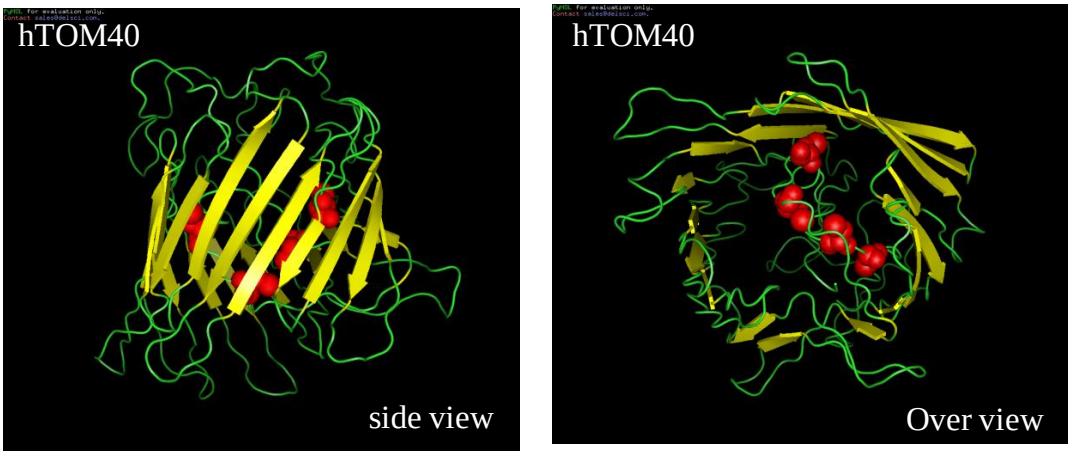

C

Figure 3.2. *In silico* analysis of hTOM40. (A). The sequence alignment of eukaryotic Tom40 by clustalW software showing that mammalian TOM40 having three conserved cysteine motifs (CXC, CX_9C & CX_3C). The cysteine residues are located in the human TOM40 at 74, 76, 86 & 90th position.

(B). Secondary structure of hTOM40 was predicted by using EASY-PRED analysis. The predicted secondary structure of hTOM40 majorly shows a β-sheet. **(C).**The pore structure of hTOM40 was predicted by using ITASSER. It shows that cysteine motifs exposed towards the intermembrane space of mitochondria.

3.3.2. Cloning, Expression, purification and raising antibodies for hTOM40

To further characterize the role of hTOM40 in cellular iron homeostasis and to elucidate the biogenesis of hTOM40, we have cloned *hTOM40*. In brief, total cDNA was made from HeLa cells RNA (Bangalore GeNei) by using reverse transcriptase enzyme. From the total cDNA, the *hTOM40* was amplified by using *hTOM40* ORF specific primers (NB57 and NB60) and the amplified product was shown in Fig 3.3A. Further, we cloned human *TOM40* gene into pET28 vector for bacterial expression (Fig 3.3B). The clone was confirmed by restriction digestion with *EcoR1&Xho1* enzymes and the sequence was confirmed by automated sequencing (Bioserve, India).

The pET28 vector harbouring *hTOM40* gene was transformed into *E.coli* Rosetta gammie bacterial strain. Expression of recombinant protein was induced with the addition of 1 mM isopropyl-β-D-thiogalactopyranoside. The recombinant protein was expressed as insoluble (Inclusion bodies) form. The insoluble recombinant protein was purified by Ni-NTA affinity column (Clontech) as described in the methods (Fig 3.3C).

The polyclonal antibodies for hTOM40 protein were raised in rabbit and mono-specific antibodies were purified using antigen coupled CNBR-sepharose beads as described in methods. To check the specificity of antibodies, the purified recombinant hTOM40 and mitochondrial fraction isolated from rat liver were separated on SDS-PAGE and western blotted (Fig 3.3D). Tom40 antibody detects the 40 KDa band that corresponds to the apparent molecular weight of TOM40in both recombinant and rat liver mitochondrial fraction lane (Fig 3.3D).

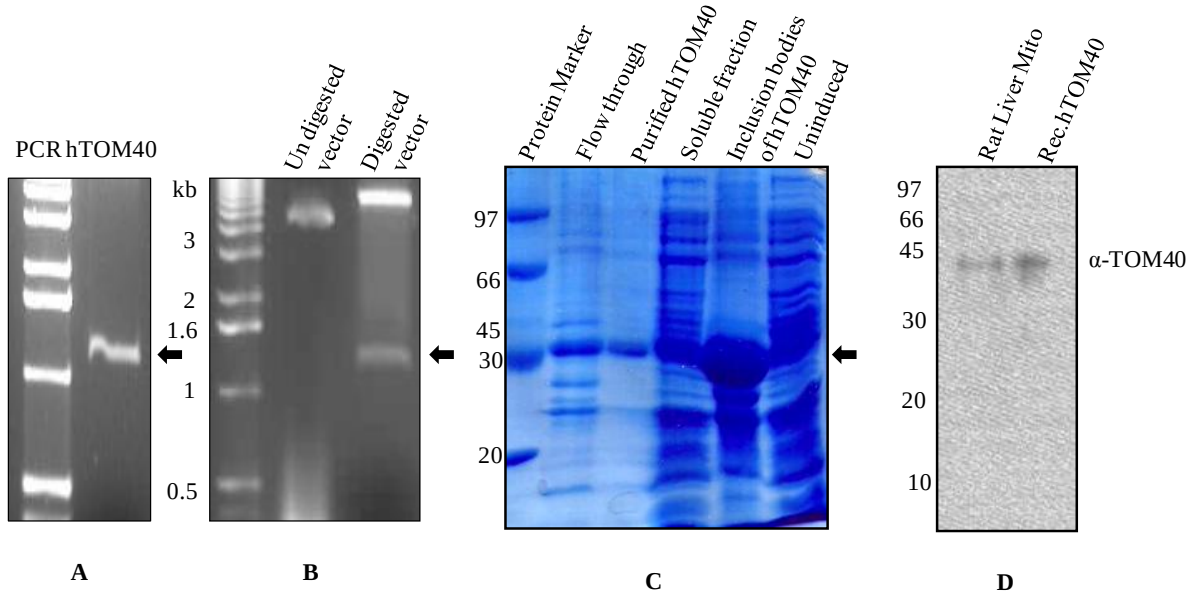

Figure 3.3. Cloning, Expression, purification and raising of antibodies against hTOM40. To characterize the hTOM40 *in vitro*, we have cloned *hTOM40* into bacterial expression vector pET28 (a^+). **(A).** 1% Agarose gel electrophoresis analysis of PCR amplified *hTOM40* gene. Arrow indicates the *hTOM40* amplicon. **(B).** Restriction digestion of pET28-*TOM40* with *EcoR1&Xho1* enzymes to confirm the clone. Arrow indicates the *hTOM40* insert. **(C).** Bacterial expressed recombinant His-hTOM40 was purified by using Ni-NTA column and further analysed by 10% SDS-PAGE. Arrow indicates the expressed His-hTOM40 protein. **(D).** Polyclonal antibodies were raised against hTOM40 in rabbit and purified. The antibody specificity was checked by western blot analysis of recombinant hTOM40 and rat liver mitochondrial fraction.

3.3.3. Human TOM40 is a 4Fe-4S cluster containing protein

Our bioinformatics results suggest that hTOM40 may contain Fe. To confirm whether hTOM40 contains Fe, the purified recombinant protein was further subjected to Atomic Emission Spectroscopy (AES) analysis (Spiller, Ang *et al.*, 2013). As shown in Fig 3.4A, recombinant hTOM40 indeed contains a significant amount of iron and a small amount of Mn. The molar ratio of protein to metal is around 0.04 indicating that like hMIA40, a certain fraction of hTOM40 has the ability to bind to iron *in vitro*.

We further investigated whether hTOM40 can bind to iron *in vivo*.To enrich for endogenous hTOM40 *in vivo*, HEK293T cells were transiently transfected with plasmid

containing pcDNA-Myc*TOM40*and incubated with ^{55}Fe for 24 hrs. Thereafter, cells were harvested, lysed and the cell lysates were subjected to immunoprecipitation with Myc antibody or non-specific IgG. The amount of radioactivity present in the immunoprecipitate was determined in a scintillation counter (Fig 3.4B). Immunoprecipitate of cell lysate upon using Myc antibody was more enriched in ^{55}Fe compared to immunoprecipitate from non specific IgG. We validated the immunoprecipitation of Myc-TOM40 by probing the immunoprecipitated samples with the antibody specific for Myc (Fig 3.4C). Taken together, our results indicate that hTOM40 binds to iron both *in vitro* and *in vivo.*

To further characterize the nature of Fe that was associated with hTOM40, we performed UV-Vis absorption spectroscopy for affinity purified recombinant hTOM40 as described in methods. When purified recombinant protein was subjected to UV-Vis spectrum, we observed a small but significant peak at 410 nm indicating the presence of 4Fe-4S cluster (Fig 3.4D) (Cai, Frederick *et al.,* 2013). A small peak may be due to loss of most of TOM40 associated Fe/S clusters during purification of protein under denaturing conditions. In summary, our results show that hTOM40 is probably a 4Fe-4S containing protein.

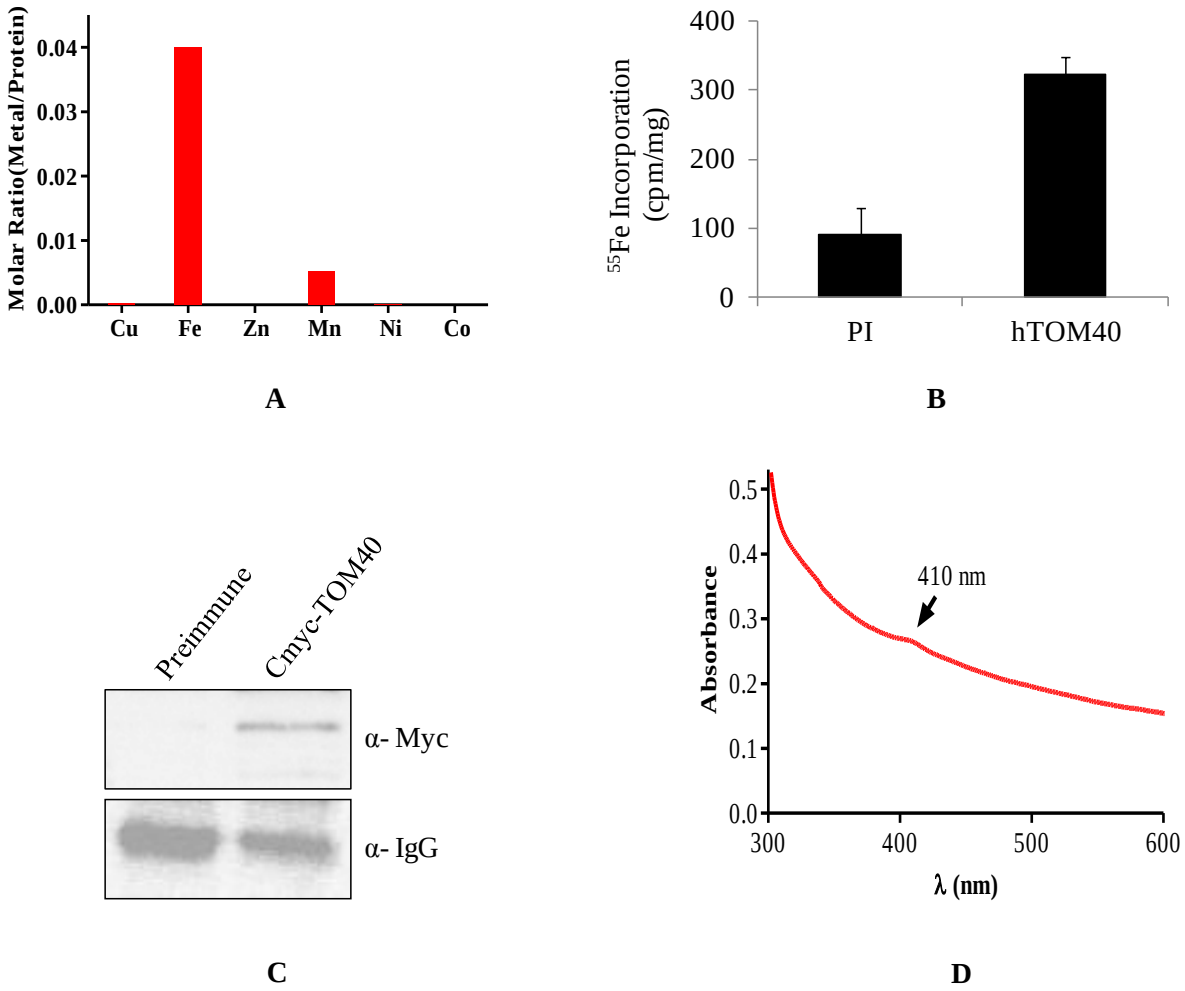

Figure 3.4. Human TOM40 is a Fe/S cluster binding protein. (A). *E.coli* lysate containing recombinant His-hTOM40 was purified by Ni-NTA column under reduced conditions. AES analysis (GSI, Hyderabad) of purified recombinant His-hTOM40 was carried out as described under methods section and the metal content is shown here. **(B).** HEK293T cells were transiently transfected for over-expression of Myc-His-hTOM40 followed by incubation with labelled ^{55}Fe. Cell lysate were prepared by using NP40 buffer as described in methods section. Immunoprecipitation was carried out with either pre-immune serum (PI) or Myc antibody. Labelled ^{55}Fe present in immunoprecipitate was measured in a scintillation counter and shown here as CPM/mg protein. **(C).** Immunoprecipitated samples were separated on SDS-PAGE and probed with antibodies specific for Myc and IgG. **(D).** UV-Vis spectra (300 nm-700 nm) of purified recombinant His-hTOM40 was carried out as described in the Methods. Arrow indicates the characteristic 4Fe-4S peak at 410 nm.

3.3.4. Effect of redox reagents on hTOM40 Fe/S cluster stability

The iron sulfur clusters were more sensitive when MIA40 was exposed to oxidative environment as described in earlier chapter (Fig 2.7B).Similarly, we observed that the characteristic 4Fe-4S cluster peak at 410 nm is gradually decreased when purified hTOM40 protein was exposed to air at room temperature Fig 3.5A. This indicates the stability of Fe/S associated with TOM40 is dependent on the redox environment.

Further, the purified TOM40 was treated either with reducing agent (DTT) or oxidative agent (H_2O_2) and analyzed the stability of Fe/S cluster by performing UV-Vis spectrum. In the presence of DTT, a characteristic absorbance peak of 4Fe-4S at 410nm is observed whereas no such peak is observed when TOM40 was treated with H_2O_2 indicating the destabilization of Fe/S cluster (Fig 3.5B). The disassembly of Fe/S cluster in hTOM40 may be due to oxidation of cysteine motifs upon exposure to hydrogen peroxide.

TOM40 is an integral membrane protein. It is known that integral membrane protein functions are modulated by the surrounding lipid molecules and interacting proteins in the membrane. Thus it is difficult to analyze the functions of membrane protein *in vivo* as they are prone to aggregation in solution. However, it is possible to extract some *in vivo* functions of membrane proteins by reconstituting them in membranes or at certain extent in detergent (Maurya and Mahalakshmi 2013). To mimic the membrane environment, we reconstituted the recombinant urea denatured TOM40 in liposomes, a unilamellar phospholipid vesicles, to study the *in vivo* functions of TOM40 as described in the Methods. We also analyzed the redox state of TOM40 proteo-liposomesby treating withor without reducing agent (Dithiothreitol) followed by non reducing SDS-PAGE and probing with hTom40 antibodies(Fig 3.5C). In the presence of reducing agent recombinant hTOM40 migrates as a 40 kDa protein. However, in the absence of reducing agent hTOM40 migrates at ~38 kDa,

which may be due to oxidation of sulfahydral groups on TOM40.However, we could not observe any metal mediated formation of higher order structures of hTOM40 *in vitro*. Thismay be due to four cysteine residues in monomeric TOM40 are sufficient to associate with 4Fe-4S cluster. Further, cell extracts from HEK293 cell lineswas treated with or without reducing agent and subjected to SDS-PAGE followed by immunoblotting with antibodies specific for Tom40 (Fig 3.5D). As shown in Fig 3.5C, TOM40 antibody detects a band at ~38 kDa in the absence of DTT and migrates at ~40 kDa band in the presence of DTT. The faster migrating band may represent an oxidized form of TOM40. Although, an equal amount of protein was present in both lanes, the amount of TOM40 detected in the lane without DTT is very low. One of the reasons that could attribute to this low signal of TOM40 is may be the formation of insoluble disulphide linked aggregates of TOM40 that is not able to enter the gel in the absence of a reducing agent.

To analyze whether hTOM40 can undergo disulfide mediated oligomerization, the reconstituted TOM40 vesicles, mitochondrial fraction isolated from rat heart and cell extracts from HEK293 cells expressing Myc tagged TOM40 were resolved on non-reducing SDS-PAGE in the presence and absence of reducing agent (DTT) and probed the whole blot either with Tom40 or Myc antibody. In the absence of DTT, hTOM40 antibody or Myc antibody detected a dimer and other higher order structures in all the samples described above (Fig 3.5E).

In summary, these results suggest that hTOM40 is an iron sulfur protein and can exist in an oxidized and reduced form and can form disulfide mediated oligomers both *in vitro* and *in vivo.*

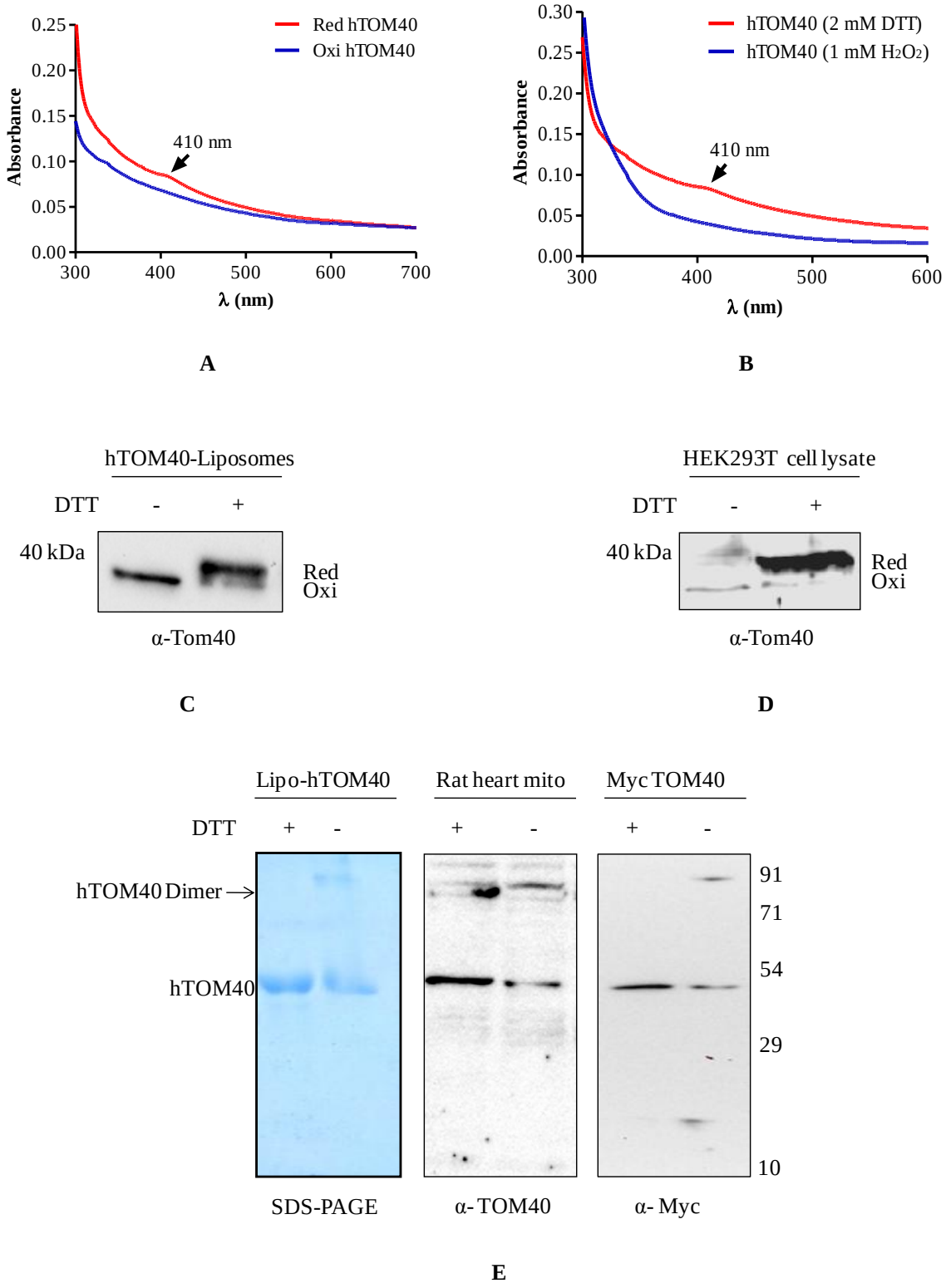

Figure 3.5. Effect of redox reagents on hTOM40 Fe/S cluster. (A). UV-Vis spectra (300 nm-700 nm) of purified recombinant His-hTOM40 were carried out as indicated in the Methods. Arrows indicate the characteristic 4Fe-4S peak at 410 nm. **(B).** UV-Vis spectra of recombinant His-hTOM40 protein in the presence and absence of 2 mM DTT is shown with wavelength on X- axis and

absorbance on Y- axis. **(C).** Analysis of hTOM40 redox state *in vitro.* Liposome reconstituted recombinant His-hTOM40 protein was treated without or with 5 mM DTT and followed by non reducing SDS-PAGE analysis. The reduced (Red) and oxidised (Oxi) states were indicated. **(D).** Analysis of cysteine redox state of hTOM40 by using reducing agent *in vivo.* HEK293T cells were treated without or with 5 mM DTT (Dithiothreitol) followed by extraction of cell lysates as described in methods and analysed the samples by western blot. **(E).** Liposome reconstituted recombinant hTOM40 protein, rat heart mitochondria and TOM40 over expressed HEK293T cell lysate were resolved on non reducing SDS-PAGE. First panel stained with coomassie R250, 2nd and 3rd panel probed with TOM40 and Myc antibodies respectively. Arrow indicates the hTOM40 dimer.

3.3.5. Role of hTOM40 in cellular iron homeostasis

Our *in vitro* and *in vivo* studies clearly demonstrate that hTOM40 binds to iron. In the second chapter we have shown that hMIA40 function as Fe/S cluster exporter in the intermembrane space of mitochondria. Being an inter membrane space protein, hMIA40 must act in concert with an outer membrane transporter to export Fe/S across outer membrane. To find out the downstream effectors of hMIA40 in iron export, we have looked for the characteristic cysteine motifs in outer mitochondrial membrane proteins (Fig 3.2A). Interestingly, we found conserved characteristic cysteine motifs ($CXCX_9CX_3C$) in outer mitochondrial channel protein hTOM40. These typical cysteine residues are important for the binding of Fe/S clusters. Based on these findings, we further hypothesized that hTOM40 may be playing a role in cellular iron homeostasis. To determine if hTOM40 has any effect on iron homeostasis, we initially depleted *hTOM40* in HEK293T cells by transiently transfecting the cells with *TOM40* shRNA.

In parallel, we also transfected HEK293T cells with scrambled shRNA to serve as a control. To ascertain the level of hTOM40, SDS-PAGE followed by immunoblot analysis was carried out on mitochondria samples that were isolated from transfected cells (Fig 3.6A). Transfection with shRNA specifically reduced TOM40 levels by 60% compared to control

cells while the level of mitochondrial Hsp70 was similar in both samples indicating equivalent loading (Fig 3.6A).

The amount of iron present in mitochondria that was isolated from the transfected cells was measured using bathophenonthroline. Depletion of hTOM40 is correlated to increased accumulation of non-heme iron in mitochondria (Fig 3.6B). We repeated this experiment by performing transfections in presence of radioactive iron. Consistent with the previous result, we observed accumulation of ^{55}Fe in mitochondria that was isolated from cells depleted in hTOM40 (Fig 3.6C). We rule out the possibility of cytosolic contamination as negligible amount of actin, a cytosolic marker protein was present in our mitochondrial preparations (Fig 2.8D). We conclude that hTOM40 may be required for export of Fe/S from mitochondria to cytosol.

Several cytosolic enzymes are dependent on Fe/S clusters that are exported from mitochondria for their activity (Kispal, Csere *et al.*, 1999). As depletion of hTOM40 affected the export of iron from mitochondria to cytosol, we additionally wished to probe if this affected the function of cytosolic enzymes that are associated with Fe/S clusters. We monitored the activity of cytosolic enzyme aconitase in control cells and cells that were depleted for hTOM40 as described for MIA40. The activity of aconitase was significantly lowered in cytosolic fraction obtained from cells that were depleted for hTOM40 compared to control sample (Fig 3.6D). The stability of cytosolic Glutamate Phosphoribosyl Pyrophosphate Amidotransferase (GPAT) is dependent on the presence of 4Fe-4S cluster and hence its stability could serve as a hallmark for the presence of cytosolic 4Fe-4S assembly (Sheftel, Stehling *et al.*, 2010). The total cell extract of the hTOM40 depleted cells and control cells were resolved on SDS-PAGE and the level of GPAT enzyme was monitored by immunoblot analysis (Fig 3.6E). We find that depletion of hTOM40 reduces the stability of

GPAT enzyme compared to control cells although comparable amount of GAPDH is present in both fractions. Further experiments like mutational studies, mitochondrial complex I activity and mitochondrial aconitase activities are required to show the role of hTOM40 in the export of Fe/S cluster across the outer mitochondrial membrane. These studies indicate that the hTOM40 has a pronounced effect on the cytosolic Fe/S cluster assembly and on the activity and stability of cytosolic enzymes present in the cytosol. Taken together, our results suggest that hTOM40 probably involved in the mitochondrial Fe/S export machinery and thereby affects cellular iron homeostasis.

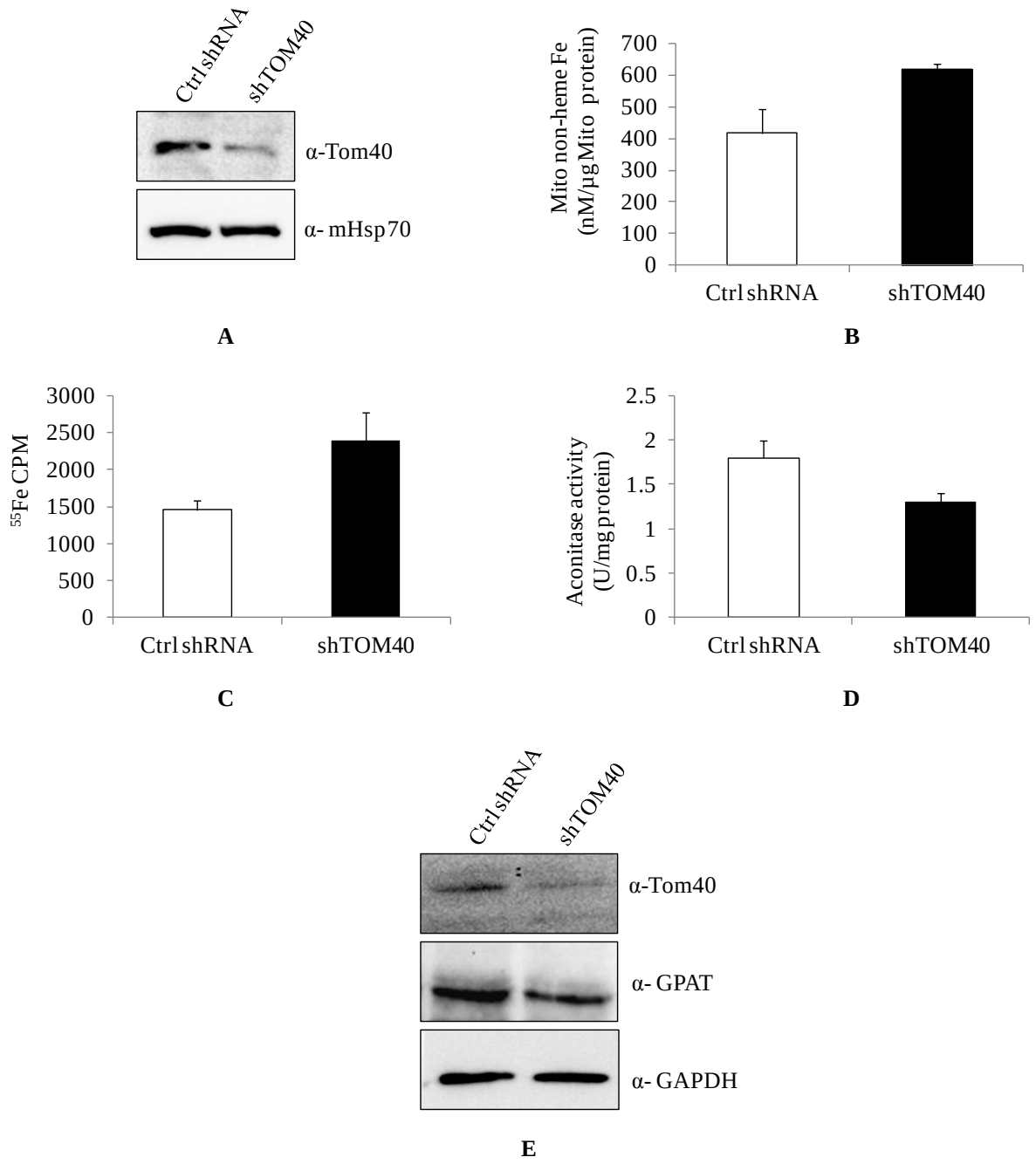

Figure 3.6. Knock down of hTOM40 result in increased levels of mitochondrial iron and decreased activity of cytosolic Fe/S proteins. (A). HEK293T cells were transfected with *TOM40* shRNA or scrambled shRNA vector. Western blot analysis of whole cell extracts of HEK293T cells. The blot was probed with Tom40 and HSP70 antibodies. HSP70 was used as an internal loading control. **(B).** Mitochondrial non-heme iron was measured by bathophenonthroline method as described in the methods section and shown here as nM/µg of mitochondrial protein. **(C).** Radiolabelled ^{55}Fe present in mitochondria was measured in a Beckman scintillation counter and shown as CPM/mg. **(D).** Cytosolic aconitase activity was measured at 240 nm and shown here as

units/mg protein. **(E).** Western blot analysis of total cell extraction of HEK293T cells treated with *hTOM40* shRNA and vector control. The blot was probed with antibodies against Tom40, GPAT and GAPDH. GAPDH was used as an internal loading control.

3.3.6. Human TOM40 interacting with hMIA40 *in vitro*

Our results show that hTOM40 has characteristic cysteine motifs, binds to Fe/S and is involved in the cellular iron homeostasis. We are hypothesizing that both TOM40 and MIA40 are components of ISC export machinery of mitochondria. It is possible that hMIA40 transfers Fe/S cluster from IMS to the outer mitochondrial membrane protein, hTOM40. TOM40 is probably involved in the export of Fe/S to cytosol. If MIA40 is interacting with TOM40 through a sulfahydral groups, a transient intermediate TOM40-MIA40 complex should be observed when we perform an experiment *in vitro* with purified proteins under non-reducing conditions. To test this hypothesis, initially, we have performed a preliminary an *in vitro* interaction assay without or with recombinant hMIA40 and ^{35}S radiolabel hTOM40. ^{35}S radiolabelled hTOM40 (Fig 3.7A) was incubated with or without affinity purified recombinant hMIA40 protein (Fig 3.7B) at room temperature for 20 min. The samples were resolved on 10% SDS-PAGE in the presence and absence of DTT. In the absence of DTT (Fig 3.7C), we observed a migration of radiolabelled TOM40 at ~40 kDa (lane no. 1). However, in the presence of MIA40, radiolabelled TOM40 migrates at 60 kDa (lane no. 2). The observed 60 kDa band is likely to represent a TOM40-MIA40 complex. However, reduced conditions do not favour the formation of hTOM40-hMIA40 complex even in the presence of recombinant MIA40 indicating that these intermediates are disulfide mediated. This *in vitro* interaction of hTOM40 with hMIA40 may suggest that Fe/S clusters are may be transferred to TOM40 from MIA40. However, further experiments with mutants and radiolabelled iron are required to confirm the transfer of Fe/S from MIA40 to TOM40.

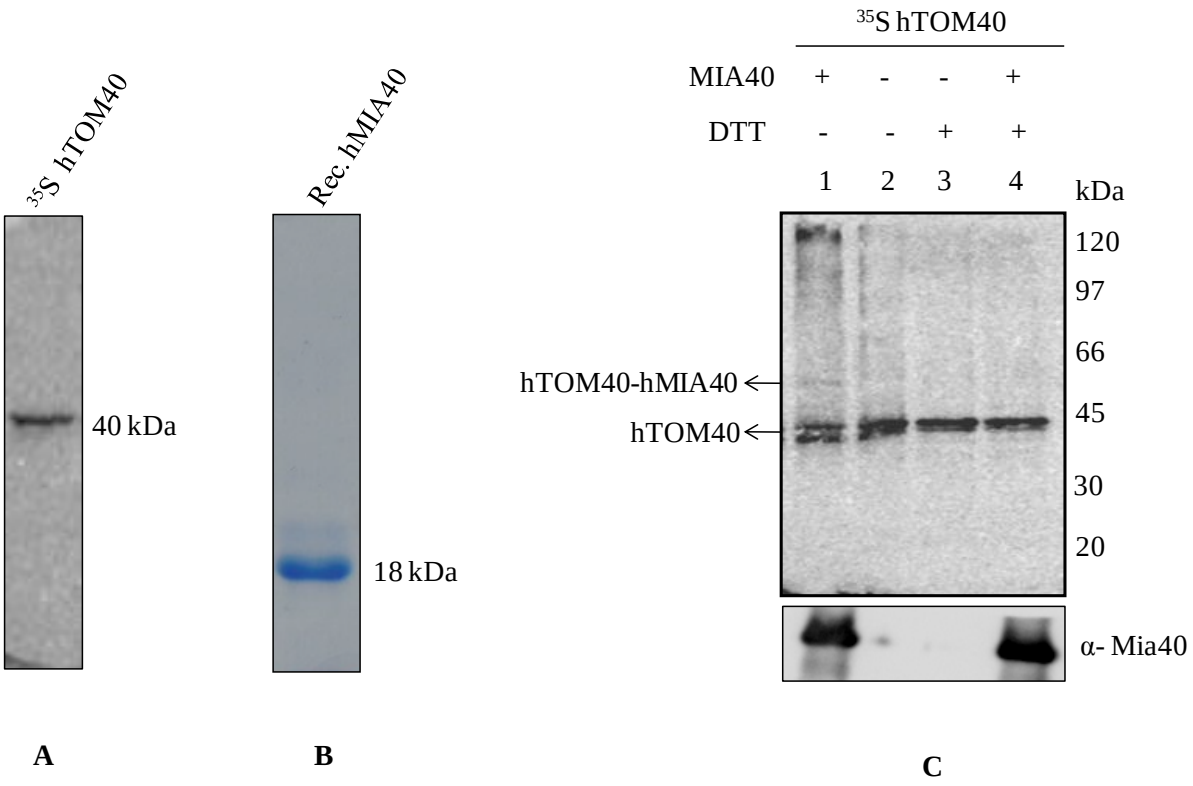

Figure 3.7. *In vitro* interaction of hMIA40 with hTOM40. (A).*In vitro* coupled Transcription/Translation system was used for synthesis of ^{35}S hTOM40 and further analysed by autoradiography. **(B).** Bacterial expressed recombinant His-hMIA40 was purified by using Ni-NTA column and analysed by 12% SDS-PAGE. **(C).** The *In vitro* Translated hTOM40 protein was incubated with recombinant His-hMIA40 protein at room temperature for 20 min and analysed by non-reducing SDS-PAGE followed by autoradiography. Arrows indicates the hTOM40 and hTOM40-hMIA40 intermediate.

3.3.7. Effect of redox reagents on pore structure of hTOM40

The redox environment is probably required for stability of Fe/S clusters associated with hTOM40. To further analyze the role of redox environment in channel or pore forming ability of recombinant hTOM40, we reconstituted the urea denatured recombinant TOM40 in liposomes in the presence and absence of DTT to mimic the oxidative and reducing conditions respectivelyas described in the methods. It has been shown that reconstituted recombinant *Neurospora* Tom40 liposomes can form structures with 2-3 pores like the native TOM complex *in vitro* under negative stained transmission electron microscopy (Ahting,

Thieffry *et al.,* 2001). We analyzed the reconstituted TOM40 vesicles by negative staining TEM analysis as described in the Methods. The electron micrographs of hTOM40 liposomes reconstituted under oxidative conditions displayed predominantly a 2-3 stain filled openings or pores whereas hTOM40 liposomes reconstituted under reducing conditions displayed structures with 1-2 pores (Fig 3.8A & B). The measured each pore size of hTOM40 is around 20 ^{0}A in diameter which is equivalent to observed pore size of native or recombinant Tom40 (Kunkele, Heins *et al.,* 1998).We performed a statistical analysis for assembled hTOM40 pore structures by visually selecting the stain filled structures from electron micrographs Fig 3.8C).The results show that TOM40 vesicles under reduced conditions display more number of structures with single pore and few structures with 2 or 3 pores whereas TOM40 vesicles that were reconstituted under oxidized conditions display structures with maximum number of 2 or 3 pores and few structures with single pore (Fig 3.8C). These results suggest that the oxidative conditions favour the formation of optimal number of pores with reconstituted TOM40 vesicles.

In summary, TEM analysis of reconstituted TOM40 vesicles confirms that oxidative conditions favours the releasing of Fe/S clusters but required for the assembly of hTOM40 or optimal pore structures formation. In contrast, reduce conditions favour the binding of Fe/S clusters to the TOM40 protein and does not form optimal pore structure *in vitro*. Further studies are required to understand the mechanistic details of Fe/S cluster binding and release, assembly of pore forming structures of TOM40 with respect to import of precursor proteins and Fe/S export from mitochondria.

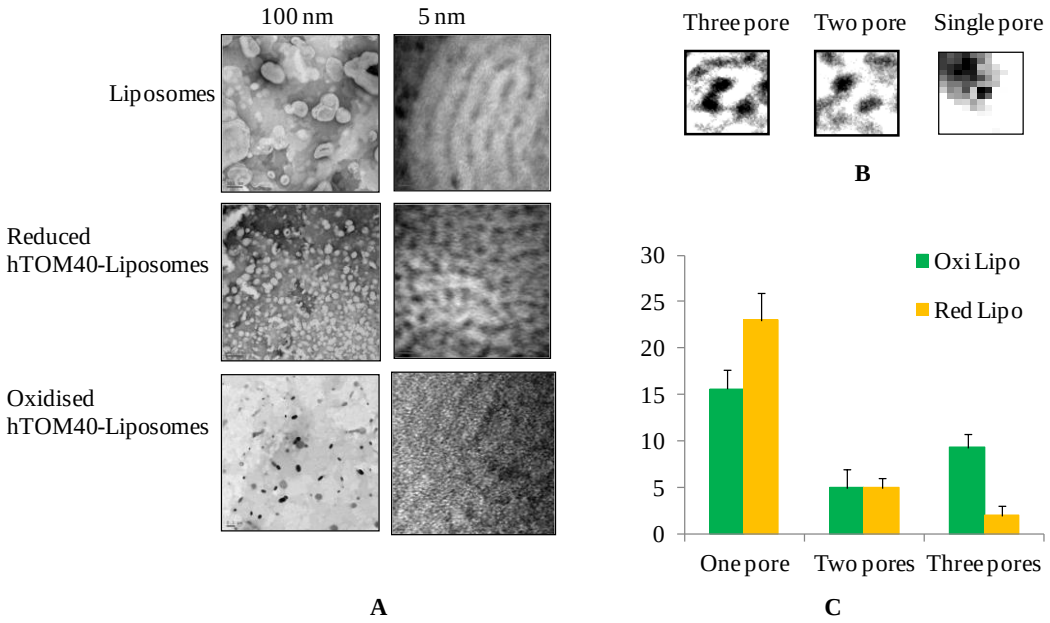

Figure 3.8. Redox reagents affect the pore structure of hTOM40. (A). hTOM40 liposomes were applied to carbon-coated grids for electron microscopy and were negatively stained with 2% Uranyl acetate and analyzed by TEM (Electron micrographs of Liposomes and hTOM40 liposomes, Scale bar-100 nm & 5 nm). **(B).** Selected images of hTOM40 pores under reduced and oxidized conditions (Pore average size 2 nm). **(C).** Statistical analysis of number of assembled pores represented by histograms.

3.3.8. Role of cysteine residues in Fe binding, mitochondrial targeting and assembly of hTOM40

Majority of Fe/S clusters in proteins are coordinated by four cysteine residues. Human TOM40 also contains four cysteine residues and they are arranged as $CXCX_9CX_3C$ motif. To understand the role of cysteines in iron binding and assembly of hTOM40, we have created a single or double cysteine mutations (C-A) by site directed mutagenesis in pcDNA3.1 vector as described in methods (Fig 3.9A). These mutants were analyzed for mitochondrial targeting by the following methods.

Confocal Microscopy: HELA cells were co-transfected with the plasmid pcDNA 3.1 harbouring either *WT hTOM40* or *hTOM40* cysteine mutants (C-A) and Mito-GFP, a GFP

sequence is tagged to mitochondrial targeting sequence, for 36 hrs. The samples were processed for confocal microscopy as mentioned in methods (Fig 3.9B). Human TOM40 wild type and cysteine mutants (C-A) are co-localized with Mito-GFP indicating that cysteine mutants does not affect the mitochondrial targeting of TOM40.

***In vitro* import assay:**Further, we analyzed the targeting of wild type and cysteine mutants to mitochondria by an *in vitro* import assay. We performed an *in vitro* transcription and translation of wild type and cysteine mutants of TOM40 by using T7 TNT quick system with ^{35}S labelled Methionine at room temperature for 90 min. We carried out an *in vitro* import of ^{35}S labelled wild type and mutants (C-A) with isolated rat liver mitochondria as described in the methods. After the import, the samples were either directly processed by centrifuging at 10,000 rpm for 10 min on sucrose cushion or treated with trypsin to remove non-imported proteins and processed on sucrose cushion. All samples were resolved on 10% SDS-PAGE and analyzed by autoradiography. Import of TOM40 was confirmed byits resistance to externally added trypsin. In the absence of protease, a full length TOM40 (~40 kDa) is observed either with wild type or mutants. This fraction is a combination of bound and imported protein. The bound protein fraction and cytosolic exposed domain of imported protein is susceptible to externally added protease. Addition of protease to yeast or mammalian mitochondria results in generation of a 38 kDa protease resistant fragment of Tom40 (Hill, Model *et al.,* 1998). In our import samples, we observed that generation of a ~38 kDa protease resistant fragment with wild type or cysteine mutants (Fig 3.9C). These results suggest that mutation of cysteine residues do not affect the mitochondrial targeting of hTOM40.

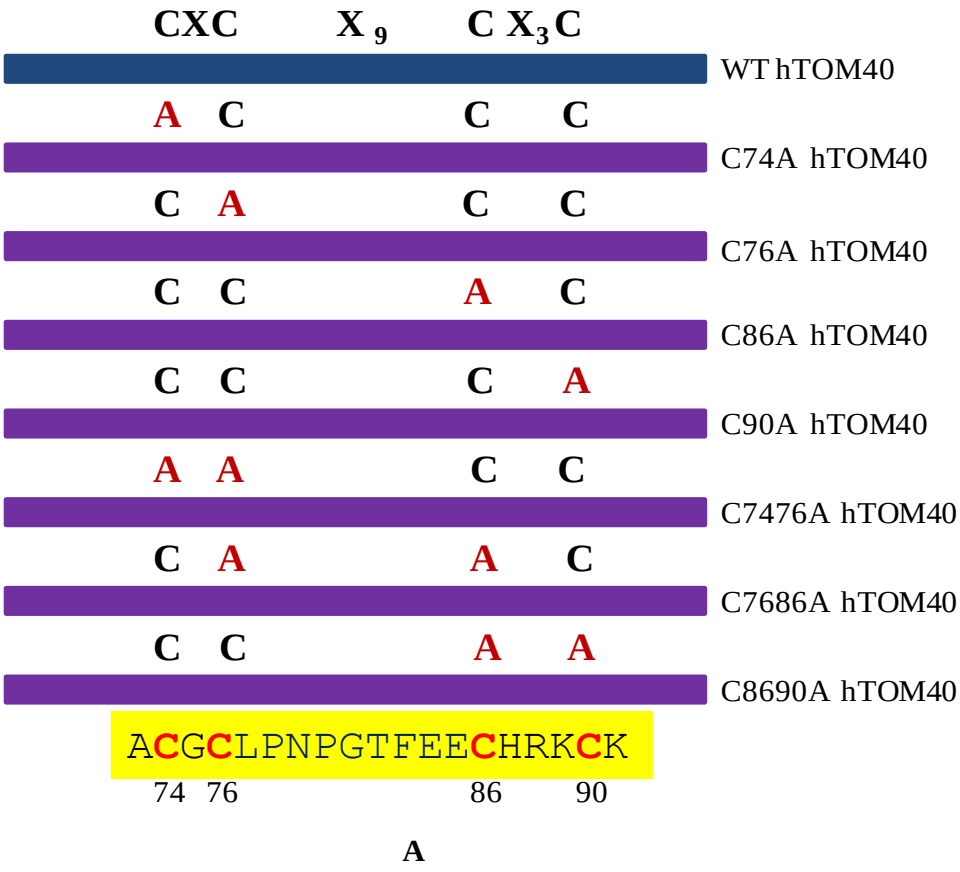
CXC X 9 C X3 C
WT hTOM40
A C C C
C74A hTOM40
C A C C
C76A hTOM40
C C A C
C86A hTOM40
C C C A
C90A hTOM40
A A C C
C7476A hTOM40
C A A C
C7686A hTOM40
C C A A
C8690A hTOM40
ACGCLPNPGTFEECHRKCK
74 76 86 90

A

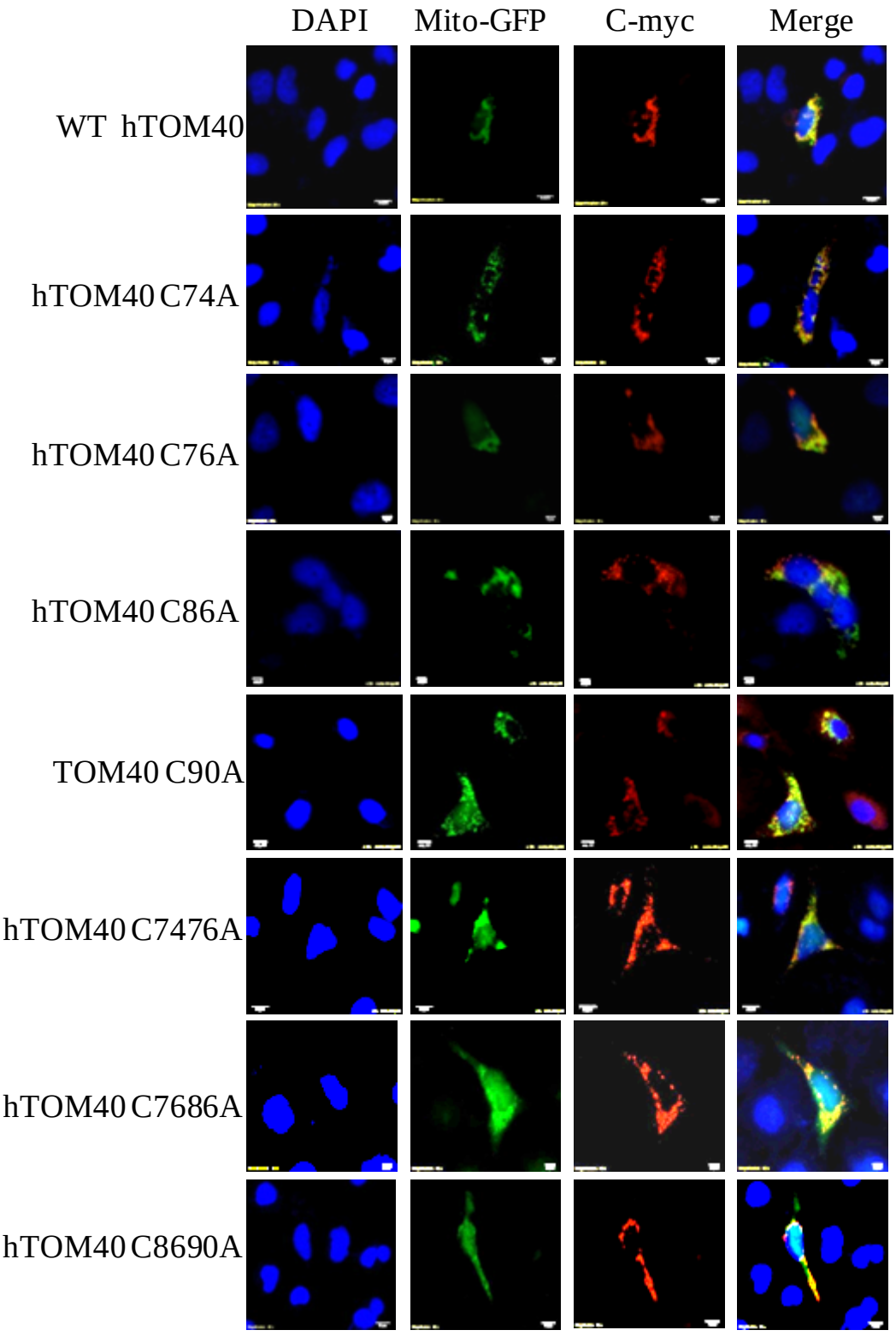
DAPI
Mito-GFP
C-myc
Merge
WT hTOM40
hTOM40 C74A
hTOM40 C76A
hTOM40 C86A
TOM40 C90A
hTOM40 C7476A
hTOM40 C7686A
hTOM40 C8690A

B

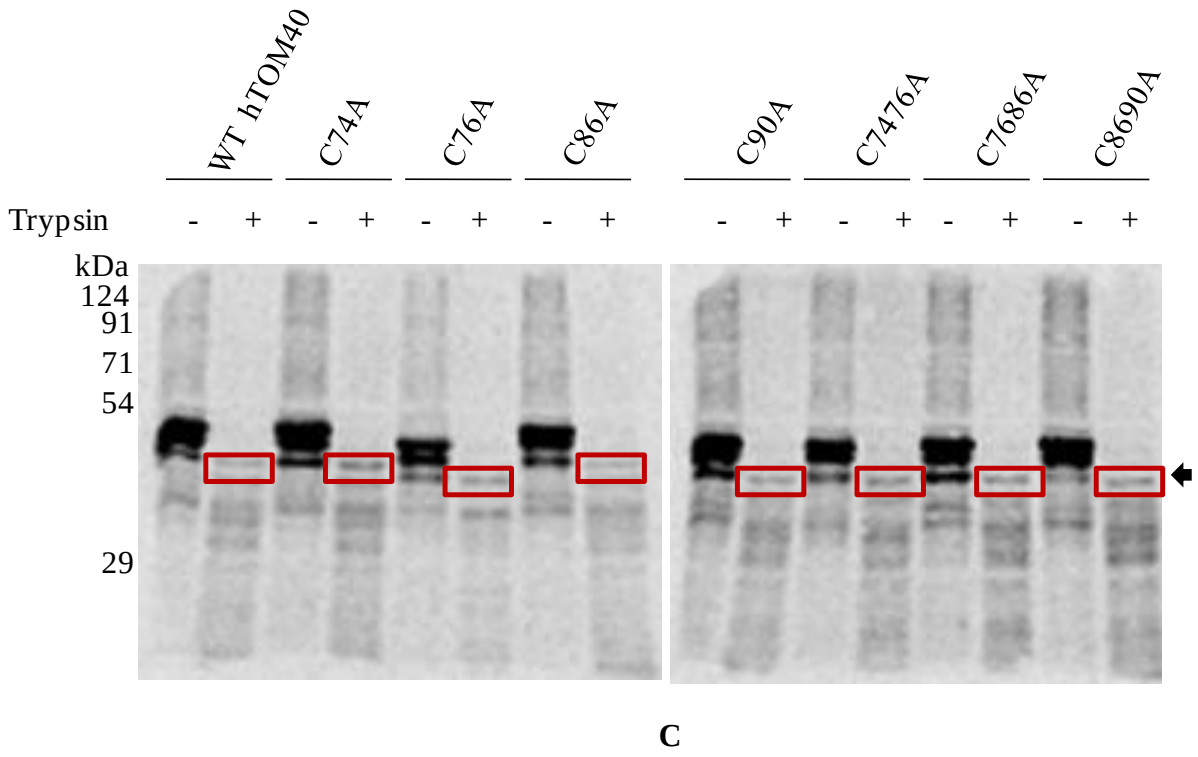

Figure 3.9. Mitochondrial targeting of hTOM40 cysteine (C-A) mutants. The hTOM40 is a nuclear encoded protein synthesized in the cytosol and targeted to mitochondria post-translationally. **(A).** Schematic representation of hTOM40 cysteine mutants showing CXC, CX_3C and CX_9C motifs. **(B).** The Myc-hTOM40 and cysteine mutants were co-transfected with Mito-GFP in HeLa cells. The cells were processed with primary and alexa flour secondary antibodies. The processed cover slips fixed on to the glass slide for further analysis by confocal microscopy (Red-hTOM40, Green-Mito GFP & Blue-Nucleus). **(C).** ^{35}Slabeled hTOM40 and cysteine mutants were imported into rat heart mitochondria at 37 ^{0}C for 60 min. After import the mitochondria were treated without or with 200 µg/ml trypsin on ice and the samples were resolved on SDS-PAGE followed by autoradiography (Arrow indicates the membrane integrated protein).

3.3.9. Role of cysteine residues on secondary structure of hTOM40

Human TOM40 is central component of TOM complex. It is an integral membrane protein with β-barrel structure that forms channel for mitochondrial targeting proteins. The hTOM40 contains a typical cysteine rich motif exposed towards the intermembrane space side. Since cysteine residues also play a crucial role in proper folding and maintaining the structural stability of proteins, we investigated whether cysteine mutants have any effect on folding and

structural stability. We cloned all the cysteine mutants of *TOM40* in pET28 (a^+) vector, expressed and purified to homogeneity (Fig 3.10A) as described in the Methods. We reconstituted the urea denatured recombinant wild type and cysteine mutants of hTOM40in 0.5% LDAO (Lauryl dimethyl amine oxide) detergent. It has been shown that LDAO detergent replaces the membranous environment and provides the native structure to the protein (Maurya and Mahalakshmi 2013). We analyzed the secondary structure of wild type and mutants by using CD. CD spectrum shows that wild type hTOM40 predominantly contains a β-barrel structure (60%) and contains low amount of α-helical structure (12.8%) (Fig 3.10B). Cysteine mutants of human TOM40 does not show any significant deviation from the observed secondary structure of wild type hTOM40 indicating that cysteine mutants does not induce any structural alteration in hTOM40 (Fig 3.10C).

In summary our results show that cysteine motif is important for binding of Fe and cysteine motif may be involved in the assembly or pores formation. However, cysteine residues do not involved in the targeting and do not alter the secondary structure of protein. Further experiments are necessary to understand the precise role of cysteine residues of TOM40 in Fe/S binding, protein import, formation of pore and structural stability.

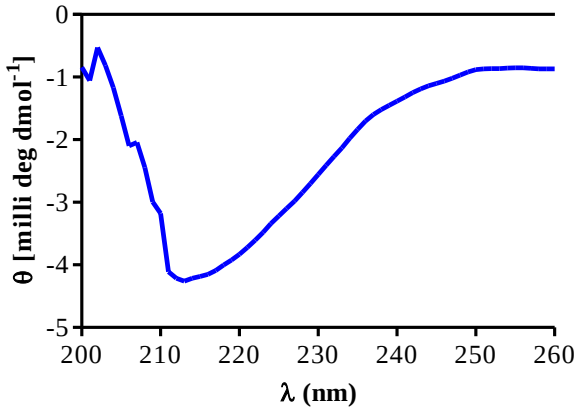

A

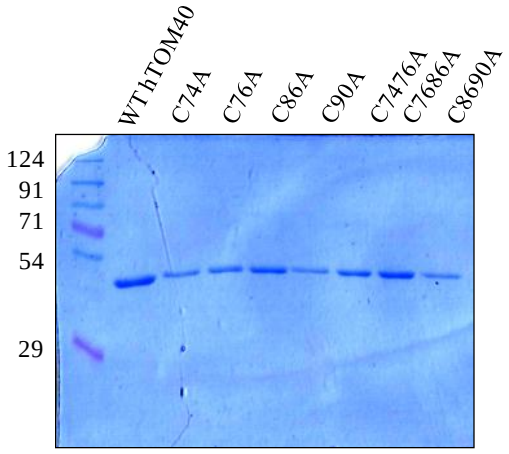

B

	Wavelength 200-260 nm		
	α-Helix (%)	β-Sheet (%)	R-Coil (%)
WT hTOM40	12.8	61.7	25.5
C74A hTOM40	13.9	59.0	27.1
C76A hTOM40	13.6	59.8	26.6
C86A hTOM40	12.4	62.7	24.9
C90A hTOM40	13.8	59.3	26.9
C7476A hTOM40	13.5	59.9	26.6
C7686A hTOM40	14.1	58.5	27.4
C8690A hTOM40	13.0	61.3	25.7

C

Figure 3.10. Secondary structure analysis of hTOM40 by CD. (A). CD spectrum (200 nm-260 nm) analysis of 0.5% LDAO reconstituted hTOM40 protein. **(B).***E.coli* lysate containing recombinant His-hTOM40 and cysteine mutants (C74A, C76A, C86A, C90A, C7476A, C7686A and C8690A) were purified by Ni-NTA column and separated on SDS-PAGE. The SDS-PAGE gel was stained with coomassie and is shown here. **(C).** The secondary structure of 0.5% LDAO reconstituted hTOM40 and cysteine mutants were measured from 200 nm to 260 nm by CD spectrum analysis. The content of β-sheet was calculated by using web based CDNN 2.1 analysis.

3.4. Discussion

Mitochondrion is an essential organelle of the cell and has multifarious roles. One of the important functions of mitochondria is the regulation of cellular iron homeostasis. It forms the main hub for synthesis and export of Fe/S clusters. The enzyme components of the ISC synthesis pathway of the mitochondria have been well characterized genetically and biochemically in yeast and bacteria (Frazzon and Dean 2003; Lill and Muhlenhoff 2006). The cytoplasm and the nucleus in higher eukaryotes have their own Fe/S assembly machinery (CIA), nevertheless, perturbations in the mitochondrial ISC pathway causes maturation defects of nuclear and cytoplasmic enzymes that are dependent on Fe/S clusters. This underscores the importance of mitochondrial ISC system in the cellular iron homeostasis. Yet, the molecular mechanism by which the mitochondrial ISC system exports iron to the cytoplasm is to be fully elucidated.

Atm1, an inner membrane protein has been identified as an iron sulfur exporter from mitochondria (Kispal, Csere *et al.*, 1997). Although the precise component that is exported by Atm1 from mitochondria is debatable, deficiency of Atm1 lead to iron overload in mitochondria, defect in cytosol and nuclear Fe/S cluster biogenesis and no effect on mitochondrial ISC machinery or stability of Fe/S clusters containing proteins (Kispal, Csere *et al.*, 1999; Lill 2009). The additional components of Fe/S export machinery that are probably working along with Atm1 includes Erv1, a sulfahydral oxidase and glutathione (Lange, Lisowsky *et al.*, 2001; Sipos, Lange *et al.*, 2002) as depletion of these proteins reflects the similar phenotype like Atm1 deficiency. Erv1 has been shown to play a role in combination with Mia40, an intermembrane space protein, in the import of numerous cysteine rich intermembrane space proteins by a oxidative folding mechanism.

We have showna novel function for hMIA40 as a Fe/S cluster exporter across the intermembrane space of mitochondria. Since, hMIA40 is an intermembrane space protein it must interact with outer membrane protein to export Fe/S cluster to the cytosol. Majority of the Fe/S clusters are coordinated with four cysteine residues of protein (Spiller, Ang *et al.,* 2013). We found hTOM40 contains conserved typical cysteine motif ($CXCX_9CX_3C$) in its N-terminal intermembrane space domain (Fig 3.2A). This typical cysteine motif is observed only in TOM40 of higher eukaryotes or mammals and does not present in lower eukaryotes. Further, modelling studies shows that cysteine residues are present in the centre of the predicted pore structure of hTOM40 and exposed towards the intermembrane space of mitochondria (Fig 3.2B & C).

Our *AES* studies using recombinant hTOM40 shows that hTOM40 binds to iron*in vitro* (Fig 3.4A). We also confirmed that hTOM40 binds to iron *in vivo* (Fig 3.4B). The visible spectrum of recombinant hTOM40 showed an absorption peak at 410 nm which is a characteristic peak for 4Fe-4S cluster. This Fe/S clusters were very sensitive to oxidative environment. Further, redox conditions stabilizes Fe/S cluster and oxidised conditions destabilizes the Fe/S cluster (Fig 3.5B). Further, SDS-PAGE analysis of hTOM40 under non-reducing conditions shows that hTOM40 exist in both reduced and oxidised states *in vitro*and *in vivo*(Fig 3.5C & D).

The TEM analysis of reconstituted hTOM40 liposomes shows that oxidative conditions are required for formation of structures with optimal number of pores (Fig 3.8B & C). We have measured the pore size of hTOM40 during TEM analysis and it is around 20 ^{0}A diameter. The observed pore size is in agreement with the published results (Kunkele, Heins *et al.,* 1998).

The biological significance of Fe/S clusters on TOM40 is not known. Here we show that the role of hTOM40 in cellular iron homeostasis. We used shRNA to deplete the levels of TOM40 in cells (Fig 3.6A). To asses the mitochondrial iron, we have used two different methods i.e. bathophenonthroline and ^{55}Fe method. These two methods show significant accumulation of mitochondrial iron with depletion of hTOM40 levels (Fig 3.6B & C). The knock down of hTOM40 in human cell lines reduced the activity of cytosolic Fe/S cluster containing enzyme (Aconitase) (Fig 3.6D). Further, the stability of GPAT (Glutamate Phosphoribosyl pyrophosphate Amidotransferase) is altered in hTOM40 knock down cells (Fig 3.6E). These results suggest that hTOM40 is probably involved in the export of mitochondrial Fe/S cluster. The confocal, *in vitro* protein import and CD spectral studies shows that cysteine mutants (C-A) of hTOM40 does not affect its targeting or do not affect its secondary structure. These results suggest that cysteine motif is probably important for binding of Fe and pore formation.

In summary our results suggests that oxidised conditions may required for the pore formation and releasing of Fe/S clusters from the hTOM40. In contrast, reduced environment favours the binding of Fe/S clusters. Based on our results, we are predicting that probably alternative cycles of redox and oxidative environment may be regulating the binding and releasing of Fe/S cluster on hTOM40 as well as assembly of TOM complex for the import of precursor proteins destined to mitochondria simultaneously.

It is known that Tom40 is involved in the mitochondrial protein import. However, we have not shown the exchange of Fe/S cluster from protein to protein as it is technically difficult. In this study, we used a simple *in vitro* protein-protein interaction assay. We show that a disulfide mediated interaction between hMIA40 and hTOM40 *in vitro* (Fig 3.7C). Based on these studies, we are predicting that there is possibility of exchange of Fe/S cluster between

two proteins. Further experiments are required to understand the role of TOM40 in cellular iron metabolism and Fe/S export.

The presence of cysteine motif only in TOM40 of higher eukaryotes is not surprising as mammalian mitochondria are involved in several pathways. Further, studies show that import mechanism and receptors may vary in higher eukaryotes particularly at the level of TOM complex.

TOM complex is an entry gate to most of the proteins targeted to mitochondria. The pore forming structure in TOM complex is TOM40, a β-barrel membrane integrated protein (Hill, Model *et al.,* 1998). TOM40 is associated with different receptor proteins of the TOM complex and can form structure with 2-3 pores. Tom40 is synthesized in the cytosol and contains information in its mature protein for mitochondrial targeting and assembly. The biogenesis of Tom40 is well characterized in lower eukaryotes. It is believed to be similar in higher eukaryotes. However, the constituents of TOM complex and its biogenesis in mammalian cells are yet to be explored in detail.*In vitro* studies with isolated mitochondria and labelled TOM40 reveal that the human TOM40 assembled into three resolvable complexes in a time-dependent manner. Initially human TOM40 precursors are found in a 500kDa complex (Intermediate 1), then as a smaller 100kDa complex (Intermediate II) andeventually forming a mature 380kDa complex (TOM Complex) in a time dependent manner. But in yeast, the assembly of Tom40 is different where it forms 500 kDa mature TOM complex. In yeast, Tom40 is found in a multi-subunit complex consisting of receptor proteins Tom20 and Tom70, a central organizing subunit Tom22 and three small proteins Tom5, Tom6, and Tom7.In mammalian mitochondria the accessory subunits of TOM complex such as Tom5 and Tom6 have not been found in the genome.In addition, our studies shows that mammalian but not yeast Tom40 undergoes disulfide mediated oligomerization

under non-reducing conditions(Ahting, Thieffry *et al.*, 2001; Model, Meisinger *et al.*, 2008). Further, mammalian mitochondria are involved in well defined apoptosis, steroid biosynthesis, calcium signaling and cancer. These differences may emphasize the fact that mammalian protein translocation is probably highly evolved to carry out additional functions such as Fe/S export.

Since the genetic mutations in proteins that are involved Fe/S biogenesis may lead to several human disorders. These diseases are ranging from ataxia such as Friedreich's ataxia (FRDA), myopathies and anaemia (Mochel, Knight *et al.*, 2008; Ye, Jeong *et al.*, 2010; Koeppen 2011). By understanding the Fe/S export mediated by hMIA40 and hTOM40 would eventually help in development of better therapeutics to various disorders due to genetic mutations in Fe/S cluster biogenesis.

BIBLIOGRAPHY

Acquaviva, F., I. De Biase, *et al.*, (2005). "Extra-mitochondrial localisation of frataxin and its association with IscU1 during enterocyte-like differentiation of the human colon adenocarcinoma cell line Caco-2." J Cell Sci**118**(Pt 17): 3917-3924.

Adam, A. C., C. Bornhovd, *et al.*, (2006). "The Nfs1 interacting protein Isd11 has an essential role in Fe/S cluster biogenesis in mitochondria." EMBO J**25**(1): 174-183.

Ahting, U., M. Thieffry, *et al.*, (2001). "Tom40, the pore-forming component of the protein-conducting TOM channel in the outer membrane of mitochondria." J Cell Biol**153**(6): 1151-1160.

Alberts, Bruce; Alexander Johnson, Julian Lewis, Martin Raff, Keith Roberts, Peter Walter (1994). Molecular Biology of the Cell. New York: Garland Publishing Inc. ISBN 0-8153-3218-1.

Alconada, A., M. Kubrich, *et al.*, (1995). "The mitochondrial receptor complex: the small subunit Mom8b/Isp6 supports association of receptors with the general insertion pore and transfer of preproteins." Mol Cell Biol**15**(11): 6196-6205.

Allen, S., V. Balabanidou, *et al.*, (2005). "Erv1 mediates the Mia40-dependent protein import pathway and provides a functional link to the respiratory chain by shuttling electrons to cytochrome c." J Mol Biol**353**(5): 937-944.

Attardi, G. and G. Schatz (1988). "Biogenesis of mitochondria." Annu Rev Cell Biol**4**: 289-333.

Balk, J. and S. Lobreaux (2005). "Biogenesis of iron-sulfur proteins in plants." Trends Plant Sci**10**(7): 324-331.

Balk, J., A. J. Pierik, *et al.*, (2004). "The hydrogenase-like Nar1p is essential for maturation of cytosolic and nuclear iron-sulphur proteins." EMBO J**23**(10): 2105-2115.

Banci, L., I. Bertini, *et al.*, (2009). "MIA40 is an oxidoreductase that catalyzes oxidative protein folding in mitochondria." Nat Struct Mol Biol**16**(2): 198-206.

Bandyopadhyay, S., K. Chandramouli, *et al.*, (2008). "Iron-sulfur cluster biosynthesis." Biochem Soc Trans**36**(Pt 6): 1112-1119.

Barros, M. H. and A. Tzagoloff (2002). "Regulation of the heme A biosynthetic pathway in Saccharomyces cerevisiae." FEBS Lett**516**(1-3): 119-123.

Beinert, H. (2000). "Iron-sulfur proteins: ancient structures, still full of surprises." J Biol Inorg Chem**5**(1): 2-15.

Beinert, H., R. H. Holm, *et al.*, (1997). "Iron-sulfur clusters: nature's modular, multipurpose structures." Science**277**(5326): 653-659.

Biederbick, A., O. Stehling, *et al.*, (2006). "Role of human mitochondrial Nfs1 in cytosolic iron-sulfur protein biogenesis and iron regulation." Mol Cell Biol**26**(15): 5675-5687.

Boal, A. K., E. Yavin, *et al.*, (2007). "DNA repair glycosylases with a [4Fe-4S] cluster: a redox cofactor for DNA-mediated charge transport?" J Inorg Biochem**101**(11-12): 1913-1921.

Bogenhagen, D. and D. A. Clayton (1977). "Mouse L cell mitochondrial DNA molecules are selected randomly for replication throughout the cell cycle." Cell**11**(4): 719-727.

Bolender, N., A. Sickmann, *et al.*, (2008). "Multiple pathways for sorting mitochondrial precursor proteins." EMBO Rep**9**(1): 42-49.

Bonomi, F., S. Iametti, *et al.*, (2011). "Facilitated transfer of IscU-[2Fe2S] clusters by chaperone-mediated ligand exchange." Biochemistry**50**(44): 9641-9650.

Bottinger, L., A. Gornicka, *et al.*, (2012). "In vivo evidence for cooperation of Mia40 and Erv1 in the oxidation of mitochondrial proteins." Mol Biol Cell**23**(20): 3957-3969.

Bridwell-Rabb, J., A. M. Winn, *et al.*, (2011). "Structure-function analysis of Friedreich's ataxia mutants reveals determinants of frataxin binding and activation of the Fe-S assembly complex." Biochemistry**50**(33): 7265-7274.

Cai, K., R. O. Frederick, *et al.*, (2013). "Human mitochondrial chaperone (mtHSP70) and cysteine desulfurase (NFS1) bind preferentially to the disordered conformation, whereas co-chaperone (HSC20) binds to the structured conformation of the iron-sulfur cluster scaffold protein (ISCU)." J Biol Chem**288**(40): 28755-28770.

Cavadini, P., G. Biasiotto, *et al.*, (2007). "RNA silencing of the mitochondrial ABCB7 transporter in HeLa cells causes an iron-deficient phenotype with mitochondrial iron overload." Blood**109**(8): 3552-3559.

Craig, E. A. and J. Marszalek (2002). "A specialized mitochondrial molecular chaperone system: a role in formation of Fe/S centers." Cell Mol Life Sci**59**(10): 1658-1665.

Csere, P., R. Lill, *et al.*, (1998). "Identification of a human mitochondrial ABC transporter, the functional orthologue of yeast Atm1p." FEBS Lett**441**(2): 266-270.

Dailey, H. A. (2002). "Terminal steps of haem biosynthesis." Biochem Soc Trans**30**(4): 590-595.

Daithankar, V. N., S. R. Farrell, *et al.*, (2009). "Augmenter of liver regeneration: substrate specificity of a flavin-dependent oxidoreductase from the mitochondrial intermembrane space." Biochemistry**48**(22): 4828-4837.

De Domenico, I., D. McVey Ward, *et al.*, (2008). "Regulation of iron acquisition and storage: consequences for iron-linked disorders." Nat Rev Mol Cell Biol**9**(1): 72-81.

de Wit, L. E. and W. Sluiter (2009). "Chapter 9 Reliable assay for measuring complex I activity in human blood lymphocytes and skin fibroblasts." Methods Enzymol**456**: 169-181.

Dekker, P. J., M. T. Ryan, *et al.*, (1998). "Preprotein translocase of the outer mitochondrial membrane: molecular dissection and assembly of the general import pore complex." Mol Cell Biol**18**(11): 6515-6524.

Dietmeier, K., A. Honlinger, *et al.*, (1997). "Tom5 functionally links mitochondrial preprotein receptors to the general import pore." Nature**388**(6638): 195-200.

Dong, X. P., X. Cheng, *et al.*, (2008). "The type IV mucolipidosis-associated protein TRPML1 is an endolysosomal iron release channel." Nature**455**(7215): 992-996.

Endo, T., H. Yamamoto, *et al.*, (2003). "Functional cooperation and separation of translocators in protein import into mitochondria, the double-membrane bounded organelles." J Cell Sci**116**(Pt 16): 3259-3267.

Fontecave, M., S. O. Choudens, *et al.*, (2005). "Mechanisms of iron-sulfur cluster assembly: the SUF machinery." J Biol Inorg Chem**10**(7): 713-721.

Frazzon, J. and D. R. Dean (2002). "Biosynthesis of the nitrogenase iron-molybdenum-cofactor from Azotobacter vinelandii." Met Ions Biol Syst**39**: 163-186.

Frazzon, J. and D. R. Dean (2003). "Formation of iron-sulfur clusters in bacteria: an emerging field in bioinorganic chemistry." Curr Opin Chem Biol**7**(2): 166-173.

Frey, T. G. and C. A. Mannella (2000). "The internal structure of mitochondria." Trends Biochem Sci**25**(7): 319-324.

Frey, T. G., C. W. Renken, *et al.*, (2002). "Insight into mitochondrial structure and function from electron tomography." Biochim Biophys Acta**1555**(1-3): 196-203.

Fuzery, A. K., J. J. Oh, *et al.*, (2011). "Three hydrophobic amino acids in Escherichia coli HscB make the greatest contribution to the stability of the HscB-IscU complex." BMC Biochem**12**: 3.

Gakh, O., P. Cavadini, *et al.*, (2002). "Mitochondrial processing peptidases." Biochim Biophys Acta**1592**(1): 63-77.

Ganz, T. (2008). "Iron homeostasis: fitting the puzzle pieces together." Cell Metab**7**(4): 288-290.

Gardner, P. R. (1997). "Superoxide-driven aconitase FE-S center cycling." Biosci Rep**17**(1): 33-42.

Gardner, P. R. and I. Fridovich (1992). "Inactivation-reactivation of aconitase in Escherichia coli. A sensitive measure of superoxide radical." J Biol Chem**267**(13): 8757-8763.

Gilkerson, R. W., J. M. Selker, *et al.*, (2003). "The cristal membrane of mitochondria is the principal site of oxidative phosphorylation." FEBS Lett**546**(2-3): 355-358.

Glick, B. S., A. Brandt, *et al.*, (1992). "Cytochromes c1 and b2 are sorted to the intermembrane space of yeast mitochondria by a stop-transfer mechanism." Cell**69**(5): 809-822.

Gorla, M. and N. B. Sepuri (2014). "Perturbation of apoptosis upon binding of tRNA to the heme domain of cytochrome c." Apoptosis**19**(1): 259-268.

Grandoni, J. A., R. L. Switzer, *et al.*, (1989). "Evidence that the iron-sulfur cluster of Bacillus subtilis glutamine phosphoribosylpyrophosphate amidotransferase determines stability of the enzyme to degradation in vivo." J Biol Chem**264**(11): 6058-6064.

Hachiya, N., K. Mihara, *et al.*, (1995). "Reconstitution of the initial steps of mitochondrial protein import." Nature**376**(6542): 705-709.

Hentze, M. W., M. U. Muckenthaler, *et al.*, (2004). "Balancing acts: molecular control of mammalian iron metabolism." Cell**117**(3): 285-297.

Henze, K. and W. Martin (2003). "Evolutionary biology: essence of mitochondria." Nature**426**(6963): 127-128.

Herrmann, J. M. and K. Hell (2005). "Chopped, trapped or tacked--protein translocation into the IMS of mitochondria." Trends Biochem Sci**30**(4): 205-211.

Herrmann, J. M. and W. Neupert (2000). "Protein transport into mitochondria." Curr Opin Microbiol**3**(2): 210-214.

Hill, K., K. Model, *et al.*, (1998). "Tom40 forms the hydrophilic channel of the mitochondrial import pore for preproteins [see comment]." Nature**395**(6701): 516-521.

Hofmann, S., U. Rothbauer, *et al.*, (2005). "Functional and mutational characterization of human MIA40 acting during import into the mitochondrial intermembrane space." J Mol Biol**353**(3): 517-528.

Honlinger, A., U. Bomer, *et al.*, (1996). "Tom7 modulates the dynamics of the mitochondrial outer membrane translocase and plays a pathway-related role in protein import." EMBO J**15**(9): 2125-2137.

Jarrett, J. T. (2005). "The novel structure and chemistry of iron-sulfur clusters in the adenosylmethionine-dependent radical enzyme biotin synthase." Arch Biochem Biophys**433**(1): 312-321.

Jensen, R. E. and A. E. Johnson (2001). "Opening the door to mitochondrial protein import." Nat Struct Biol**8**(12): 1008-1010.

Johnson, D. C., D. R. Dean, *et al.*, (2005). "Structure, function, and formation of biological iron-sulfur clusters." Annu Rev Biochem**74**: 247-281.

Keel, S. B., R. T. Doty, *et al.*, (2008). "A heme export protein is required for red blood cell differentiation and iron homeostasis." Science**319**(5864): 825-828.

Kiebler, M., P. Keil, *et al.*, (1993). "The mitochondrial receptor complex: a central role of MOM22 in mediating preprotein transfer from receptors to the general insertion pore." Cell**74**(3): 483-492.

Kispal, G., P. Csere, *et al.*, (1997). "The ABC transporter Atm1p is required for mitochondrial iron homeostasis." FEBS Lett**418**(3): 346-350.

Kispal, G., P. Csere, *et al.*, (1999). "The mitochondrial proteins Atm1p and Nfs1p are essential for biogenesis of cytosolic Fe/S proteins." EMBO J**18**(14): 3981-3989.

Koehler, C. M., S. Merchant, *et al.*, (1999). "How membrane proteins travel across the mitochondrial intermembrane space." Trends Biochem Sci**24**(11): 428-432.

Koeppen, A. H. (2011). "Friedreich's ataxia: pathology, pathogenesis, and molecular genetics." J Neurol Sci**303**(1-2): 1-12.

Kollberg, G., M. Tulinius, *et al.*, (2009). "Clinical manifestation and a new ISCU mutation in iron-sulphur cluster deficiency myopathy." Brain**132**(Pt 8): 2170-2179.

Kunkele, K. P., S. Heins, *et al.*, (1998). "The preprotein translocation channel of the outer membrane of mitochondria." Cell**93**(6): 1009-1019.

Laemmli, U. K. (1970). "Cleavage of structural proteins during the assembly of the head of bacteriophage T4." Nature**227**(5259): 680-685.

Lange, H., T. Lisowsky, *et al.*, (2001). "An essential function of the mitochondrial sulfhydryl oxidase Erv1p/ALR in the maturation of cytosolic Fe/S proteins." EMBO Rep**2**(8): 715-720.

Leighton, J. and G. Schatz (1995). "An ABC transporter in the mitochondrial inner membrane is required for normal growth of yeast." EMBO J**14**(1): 188-195.

Li, K., W. H. Tong, *et al.*, (2006). "Roles of the mammalian cytosolic cysteine desulfurase, ISCS, and scaffold protein, ISCU, in iron-sulfur cluster assembly." J Biol Chem**281**(18): 12344-12351.

Lill, R. (2009). "Function and biogenesis of iron-sulphur proteins." Nature**460**(7257): 831-838.

Lill, R. and G. Kispal (2000). "Maturation of cellular Fe-S proteins: an essential function of mitochondria." Trends Biochem Sci**25**(8): 352-356.

Lill, R. and U. Muhlenhoff (2006). "Iron-sulfur protein biogenesis in eukaryotes: components and mechanisms." Annu Rev Cell Dev Biol**22**: 457-486.

Lill, R. and U. Muhlenhoff (2008). "Maturation of iron-sulfur proteins in eukaryotes: mechanisms, connected processes, and diseases." Annu Rev Biochem**77**: 669-700.

Lithgow, T., B. S. Glick, *et al.*, (1995). "The protein import receptor of mitochondria." Trends Biochem Sci**20**(3): 98-101.

Liu, A. and A. Graslund (2000). "Electron paramagnetic resonance evidence for a novel interconversion of [3Fe-4S](+) and [4Fe-4S](+) clusters with endogenous iron and sulfide in anaerobic ribonucleotide reductase activase in vitro." J Biol Chem**275**(17): 12367-12373.

Lutz, T., W. Neupert, *et al.*, (2003). "Import of small Tim proteins into the mitochondrial intermembrane space." EMBO J**22**(17): 4400-4408.

Makaroff, C. A., J. L. Paluh, *et al.*, (1986). "Mutagenesis of ligands to the [4 Fe-4S] center of Bacillus subtilis glutamine phosphoribosylpyrophosphate amidotransferase." J Biol Chem**261**(24): 11416-11423.

Mannella, C. A., D. R. Pfeiffer, *et al.*, (2001). "Topology of the mitochondrial inner membrane: dynamics and bioenergetic implications." IUBMB Life**52**(3-5): 93-100.

Martelli, A., M. Napierala, *et al.*, (2012). "Understanding the genetic and molecular pathogenesis of Friedreich's ataxia through animal and cellular models." Dis Model Mech**5**(2): 165-176.

Maurya, S. R. and R. Mahalakshmi (2013). "Modulation of human mitochondrial voltage-dependent anion channel 2 (hVDAC-2) structural stability by cysteine-assisted barrel-lipid interactions." J Biol Chem**288**(35): 25584-25592.

Mesecke, N., K. Bihlmaier, *et al.*, (2008). "The zinc-binding protein Hot13 promotes oxidation of the mitochondrial import receptor Mia40." EMBO Rep**9**(11): 1107-1113.

Mesecke, N., N. Terziyska, *et al.*, (2005). "A disulfide relay system in the intermembrane space of mitochondria that mediates protein import." Cell**121**(7): 1059-1069.

Mochel, F., M. A. Knight, *et al.*, (2008). "Splice mutation in the iron-sulfur cluster scaffold protein ISCU causes myopathy with exercise intolerance." Am J Hum Genet**82**(3): 652-660.

Model, K., C. Meisinger, *et al.*, (2008). "Cryo-electron microscopy structure of a yeast mitochondrial preprotein translocase." J Mol Biol**383**(5): 1049-1057.

Moraes, C. T. (2001). "What regulates mitochondrial DNA copy number in animal cells?" Trends Genet**17**(4): 199-205.

Morgan, B., S. K. Ang, *et al.*, (2009). "Zinc can play chaperone-like and inhibitor roles during import of mitochondrial small Tim proteins." J Biol Chem**284**(11): 6818-6825.

Moser, C. C., T. A. Farid, *et al.*, (2006). "Electron tunneling chains of mitochondria." Biochim Biophys Acta**1757**(9-10): 1096-1109.

Moyes, C. D. and D. A. Hood (2003). "Origins and consequences of mitochondrial variation in vertebrate muscle." Annu Rev Physiol**65**: 177-201.

Muhlenhoff, U., J. Balk, *et al.*, (2004). "Functional characterization of the eukaryotic cysteine desulfurase Nfs1p from Saccharomyces cerevisiae." J Biol Chem**279**(35): 36906-36915.

Muhlenhoff, U., N. Richhardt, *et al.*, (2002). "Characterization of iron-sulfur protein assembly in isolated mitochondria. A requirement for ATP, NADH, and reduced iron." J Biol Chem**277**(33): 29810-29816.

Napier, I., P. Ponka, *et al.*, (2005). "Iron trafficking in the mitochondrion: novel pathways revealed by disease." Blood**105**(5): 1867-1874.

Netz, D. J., A. J. Pierik, *et al.*, (2007). "The Cfd1-Nbp35 complex acts as a scaffold for iron-sulfur protein assembly in the yeast cytosol." Nat Chem Biol**3**(5): 278-286.

Netz, D. J., C. M. Stith, *et al.*, (2012). "Eukaryotic DNA polymerases require an iron-sulfur cluster for the formation of active complexes." Nat Chem Biol**8**(1): 125-132.

Netz, D. J., M. Stumpfig, *et al.*, (2010). "Tah18 transfers electrons to Dre2 in cytosolic iron-sulfur protein biogenesis." Nat Chem Biol**6**(10): 758-765.

Neupert, W. and J. M. Herrmann (2007). "Translocation of proteins into mitochondria." Annu Rev Biochem**76**: 723-749.

Nordin, A., E. Larsson, *et al.*, (2012). "The defective splicing caused by the ISCU intron mutation in patients with myopathy with lactic acidosis is repressed by PTBP1 but can be derepressed by IGF2BP1." Hum Mutat**33**(3): 467-470.

Paradies, G., G. Petrosillo, *et al.*, (1997). "Cardiolipin-dependent decrease of cytochrome c oxidase activity in heart mitochondria from hypothyroid rats." Biochim Biophys Acta**1319**(1): 5-8.

Paradies, G. and F. M. Ruggiero (1990). "Age-related changes in the activity of the pyruvate carrier and in the lipid composition in rat-heart mitochondria." Biochim Biophys Acta**1016**(2): 207-212.

Pfanner, N. and A. Geissler (2001). "Versatility of the mitochondrial protein import machinery." Nat Rev Mol Cell Biol**2**(5): 339-349.

Pfanner, N., N. Wiedemann, *et al.*, (2004). "Assembling the mitochondrial outer membrane." Nat Struct Mol Biol**11**(11): 1044-1048.

Pondarre, C., B. B. Antiochos, *et al.*, (2006). "The mitochondrial ATP-binding cassette transporter Abcb7 is essential in mice and participates in cytosolic iron-sulfur cluster biogenesis." Hum Mol Genet**15**(6): 953-964.

Poyton, R. O. and J. E. McEwen (1996). "Crosstalk between nuclear and mitochondrial genomes." Annu Rev Biochem**65**: 563-607.

Prischi, F., P. V. Konarev, *et al.*, (2010). "Structural bases for the interaction of frataxin with the central components of iron-sulphur cluster assembly." Nat Commun**1**: 95.

Py, B. and F. Barras (2010). "Building Fe-S proteins: bacterial strategies." Nat Rev Microbiol**8**(6): 436-446.

Qi, W. and J. A. Cowan (2011). "Mechanism of glutaredoxin-ISU [2Fe-2S] cluster exchange." Chem Commun (Camb)**47**(17): 4989-4991.

Quigley, J. G., Z. Yang, *et al.*, (2004). "Identification of a human heme exporter that is essential for erythropoiesis." Cell**118**(6): 757-766.

Raulfs, E. C., I. P. O'Carroll, *et al.*, (2008). "In vivo iron-sulfur cluster formation." Proc Natl Acad Sci U S A**105**(25): 8591-8596.

Rees, D. C. (2002). "Great metalloclusters in enzymology." Annu Rev Biochem**71**: 221-246.

Rees, D. C. and J. B. Howard (2000). "Nitrogenase: standing at the crossroads." Curr Opin Chem Biol**4**(5): 559-566.

Rees, D. C. and J. B. Howard (2003). "The interface between the biological and inorganic worlds: iron-sulfur metalloclusters." Science**300**(5621): 929-931.

Renis, M., P. Cantatore, *et al.*, (1989). "Content of mitochondrial DNA and of three mitochondrial RNAs in developing and adult rat cerebellum." J Neurochem**52**(3): 750-754.

Richards, T. A. and M. van der Giezen (2006). "Evolution of the Isd11-IscS complex reveals a single alpha-proteobacterial endosymbiosis for all eukaryotes." Mol Biol Evol**23**(7): 1341-1344.

Robin, E. D. and R. Wong (1988). "Mitochondrial DNA molecules and virtual number of mitochondria per cell in mammalian cells." J Cell Physiol**136**(3): 507-513.

Rouault, T. A. (2006). "The role of iron regulatory proteins in mammalian iron homeostasis and disease." Nat Chem Biol**2**(8): 406-414.

Rouault, T. A. (2012). "Biogenesis of iron-sulfur clusters in mammalian cells: new insights and relevance to human disease." Dis Model Mech**5**(2): 155-164.

Rouault, T. A. and W. H. Tong (2005). "Iron-sulphur cluster biogenesis and mitochondrial iron homeostasis." Nat Rev Mol Cell Biol**6**(4): 345-351.

Ruzicka, F. J. and H. Beinert (1975). "A new membrane iron-sulfur flavoprotein of the mitochondrial electron transfer system. The entrance point of the fatty acyl dehydrogenation pathway?" Biochem Biophys Res Commun**66**(2): 622-631.

Ryter, S. W. and R. M. Tyrrell (2000). "The heme synthesis and degradation pathways: role in oxidant sensitivity. Heme oxygenase has both pro- and antioxidant properties." Free Radic Biol Med**28**(2): 289-309.

Saitoh, T., M. Igura, *et al.,* (2007). "Tom20 recognizes mitochondrial presequences through dynamic equilibrium among multiple bound states." EMBO J**26**(22): 4777-4787.

Scarpulla, R. C. (1997). "Nuclear control of respiratory chain expression in mammalian cells." J Bioenerg Biomembr**29**(2): 109-119.

Schmucker, S., A. Martelli, *et al.,* (2011). "Mammalian frataxin: an essential function for cellular viability through an interaction with a preformed ISCU/NFS1/ISD11 iron-sulfur assembly complex." PLoS One**6**(1): e16199.

Schnackerz, K. D., D. Dobritzsch, *et al.,* (2004). "Dihydropyrimidine dehydrogenase: a flavoprotein with four iron-sulfur clusters." Biochim Biophys Acta**1701**(1-2): 61-74.

Shadel, G. S. and D. A. Clayton (1997). "Mitochondrial DNA maintenance in vertebrates." Annu Rev Biochem**66**: 409-435.

Shaw, G. C., J. J. Cope, *et al.,* (2006). "Mitoferrin is essential for erythroid iron assimilation." Nature**440**(7080): 96-100.

Shay, J. W., D. J. Pierce, *et al.,* (1990). "Mitochondrial DNA copy number is proportional to total cell DNA under a variety of growth conditions." J Biol Chem**265**(25): 14802-14807.

Sheftel, A. D., O. Stehling, *et al.,* (2010). "Humans possess two mitochondrial ferredoxins, Fdx1 and Fdx2, with distinct roles in steroidogenesis, heme, and Fe/S cluster biosynthesis." Proc Natl Acad Sci U S A**107**(26): 11775-11780.

Shepherd, M., T. A. Dailey, *et al.,* (2006). "A new class of [2Fe-2S]-cluster-containing protoporphyrin (IX) ferrochelatases." Biochem J**397**(1): 47-52.

Shi, H., K. Z. Bencze, *et al.,* (2008). "A cytosolic iron chaperone that delivers iron to ferritin." Science**320**(5880): 1207-1210.

Shi, R., A. Proteau, *et al.,* (2010). "Structural basis for Fe-S cluster assembly and tRNA thiolation mediated by IscS protein-protein interactions." PLoS Biol**8**(4): e1000354.

Shi, Y., M. C. Ghosh, *et al.,* (2009). "Human ISD11 is essential for both iron-sulfur cluster assembly and maintenance of normal cellular iron homeostasis." Hum Mol Genet**18**(16): 3014-3025.

Sipos, K., H. Lange, *et al.,* (2002). "Maturation of cytosolic iron-sulfur proteins requires glutathione." J Biol Chem**277**(30): 26944-26949.

Song, D. and F. S. Lee (2008). "A role for IOP1 in mammalian cytosolic iron-sulfur protein biogenesis." J Biol Chem**283**(14): 9231-9238.

Spiller, M. P., S. K. Ang, *et al.*, (2013). "Identification and characterization of mitochondrial Mia40 as an iron-sulfur protein." Biochem J**455**(1): 27-35.

Srinivasan, V., D. J. Netz, *et al.*, (2007). "Structure of the yeast WD40 domain protein Cia1, a component acting late in iron-sulfur protein biogenesis." Structure**15**(10): 1246-1257.

Stehling, O., H. P. Elsasser, *et al.*, (2004). "Iron-sulfur protein maturation in human cells: evidence for a function of frataxin." Hum Mol Genet**13**(23): 3007-3015.

Stehling, O., D. J. Netz, *et al.*, (2008). "Human Nbp35 is essential for both cytosolic iron-sulfur protein assembly and iron homeostasis." Mol Cell Biol**28**(17): 5517-5528.

Steiner, H., A. Zollner, *et al.*, (1995). "Biogenesis of mitochondrial heme lyases in yeast. Import and folding in the intermembrane space." J Biol Chem**270**(39): 22842-22849.

Stemmler, T. L., E. Lesuisse, *et al.*, (2010). "Frataxin and mitochondrial FeS cluster biogenesis." J Biol Chem**285**(35): 26737-26743.

Stephens, P. J., D. R. Jollie, *et al.*, (1996). "Protein Control of Redox Potentials of Ironminus signSulfur Proteins." Chem Rev**96**(7): 2491-2514.

Takahashi, M. and D. A. Hood (1993). "Chronic stimulation-induced changes in mitochondria and performance in rat skeletal muscle." J Appl Physiol (1985)**74**(2): 934-941.

Tangeras, A., T. Flatmark, *et al.*, (1980). "Mitochondrial iron not bound in heme and iron-sulfur centers. Estimation, compartmentation and redox state." Biochim Biophys Acta**589**(2): 162-175.

Terziyska, N., B. Grumbt, *et al.*, (2009). "Structural and functional roles of the conserved cysteine residues of the redox-regulated import receptor Mia40 in the intermembrane space of mitochondria." J Biol Chem**284**(3): 1353-1363.

Terziyska, N., T. Lutz, *et al.*, (2005). "Mia40, a novel factor for protein import into the intermembrane space of mitochondria is able to bind metal ions." FEBS Lett**579**(1): 179-184.

Tong, W. H. and T. A. Rouault (2006). "Functions of mitochondrial ISCU and cytosolic ISCU in mammalian iron-sulfur cluster biogenesis and iron homeostasis." Cell Metab**3**(3): 199-210.

Tsai, C. L. and D. P. Barondeau (2010). "Human frataxin is an allosteric switch that activates the Fe-S cluster biosynthetic complex." Biochemistry**49**(43): 9132-9139.

Uhrigshardt, H., A. Singh, *et al.*, (2010). "Characterization of the human HSC20, an unusual DnaJ type III protein, involved in iron-sulfur cluster biogenesis." Hum Mol Genet**19**(19): 3816-3834.

van Wilpe, S., M. T. Ryan, *et al.*, (1999). "Tom22 is a multifunctional organizer of the mitochondrial preprotein translocase." Nature**401**(6752): 485-489.

Varghese, S., Y. Tang, *et al.*, (2003). "Contrasting sensitivities of Escherichia coli aconitases A and B to oxidation and iron depletion." J Bacteriol**185**(1): 221-230.

Vickery, L. E. and J. R. Cupp-Vickery (2007). "Molecular chaperones HscA/Ssq1 and HscB/Jac1 and their roles in iron-sulfur protein maturation." Crit Rev Biochem Mol Biol**42**(2): 95-111.

Viel, E. C., K. Benkirane, *et al.*, (2008). "Xanthine oxidase and mitochondria contribute to vascular superoxide anion generation in DOCA-salt hypertensive rats." Am J Physiol Heart Circ Physiol**295**(1): H281-288.

von Heijne, G. (1986). "Mitochondrial targeting sequences may form amphiphilic helices." EMBO J**5**(6): 1335-1342.

Walden, W. E., A. I. Selezneva, *et al.*, (2006). "Structure of dual function iron regulatory protein 1 complexed with ferritin IRE-RNA." Science**314**(5807): 1903-1908.

Wallander, M. L., E. A. Leibold, *et al.*, (2006). "Molecular control of vertebrate iron homeostasis by iron regulatory proteins." Biochim Biophys Acta**1763**(7): 668-689.

Wiedemann, N., E. Urzica, *et al.*, (2006). "Essential role of Isd11 in mitochondrial iron-sulfur cluster synthesis on Isu scaffold proteins." EMBO J**25**(1): 184-195.

Wiesner, R. J., T. T. Kurowski, *et al.*, (1992). "Regulation by thyroid hormone of nuclear and mitochondrial genes encoding subunits of cytochrome-c oxidase in rat liver and skeletal muscle." Mol Endocrinol**6**(9): 1458-1467.

Williams, R. S., S. Salmons, *et al.*, (1986). "Regulation of nuclear and mitochondrial gene expression by contractile activity in skeletal muscle." J Biol Chem**261**(1): 376-380.

Ye, H., S. Y. Jeong, *et al.*, (2010). "Glutaredoxin 5 deficiency causes sideroblastic anemia by specifically impairing heme biosynthesis and depleting cytosolic iron in human erythroblasts." J Clin Invest**120**(5): 1749-1761.

Zhang, Y., E. R. Lyver, *et al.*, (2008). "Dre2, a conserved eukaryotic Fe/S cluster protein, functions in cytosolic Fe/S protein biogenesis." Mol Cell Biol**28**(18): 5569-5582.

Zheng, L., V. L. Cash, *et al.*, (1998). "Assembly of iron-sulfur clusters. Identification of an iscSUA-hscBA-fdx gene cluster from Azotobacter vinelandii." J Biol Chem**273**(21): 13264-13272.

PUBLICATIONS

Mge1, a nucleotide exchange factor of Hsp70, acts as an oxidative sensor to regulate mitochondrial Hsp70 function

Adinarayana Marada, Praveen Kumar Allu, Anjaneyulu Murari, BhoomiReddy PullaReddy, Prasad Tammineni, Venkata Ramana Thiriveedi, Jayasree Danduprolu, and Naresh Babu V. Sepuri
Department of Biochemistry, School of Life Sciences, University of Hyderabad, Hyderabad 500046, India

ABSTRACT **Despite the growing evidence of the role of oxidative stress in disease, its molecular mechanism of action remains poorly understood. The yeast *Saccharomyces cerevisiae* provides a valuable model system in which to elucidate the effects of oxidative stress on mitochondria in higher eukaryotes. Dimeric yeast Mge1, the cochaperone of heat shock protein 70 (Hsp70), is essential for exchanging ATP for ADP on Hsp70 and thus for recycling of Hsp70 for mitochondrial protein import and folding. Here we show an oxidative stress–dependent decrease in Mge1 dimer formation accompanied by a concomitant decrease in Mge1–Hsp70 complex formation in vitro. The Mge1-M155L substitution mutant stabilizes both Mge1 dimer and Mge1–Hsp70 complex formation. Most important, the Mge1-M155L mutant rescues the slow-growth phenomenon associated with the wild-type Mge1 strain in the presence of H_2O_2 in vivo, stimulation of the ATPase activity of Hsp70, and the protein import defect during oxidative stress in vitro. Furthermore, cross-linking studies reveal that Mge1–Hsp70 complex formation in mitochondria isolated from wild-type Mge1 cells is more susceptible to reactive oxygen species compared with mitochondria from Mge1-M155L cells. This novel oxidative sensor capability of yeast Mge1 might represent an evolutionarily conserved function, given that human recombinant dimeric Mge1 is also sensitive to H_2O_2.**

Monitoring Editor
Ramanujan S. Hegde
National Institutes of Health

Received: Oct 5, 2012
Revised: Jan 8, 2013
Accepted: Jan 14, 2013

INTRODUCTION

Mitochondria are essential organelles involved in many cellular processes, such as energy metabolism and apoptosis. Although the mitochondrion has its own genome, it depends on the nucleus for optimal functioning (Chacinska *et al.*, 2009). Based on their signal sequence, mitochondrial proteins encoded by nuclear DNA are targeted to different subcompartments of mitochondria through a translocase system present on outer and inner mitochondrial membranes known as the translocase of outer membrane (TOM) and translocase of inner membrane (TIM) complexes, respectively (Schulke *et al.*, 1997, 1999; Endo *et al.*, 2003; Kutik *et al.*, 2007; Neupert and Herrmann, 2007). Targeting of precursor protein to the matrix involves an interplay among many proteins; however, the final step of this process is mediated by Tim44 and a translocation motor that contains mitochondrial heat shock protein 70 (mHsp70), Pam16, Pam18, and the nucleotide exchange factor Mge1 (Azem *et al.*, 1997; Mokranjac *et al.*, 2007; Stojanovski *et al.*, 2007; Schiller *et al.*, 2008). Hsp70, in combination with Tim44, binds to the emerging end of the transit peptide from the TIM channel in an ATP-dependent manner, and the ATPase cycle of mHsp70 leads to pulling or vectorial translocation of preproteins across the inner mitochondrial membrane (Matouschek *et al.*, 2000; Okamoto *et al.*, 2002; Liu *et al.*, 2003). Mge1, a component of this translocation motor, accelerates the exchange of ATP for ADP on mHsp70 and promotes a change from the high–substrate affinity conformation of mHsp70 to a lower–substrate affinity form with a concomitant release of precursor protein from mHsp70 to begin the next round of translocation

This article was published online ahead of print in MBoC in Press (http://www.molbiolcell.org/cgi/doi/10.1091/mbc.E12-10-0719) on January 23, 2013.

Address correspondence to: Naresh Babu V. Sepuri (nareshuohyd@gmail.com or nbvssl@uohyd.ernet.in).

Abbreviations used: Ccpo, cytochrome *c* peroxidase; DHFR, dihydrofolate reductase; HSP 70, heat shock protein 70; ROS, reactive oxygen species; Tim, translocase of inner membrane; Tom, translocase of outer membrane.

Supplemental Material can be found at:
http://www.molbiolcell.org/content/suppl/2013/01/21/mbc.E12-10-0719v1.DC1.html

Cell Biology:

The Import of the Transcription Factor STAT3 into Mitochondria Depends on GRIM-19, a Component of the Electron Transport Chain

Prasad Tammineni, Chandrashekhar Anugula, Fareed Mohammed, Murari Anjaneyulu, Andrew C. Larner and Naresh Babu Venkata Sepuri

J. Biol. Chem. 2013, 288:4723-4732.
doi: 10.1074/jbc.M112.378984 originally published online December 27, 2012

---

1. Anjaneyulu Murari, Venkata Ramana Thiriveedi, Fareed Mohammad, Viswamithra Vengaldas, Madhavi Gorla, Prasad Tammineni, Thanuja Krishnamoorthy and Naresh Babu V.Sepuri*. **Role of Human Mitochondrial MIA40 (CHCD4) in the Maturation of Cytosolic Fe/S Cluster Proteins.** Under communication with Journal of Biological Chemistry

2. Anjaneyulu Murari, Venkata Ramana Thiriveedi, Viswamithra Vengaldas and Naresh Babu V.Sepuri*. **Mammalian TOM40 is a Fe/S protein.** Manuscript is under preparation.